

Winter 2003

Hydrodynamic behavior and thermal stability of a PEGylated protein: Studies with hen egg lysozyme

Yatin R. Gokarn

University of New Hampshire, Durham

Follow this and additional works at: <https://scholars.unh.edu/dissertation>

Recommended Citation

Gokarn, Yatin R., "Hydrodynamic behavior and thermal stability of a PEGylated protein: Studies with hen egg lysozyme" (2003).
Doctoral Dissertations. 192.

<https://scholars.unh.edu/dissertation/192>

This Dissertation is brought to you for free and open access by the Student Scholarship at University of New Hampshire Scholars' Repository. It has been accepted for inclusion in Doctoral Dissertations by an authorized administrator of University of New Hampshire Scholars' Repository. For more information, please contact nicole.hentz@unh.edu.

HYDRODYNAMIC BEHAVIOR AND THERMAL STABILITY
OF A PEGYLATED PROTEIN: STUDIES WITH HEN EGG
LYSOZYME

By

YATIN R. GOKARN

B. Chem. Eng. University of Bombay, 1992

M.S. University of New Hampshire, 1995

M.S. University of New Hampshire, 1998

DISSERTATION

Submitted to the University of New Hampshire
in Partial Fulfillment of
the Requirements for the Degree of

Doctor of Philosophy

in

Biochemistry

December, 2003

UMI Number: 3111505

INFORMATION TO USERS

The quality of this reproduction is dependent upon the quality of the copy submitted. Broken or indistinct print, colored or poor quality illustrations and photographs, print bleed-through, substandard margins, and improper alignment can adversely affect reproduction.

In the unlikely event that the author did not send a complete manuscript and there are missing pages, these will be noted. Also, if unauthorized copyright material had to be removed, a note will indicate the deletion.

UMI[®]

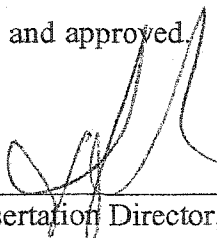
UMI Microform 3111505

Copyright 2004 by ProQuest Information and Learning Company.

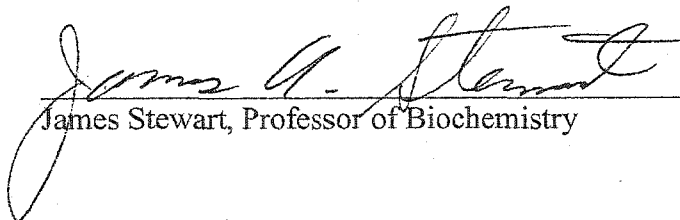
All rights reserved. This microform edition is protected against unauthorized copying under Title 17, United States Code.

ProQuest Information and Learning Company
300 North Zeeb Road
P.O. Box 1346
Ann Arbor, MI 48106-1346

This dissertation has been examined and approved.



Dissertation Director, Thomas M. Laue
Professor of Biochemistry



James Stewart, Professor of Biochemistry



Clyde Denis, Professor of Biochemistry



G. Eric Schaller, Associate Professor of Biochemistry



P. T. Vasudevan, Professor of Chemical Engineering

09/09/03

Date

To Jyotsna

ACKNOWLEDGEMENTS

I really have offshore banking to thank for a career in Biochemistry. If it were not for a company funded through the Cayman Islands, I would have never experienced the most delightful years of my scientific career (and probably the best ever). From what I vaguely understood then, Dr. Bruce (last name left out to protect the not so innocent) was going to fund his company through a rather complicated transaction in the Cayman Islands, and my funding was contingent upon this deal going through. I do not know what deal Tom struck with Bruce to keep me in the country, I didn't ask then, and I won't ask now. I am here; I have finished two degrees from the lab and have a good life. In short...*Mogambo is happy.*

Prior to formally joining the lab, I was introduced to some of its illustrious members during a make-up exam in Biochemistry 851 that Tom (L) was teaching in 1994. I was down with the Flu, and Tom was kind enough to allow me to reschedule it the following week. I arrived at the designated room, a small room in Spaulding that had amongst other things, a spectacled, stuffed eagle, an inflatable figurine of Münk's 'Shriek', Tom Moody, and a silent, menacing, ultra-muscular 240+ lb Steve Eaton. I introduced myself to them; Tom glanced at me, acknowledged my presence, and continued working on his computer, while Steve stared at me for a second, and pointed me to a chair and desk right next to him. As I picked up the exam from Steve, I noticed a quote posted on his computer next to a plastic skull stuck on a pencil. It read, "I wonder what your head would look like on a stick". Steve saw me read it, smiled at me, handed

me the exam, and without a word proceeded to work on his computer. For the next 2 hours, I didn't quite dare to look at him, till he said "time" (that is the only thing that anyone - him, Tom (M) or I had said during this period). I stopped that very second, promptly handed him the sheet, and walked out. Little did I know then how funny, gentle, and helpful Steve really is. Although I wouldn't recommend doing anything that would get him mad.

I guess I recounted this incident, as it is my first memory of this very strange, odd, crazy, yet hilarious, energetic, and ever-curious lab. The Laue-lab folks have given much to me over these years. I cannot thank Tom Laue enough. Still, Thank you, Tom, for believing in me, for your patience through my indecision about doing the PhD, for teaching me how to think, how to respect science, how to enjoy science, for asking me what I had learnt and not what the result was. And, for never once asking me why I rolled in at noon.

Thank you, Sue Lucius, for taking such good care of me and looking after me, for keeping me registered each semester, for the much needed & timely pay-checks, for listening to all my trials and tribulations, for chastising me for being thrown out of grad school, and for calling me to wake me up so that I wouldn't miss the pizza at lab lunch meetings!

Thank you, Kari Hartman & Sue Chase for your support and help in helping me accomplish the PhD. Thanks, Tom Moody, for being just you. Your scientific, worldly, and otherworldly knowledge has never ceased to amaze me, Thanks Rachel (hang in there, and get the sucker done!), Jeff, Tom & Tim for being such good friends.

Thank you, Jo, for surviving these four, crazy years, my absent mindedness, my obsession with food and science. I just cannot imagine how you continue to put with my madness. I simply couldn't have done this without your love, strength, and endurance.

Thank you, Amma, Pappa, Kakas, Anna, Vinaya, Ravi, Megha & our family for your love and support. Aniyaar, Li (chevereke, got it done, eh?), Sada, Rick - thanks for your prodding, encouragement, and motivation.

I would also like to acknowledge Searle/Pharmaica/Pfizer for their kind financial support and consent, Matt McLean for his help with the MALDI-TOF studies, and Dr. Lin from MicroCal for generating the raw DSC data.

It still hasn't quite sunk in that, now, some will address me as Dr. Gokarn. Although the question still remains - am I worthy of this title? In 1998, I didn't think I was, for the present I will take Tom's word for it. For the future, I still have to prove it to myself. I am sure about one thing, I couldn't have asked for a better start.....

TABLE OF CONTENTS

DEDICATION.....	iii
ACKNOWLEDGEMENTS.....	iv
LIST OF TABLES.....	x
LIST OF FIGURES.....	xii
LIST OF SYMBOLS.....	xviii
ABSTRACT.....	xx
1 INTRODUCTION.....	1
1.1 Dissertation Objectives.....	4
1.2 Thermal Stability of PEGylated Proteins.....	5
1.3 Hydrodynamic Behavior of PEGylated Proteins.....	13
1.4 Hen Egg Lysozyme as a Model Protein.....	17
2 EXPERIMENTAL.....	19
2.1 Research Design.....	19
2.2 Synthesis and Purification of PEGylated Hen Egg Lysozyme.....	21
2.3 Concentration Determination of HEL and PEGylated HEL molecules.....	22
2.4 Sodium Dodecyl Sulfate-Polyacrylamide Gel Electrophoresis.....	24
2.5 Matrix Assisted Laser Desorption & Ionization –Time of Flight (MALDI-TOF) Measurements.....	26
2.6 Molecular Weight Determination by Static Light Scattering.....	27
2.7 Fluorescence Spectroscopy.....	29
2.8 Circular Dichroism Spectroscopic Studies.....	30
2.8.1 Near-UV-CD Experiments.....	30
2.8.2 Far-UV-CD Experiments.....	30
2.9 Determination of Partial Specific Volume.....	31
2.10 Sedimentation Velocity Experiments.....	32
2.11 Dynamic Light Scattering Measurements.....	36
2.12 Thermal Unfolding Studies Using UV Spectroscopy.....	37
2.13 Differential Scanning Calorimetry.....	40
2.14 Turbidity Measurements to Monitor Aggregation.....	41

2.15	Aggregation Experiments Using Size Exclusion-High Performance Liquid Chromatography	43
2.16	Digital Visualization of Aggregation	44
3	RESULTS AND DISCUSSION	45
3.1	Synthesis & Characterization of PEGylated Hen Egg Lysozyme	45
3.1.1	Choice of PEGylation Chemistry	45
3.1.2	Heterogeneity in the PEGylated HEL Molecules	46
3.1.3	Determination of Molecular Weights	51
3.1.3.1	MALDI-TOF Measurements	55
3.1.3.2	Static Light Scattering Measurements	56
3.1.3.3	Sedimentation Velocity Experiments	63
3.1.4	Effect of PEGylation on the Secondary Structure of HEL	67
3.1.5	Effect of PEGylation on the Tertiary Structure of HEL	69
3.2	Hydrodynamic Behavior of PEG	73
3.3	Effect of PEGylation on the Hydrodynamic Behavior of HEL	76
3.3.1	Effect of PEGylation on the Sedimentation Properties of HEL	76
3.3.2	Hydrodynamic Nonideality	79
3.3.3	Hydrodynamic Radii of HEL and PEGylated HEL Molecules	82
3.4	Equilibrium Thermal Unfolding Studies	86
3.4.1	Thermal Unfolding Studies of Hen Egg Lysozyme	87
3.4.1.1	Difference Spectrum Method	87
3.4.2	Differential Scanning Calorimetry Results	91
3.4.3	Effect of Free PEG on the T_m of Hen Egg Lysozyme	97
3.4.4	Effect of PEGylation on HEL unfolding	103
3.4.4.1	Effect on T_m	106
3.4.4.2	Effect on the Unfolding Mechanism	111
3.4.4.3	Effect on ΔH and ΔC_p	111
3.5	Kinetic Aggregation Studies	112
3.5.1	Aggregation Studies Using Turbidimetry	113
3.5.1.1	Aggregation Assay	113
3.5.2	Effect of Free PEG on the Aggregation Rate of HEL	114
3.5.3	Effect of PEGylation on the Aggregation of HEL	117
3.5.4	Aggregation Studies Using SE-HPLC	122
4	SUMMARY AND CONCLUSIONS	125
4.1	Characterization of PEG-HEL Molecules	125
4.1.1	Purity Analysis	125
4.1.2	Molecular Weights	126
4.1.3	Effect on HEL Structure	128
4.2	Hydrodynamic Behavior of PEG-HEL molecules	128
4.2.1	Sedimentation Properties & Hydrodynamic Radii	128
4.2.2	Solution Conformation	129
4.3	Effect of PEGylation on the Thermal Stability of HEL	130
4.3.1	Equilibrium Unfolding Studies	130

4.3.2	Kinetic Aggregation Studies	131
4.3.3	Reaction Model for the Aggregation of PEGylated Proteins.....	132
REFERENCES		133

LIST OF TABLES

Table 1: FDA approved PEGylated protein drugs	3
Table 2: PEGylated protein drug candidates in development	3
Table 3: Amino acid composition of Hen Egg Lysozyme	17
Table 4: Properties of Hen Egg Lysozyme	18
Table 5: Techniques employed to characterize PEG-HEL molecules.....	19
Table 6: Techniques employed to study the thermal denaturation of HEL and PEG-HEL	20
Table 7: Techniques employed to study the aggregation rate of HEL and PEG-HEL	21
Table 8: Apparent molecular weights of HEL, and PEGylated HEL determined from the Coomassie Blue stained SDS-PAGE gel.....	52
Table 9: Molecular Weights of PEG1-HEL, PEG2-HEL, and PEG3-HEL determined using MALDI-TOF Measurements	55
Table 10: Results from the static light scattering analysis of PEG, PEG1-HEL, and PEG2-HEL.....	62
Table 11: Comparison of the molecular weights of PEG, PEG1-HEL, and PEG2-HEL determined using MALDI-TOF and static light scattering measurements	62
Table 12: Partial specific volume of different PEG molecules with varying chain lengths and/or branching measured in 25 mM phosphate, 125 mM NaCl, pH 7.5.	64
Table 13: Summary of the sedimentation velocity data used to determine the molecular weights of HEL and various PEG-HEL molecules	65
Table 14: Comparison of the molecular weights of HEL, PEG, and various PEG-HEL molecules determined using MALDI-TOF, static light scattering (SLS) and sedimentation velocity (SV) measurements	66
Table 15: Hydrodynamic radii of PEG molecules of varying chain lengths	73
Table 16. s^* values of HEL, and various PEG-HEL molecules determined using $g^*(s^*)$ versus s^* analysis	76

Table 17. s and D values of PEG1-HEL and PEG2-HEL determined at different protein concentrations using the software programs SVEDBERG and DCDT+	82
Table 18. Stokes radii of HEL and various PEG-HEL molecules determined from sedimentation velocity and DLS experiments	83
Table 19. Thermodynamic parameters governing the thermal unfolding of HEL: values determined using the difference spectrum method	89
Table 20. Reversibility of the thermal unfolding of PEG3-HEL monitored via the difference spectrum method	91
Table 21. Thermodynamic parameters for thermal unfolding of HEL determined from the Cap-DSC, VP-DSC, and the difference spectrum method	94
Table 22. Thermodynamic parameters for the thermal unfolding of HEL in the presence of PEG 400 and PEG 20 kD	101
Table 23. Thermodynamic parameters for thermal unfolding of PEG-HEL molecules determined from the Cap-DSC, VP-DSC, and the Difference Spectrum method ..	104

LIST OF FIGURES

Figure 1: Schematic of the preferential exclusion mechanism. Preferential exclusion of certain excipients from the protein surface leads to an increase in the melting temperature (T_m) of the protein.	8
Figure 2: Preferential Exclusion and PEG. Although PEG is preferentially excluded, it can interact with the exposed hydrophobic patches and stabilize the D form, which leads to a decrease in T_m	11
Figure 3. Pictorial representation of the synthesis and purification of PEGylated HEL molecules	23
Figure 4. UV Spectra of HEL, PEG1-HEL, PEG2-HEL, and PEG3-HEL. Experiments conducted in 25 mM sodium phosphate, 125 mM NaCl, pH 7.5 at room. All spectra are normalized to an arbitrary absorbance value of 1.5 at 281 nm to facilitate comparison.....	23
Figure 5. The reductive amination reaction of aldehydes and primary amines was employed for the PEGylation of HEL using methoxyPEG-propionaldehyde. The reaction was conducted at pH 4.5 in the presence of NaCNBH ₃ to selectively target the N terminal α -amine.	47
Figure 6a & b : SDS-PAGE analysis of HEL, and PEG-HEL (a) - Coomassie Blue stain. The molecular weight standards are in lanes 1 and 8, while HEL, PEG1-HEL, PEG2-HEL, and PEG3-HEL are in lanes 3-6 respectively. (b) – barium iodide stain. PEG1-HEL, PEG2-HEL, and PEG3-HEL are in lanes 1, 2, and 3 respectively.....	47
Figure 7a & b: MALDI-TOF Spectra of PEG1-HEL. Experiments were conducted in a Perceptive Biosystems DE STR time-of-flight mass spectrometer with samples prepared in a sinapinic acid matrix. The broad peak (34–39 kD) presented in panel b represents the heterogeneity in mass within the purified PEG1-HEL resulting from the polydispersity of PEG.	49
Figure 8: MALDI-TOF Spectrum of PEG2-HEL. Experiments were conducted in a Perceptive Biosystems mass spectrometer with samples prepared in a sinapinic acid matrix.	50
Figure 9.: MALDI-TOF Spectrum of PEG3-HEL. Experiments were conducted in a Perceptive Biosystems mass spectrometer with samples prepared in a sinapinic acid matrix.	50

Figure 10. Estimation of apparent molecular weight using SDS-PAGE-calibration curve constructed by plotting the natural log of the molecular weight of standards versus their migration distance (mm) relative to the 10 kD marker. Equation describing the calibration curve was obtained by linear regression.....	53
Figure 11. Comparison of estimated versus expected molecular weights for HEL, and various PEG-HEL molecules. The extent of error in estimation of the molecular weight is measured in terms of the departure from the $M_{est} - M_{exp}$ diagonal.	53
Figure 12 Size Exclusion-HPLC analysis of PEG1-HEL and PEG2-HEL. Experiments were conducted in a HP 1100 HPLC system with simultaneous UV (shown below), RI and LS detection. PEG1-HEL and PEG2-HEL are observed to contain a small amount of non-covalent aggregates at 2 and 2.3 % respectively.	57
Figure 13. Size Exclusion-HPLC coupled Static Light Scattering analysis of mPEG propionaldehyde-20 kD. Experiments were conducted in a HP 1100 HPLC system with simultaneous RI and 90° LS detection. The weight average molecular weight of the PEG monomer (Region I) was determined to be 21470.	59
Figure 14. Size Exclusion-HPLC coupled Static Light Scattering analysis of PEG1-HEL. Experiments were conducted in a HP 1100 HPLC system with simultaneous RI and 90° LS detection. The weight average molecular weight of the PEG1-HEL monomer (Region I) was determined to be 34430.	60
Figure 15. Size Exclusion-HPLC coupled Static Light Scattering analysis of PEG2-HEL. Experiments were conducted in a HP 1100 HPLC system with simultaneous RI and 90° LS detection. The weight average molecular weight of the PEG2-HEL monomer (Region I) was determined to be 53870.	61
Figure 16. The effect of sample concentration on the molecular weights of PEG1-HEL and PEG2-HEL determined by sedimentation velocity experiments. Experiments conducted at 20 °C in 25 mM phosphate, 125 mM NaCl, pH 7.5.	68
Figure 17. Far-UV CD Spectra of HEL, PEG1-HEL, and PEG2-HEL. Experiments were conducted with 0.2 mg/mL HEL, 0.17 mg/mL PEG1-HEL, 0.2 mg/mL PEG2-HEL respectively in 25 mM sodium phosphate, 125 mM NaCl, pH 7.5 at room temperature.	68
Figure 18. Near-UV-CD Spectra of HEL, PEG1-HEL, and PEG2-HEL. Experiments were conducted with 0.4 mg/mL HEL, PEG1-HEL, PEG2-HEL respectively in 25 mM sodium phosphate, 125 mM NaCl, pH 7.5 at room temperature.....	70
Figure 19. Fluorescence emission spectra of HEL, PEG1-HEL, and PEG2-HEL. Experiments were conducted with 0.4 mg/mL HEL, PEG1-HEL, & PEG2-HEL respectively in 25 mM sodium phosphate, 125 mM NaCl, pH 7.5 using an excitation wavelength of 295 nm.....	70

Figure 20. A plot between the natural log of the Stokes radii versus the molecular weights of the five PEG molecules for studying the solution behavior of PEG	77
Figure 21. $g^*(s^*)$ analysis of HEL, PEG1-HEL, PEG2-HEL, and PEG3-HEL. Sedimentation velocity experiments were conducted at 50,000 RPM and 20 °C in a Beckman XL-I analytical ultracentrifuge using absorbance optics.	77
Figure 22. Effect of concentration on the sedimentation coefficient of PEG1-HEL and PEG2-HEL. Sedimentation velocity experiments were conducted in 25 mM phosphate, 125 mM NaCl, pH 7.5 at 50,000 RPM and 20 °C in a Beckman XL-I analytical ultracentrifuge using absorbance optics.	81
Figure 23. Effect of concentration on the diffusion coefficient of PEG1-HEL and PEG2-HEL. Sedimentation velocity experiments were conducted in 25 mM phosphate, 125 mM NaCl, pH 7.5 at 50,000 RPM and 20 °C in a Beckman XL-I analytical ultracentrifuge using absorbance optics.	81
Figure 24. A plot between the natural log of the Stokes radii versus the natural log of the nominal molecular weights of the three PEG-HEL molecules	85
Figure 25. Panel a –A representative plot depicting the thermal unfolding of HEL in 40 mM glycine-HCl, pH 3.0 buffer. Experiments were conducted with 1 mg/mL HEL using a temperature ramp rate of 60 °C/hr. The unfolding was monitored spectrophotometrically at 301 nm. The residuals of the fit are presented as solid circles in panel b.	88
Figure 26. Panel a: Reversibility of the thermal unfolding of PEG3-HEL monitored spectrophotometrically at 301 nm. Experiment conducted with 0.3 mg/mL PEG3-HEL in 40 mM glycine, pH 3.0 buffer at a temperature ramping rate of 60°C/hr. The data gathered during the ramp-up cycle of the experiment are represented by closed circles, and data gathered during the ramp down cycle are represented by inverted triangles. The reversibility of thermal unfolding of PEG3-HEL was calculated to be 74 % based on the ratio of the $\Delta H_{\text{down}}/\Delta H_{\text{up}}$	90
Figure 27. Panel a: Thermogram depicting the thermal unfolding of HEL in the Cap-DSC. Experiment conducted with 1 mg/mL HEL in 40 mM glycine, pH 3.0 buffer using a temperature ramp rate of 220°C/hr. Panel b: Thermogram depicting the reversibility in the thermal unfolding of HEL. The % reversibility ($\Delta H_2/\Delta H_1$) was calculated to be 88.6 %.	92
Figure 28. Panel a: Thermogram depicting the thermal unfolding of HEL in the VP-DSC. Experiment conducted with 1 mg/mL HEL in 40 mM glycine, pH 3.0 buffer using a ramp rate of 60 °C/hr. Panel b: Thermogram depicting the reversibility in the thermal unfolding of HEL. The % reversibility was calculated to be 75 %.	93
Figure 29. Panel (a): A representative plot depicting the thermal unfolding of HEL in the presence of 30 % PEG 400 monitored spectrophotometrically at 301 nm (a). Experiment conducted with 1 mg/mL HEL in 40 mM glycine, pH 3.0 buffer in the	

presence of 30 % (w/v) PEG 400 at a temperature ramping rate of 60°C/hr. The experimental data are represented as open circles (○) while the fit to the experimental data is represented as a solid line (—). The residuals of the fit are presented as solid circles (●) in Panel (b).....	98
Figure 30. Panel a: A representative plot depicting the thermal Unfolding of HEL in the presence of 30 % PEG 20000 monitored spectrophotometrically at 301 nm. Experiment conducted with 1 mg/mL HEL in 40 mM glycine, pH 3.0 buffer in the presence of 30 % (w/v) PEG 20,000 at a temperature ramping rate of 60°C/hr. The experimental data are represented as open circles (○) while the fit to the experimental data is represented as a solid line (—). The residuals of the fit are presented as solid circles (●) in panel b.	99
Figure 31. Thermal unfolding of HEL in the Presence of 0, 10, 20 and 30 % (w/v) PEG 400. Experiments were conducted with 1 mg/mL HEL in 40 mM glycine, pH 3.0 buffer at temperature ramp rate of 60 ° C/hr.	100
Figure 32. Thermal Unfolding of Hen Egg Lysozyme in the Presence of 15% and 30 % (w/v) PEG 20 kD. Experiments were conducted with 1 mg/mL lysozyme in 40 mM glycine, pH 3.0 buffer in the presence of 0, 15 % and 30 % (w/v) PEG 20 kD respectively at a temperature ramp rate of 60 ° C/hr.....	100
Figure 33. The Effect of high concentrations of PEG 400 and PEG 20 kD on the melting temperature of HEL. Experiments were conducted with 1 mg/mL Lysozyme in 40 mM glycine, pH 3.0 buffer in the Presence of 0, 15 & 30 % (w/v) PEG 400, and 15 % & 30 % (w/v) PEG 20kD respectively at a temperature ramp rate of 60 ° C/hr.	102
Figure 34. Panel a: A representative plot depicting the thermal unfolding of PEG2-HEL monitored spectrophotometrically at 301 nm. Experiment conducted with 0.5 mg/mL PEG2-HEL in 40 mM glycine, pH 3.0 buffer at a temperature ramping rate of 60°C/hr. The experimental data are represented as open circles (○) while the fit to the experimental data is represented as a solid line (—). The residuals of the fit are presented as solid circles (●) in panel b.	105
Figure 35. Panel a: Thermogram depicting the thermal unfolding of PEG1-HEL monitored calorimetrically in the VP-Cap-DSC. Experiment conducted with 1 mg/mL HEL in 40 mM glycine, pH 3.0 buffer at a temperature ramping rate of 220°C/hr. The experimental data are represented as open circles (○) while the fit to the experimental data is represented as a solid line (—).....	107
Figure 36. Panel a: Thermogram depicting the thermal unfolding of PEG1-HEL monitored calorimetrically in the VP-DSC. Experiment conducted with 1 mg/mL HEL in 40 mM glycine, pH 3.0 buffer at a temperature ramping rate of 60 °C/hr. The experimental data are in open circles (○), while the fit to the experimental data is represented by the solid line (—).....	107

Figure 37. Comparison of the thermal unfolding of HEL, PEG1-HEL, PEG2-HEL & PEG3-HEL. Experiments conducted in a 40 mM glycine, pH 3.0 buffer Thermal unfolding monitored via the Difference Spectrum method using a ramp rate of 60 °C/hr.....	108
Figure 38. Comparison of the thermal unfolding of HEL, PEG1-HEL and PEG2-HEL. Experiments conducted with 1 mg/mL HEL, 1 mg/mL PEG1-HEL, and 0.8 mg/mL PEG2-HEL respectively in 40 mM glycine, pH 3.0 buffer in a Cap-VP-DSC at a temperature scan rate of 220 °C/hr.....	108
Figure 39. Comparison of the thermal unfolding of HEL, PEG1-HEL and PEG2-HEL. Experiments conducted with 1 mg/mL HEL, 1 mg/mL PEG1-HEL, and 0.4 mg/mL PEG2-HEL respectively in 40 mM glycine, pH 3.0 buffer in a VP-DSC at a temperature scan rate of 60 °C/hr.....	109
Figure 40. Comparison between the effects of free PEG 20 kD and of PEGylation with PEG 20kD on the melting temperature (T_m) of HEL. Experiments were conducted in 40 mM glycine, pH 3.0 buffer at a temperature ramp rate of 60 °C/hr. The thermal unfolding was spectrophotometrically monitored at 301 nm.	109
Figure 41. The Effect of PEGylation on the melting temperature (T_m) of HEL. Experiments were conducted with HEL, PEG1-HEL, PEG2-HEL, and PEG3-HEL in 40 mM glycine, pH 3.0 buffer at a temperature ramp rate of 60 °C/hr. The thermal unfolding was monitored spectrophotometrically at 301 nm.	110
Figure 42. A representative plot depicting the aggregation of HEL monitored turbidimetrically at 320 nm. Experiment conducted with 1 mg/mL HEL in a 25 mM sodium phosphate, 125 mM NaCl, pH 7.5 buffer at 75 °C.....	115
Figure 43. A plot depicting the variation in the turbidimetric assay for monitoring the heat induced aggregation of HEL. Experiments conducted with freshly prepared 1 mg/mL HEL solutions in a 25 mM sodium phosphate, 125 mM NaCl, pH 7.5 buffer on four different days (I-IV). The aggregation reaction was monitored turbidimetrically at 320 nm at 75 °C.....	115
Figure 44. A plot depicting the effect of 4% PEG 20 kD on the heat induced aggregation of HEL: Set I. The aggregation reaction was monitored turbidimetrically at 320 nm at 75 °C.	116
Figure 45. A plot depicting the effect of 4% PEG 20 kD on the heat induced aggregation of HEL: Set II. The aggregation reaction was monitored turbidimetrically at 320 nm at 75 °C.	116
Figure 46. A plot depicting the effect of 4% (w/v) PEG 20 kD on the heat induced aggregation of HEL: Set III. The aggregation reaction was monitored turbidimetrically at 320 nm at 75 °C.....	118

- Figure 47. A plot depicting the aggregation of PEG1-HEL monitored turbidimetrically at 320 nm. Experiments (n = 4) conducted with 1 mg/mL PEG1-HEL in a 25 mM sodium phosphate, 125 mM NaCl, pH 7.5 buffer at 75 °C..... 118
- Figure 48. A plot depicting the aggregation of PEG2-HEL monitored turbidimetrically at 320 nm. Experiments (n = 3) conducted with 1 mg/mL PEG2-HEL in a 25 mM sodium phosphate, 125 mM NaCl, pH 7.5 buffer at 75 °C..... 119
- Figure 49. A plot depicting the effect of PEGylation on the heat induced aggregation of HEL. Experiments conducted with 1 mg/mL HEL, 1 mg/mL HEL + 4 % PEG 20 kD, 1 mg/mL PEG1-HEL, and 1 mg/mL PEG2-HEL respectively in a 25 mM sodium phosphate, 125 mM NaCl, pH 7.5 buffer. The aggregation reaction was monitored turbidimetrically at 320 nm at 75 °C..... 119
- Figure 50. Non-reducing SDS-PAGE analysis of PEG1-HEL and PEG2-HEL post turbidimetric aggregation assay (incubation at 75 °C for 25 minutes). Panel (a): Gel stained with the Coomassie Blue Stain. The PEG1-HEL, and PEG2-HEL controls (prior to heat treatment) are in lanes 1 and 5 respectively, while the heat treated PEG1-HEL & PEG2-HEL samples (n =3) are in lanes 2-4, and 6-8 respectively. Panel (b): Gel stained with a barium iodide stain, specific for PEG. The PEG1-HEL, and PEG2-HEL controls (prior to heat treatment) are in lanes 4 and 8 respectively, while the heat treated PEG1-HEL & PEG2-HEL samples (n = 3) are in lanes 1-3, and 5-7 respectively. 121
- Figure 51. Reducing SDS-PAGE analysis of PEG1-HEL and PEG2-HEL post turbidimetric aggregation assay. Panel (a): 12% gel stained with the Coomassie Blue Stain. The PEG1-HEL, and PEG2-HEL controls (prior to heat treatment) are in lanes 1 and 5 respectively, while the heat treated PEG1-HEL & PEG2-HEL samples (n =3) are in lanes 2-4, and 6-8 respectively. Panel (b): 4 –15% gel stained with a barium iodide stain, specific for PEG. The PEG1-HEL, and PEG2-HEL controls (prior to heat treatment) are in lanes 4 and 8 respectively, while the heat treated PEG1-HEL & PEG2-HEL samples (n =3) are in lanes 1-3, and 5-7 respectively.. 121
- Figure 52. Comparison of the rates of heat induced aggregation in HEL, PEG1-HEL and PEG2-HEL. Experiments were conducted with 0.9 mg/mL HEL, PEG1-HEL and PEG2-HEL respectively in a 25 mM sodium phosphate, 125 mM NaCl, pH 7.5 buffer. The aggregation reaction was conducted 75 °C for 25-30 minutes (s indicated below). Samples were analyzed using SE-HPLC in terms of % monomer remaining post reaction. 124
- Figure 53. Visualization of the heat induced aggregation of HEL, PEG1-HEL and PEG2-HEL. Vials containing PBS (25 mM sodium phosphate, 125 mM NaCl, pH 7.5), and 0.9 mg/mL HEL, PEG1-HEL & PEG2-HEL in PBS were incubated at 75 °C for 25 minutes, and then digitally photographed. 124

LIST OF SYMBOLS

ΔC_p	Heat capacity change during unfolding (kcal/mol-°C)
D	Diffusion coefficient (cm ² /sec)
D ^o	Diffusion coefficient at infinite dilution (cm ² /sec)
dn/dc	Refractive index increment
ΔG_{unf}	Gibbs free energy of unfolding (kcal/mol)
ΔH_{cal}	Calorimetric enthalpy of unfolding (kcal/mol)
ΔH_v	Van't-Hoff's enthalpy (kcal/mol)
ΔH_m	Enthalpy of unfolding estimated from the difference spectrum method (kcal/mol)
LS ₉₀	90 ° light scattering signal
λ_{max}	wavelength of maximum fluorescence intensity
MW	Molecular weight (Daltons or kilo-daltons)
M _w	weight average molecular weight (Daltons or kilo-Daltons)
M _n	Number average molecular weight (Daltons or kilo-Daltons)
η	solvent viscosity (poise)
N _a	Avogadro's number
ρ	solvent density (g/mL)
R _h	Stokes radius (Å or nm)
R	Universal gas constant
RI	Refractive index signal

s	Sedimentation coefficient
s°	Sedimentation coefficient at infinite dilution
T	Temperature ($^\circ\text{C}$ or K)
T_m	Melting temperature of unfolding ($^\circ\text{C}$)
\bar{v}	Partial specific volume (mL/g)

ABSTRACT

HYDRODYNAMIC BEHAVIOR AND THERMAL STABILITY OF A PEGYLATED PROTEIN: STUDIES WITH HEN EGG LYSOZYME

By

Yatin R. Gokarn

University of New Hampshire, December, 2003

We studied the effect of covalent attachment of polyethylene glycol (PEGylation) on the hydrodynamic behavior and thermal stability of a model protein - Hen Egg Lysozyme (HEL). HEL was modified with a linear, 20-kD, PEG to produce mono (PEG1-HEL), di (PEG2-HEL), and triPEGylated (PEG3-HEL) species.

The hydrodynamic properties of HEL were altered upon PEGylation. A decrease in sedimentation (s) and diffusion (D) coefficients was observed for all three PEG-HEL molecules in comparison to HEL (1.81 s). Despite differences in molecular weights of the PEG-HEL molecules ($\sim 34, 55$ and 80 kD), their s values were very close (1.0–1.1 s). Significant hydrodynamic non-ideality was observed for the PEG-HEL molecules, however, their Stokes radii (R_h) calculated from D^{01} values were in agreement with dynamic light scattering (DLS) measurements. The R_h of HEL increased dramatically from 20 \AA to $\sim 50 \text{ \AA}$ upon modification with a single 20-kD PEG chain. PEG2-HEL and PEG3-HEL had even larger radii of $\sim 68 \text{ \AA}$ and 74 \AA . DLS studies with various PEGs

¹ D^0 – Diffusion coefficient value extrapolated to infinite dilution

(MW 5000 – 40,000) indicated that PEG is a random coil in solution. The R_h of PEG1-HEL and PEG2-HEL were measured to be only ~ 10 % larger than the 20-kD (43 Å) and 40-kD (60 Å) PEG chains. These data suggest that the covalently tethered PEG(s) predominantly govern the solution conformation of the PEG-HEL molecules.

The thermal stability of PEGylated HEL was evaluated by employing the Eyring-Lumry model ($N \xrightleftharpoons{T_m} D \xrightarrow{k_a} A$)² for protein aggregation. A decrease in the melting temperature (T_m) of HEL unfolding was observed with increasing degree of PEGylation, which is indicative of thermodynamic instability. A T_m drop of up to 2.5 °C (DSC) and 4.0 °C (Difference Spectrum method) was observed for the PEG-HEL molecules. In contrast, turbidimetric studies showed that the kinetic aggregation rate (k_a) of the PEG-HEL molecules was dramatically lower in comparison to the native HEL. Size exclusion HPLC indicated that the extent of aggregation decreased with increasing degree of PEGylation; only 34 % of the HEL monomer remained after incubation at 75°C for 30 minutes, while 68 % and 79 % of the PEG1-HEL and PEG2-HEL monomers were present. These data suggest that the thermal stability of PEGylated HEL is kinetically controlled. The T_m may not be a true indicator of the stability of a PEG-protein with respect to aggregation.

² N – native state, D – denatured state, A – aggregate

Chapter 1

INTRODUCTION

Beginning in the 1970s, the polymer polyethylene glycol or PEG has continually found widespread applications in the field of biotechnology. A key property of PEG is that when attached to molecules or surfaces, it provides a biocompatible, protective coating. PEG is non-toxic, non-immunogenic, and is approved by the FDA for internal and topical use in humans [1]. In the pharmaceutical industry there is tremendous interest in the covalent attachment of PEG chains to drugs, a technique known as PEGylation. Although PEGylation is possible with small molecules, peptides & proteins, to date its advantages have been realized mainly in the area of protein PEGylation. This is particularly true for protein-drugs that exhibit poor pharmacokinetic, safety, solubility or stability profiles. In such cases, PEGylation offers several distinct benefits:

- 1) PEGylation greatly reduces the renal clearance of proteins that would otherwise be eliminated via this mechanism. This is because the covalently linked PEG chain(s) dramatically increase molecular size, which enables these molecules to avoid glomerular filtration. As a result, PEG-proteins are observed to have significantly longer in-vivo half-lives providing for a sustained duration effect [2].
- 2) PEGylation has been demonstrated to reduce the toxic or neutralizing immunogenic/antigenic responses elicited by certain therapeutic proteins. In cases

where toxicity has been observed, PEGylation has enabled the development of safer drugs (or candidates) [9]. And when neutralizing immunogenic or antigenic responses have posed efficacy issues, PEGylated proteins have been shown to exhibit much longer efficacious half-lives leading to a sustained duration effect [3]. These effects of PEGylation have been attributed to the extensive hydration of PEG and to the steric hindrance offered by the polymer. Both factors are believed to help mask the response eliciting residues on a protein surface from immunogenic and antigenic recognition.

- 3) PEG is amphipathic in nature; using PEGylation, its hydrophilic property has been exploited to enhance the aqueous solubility of poorly soluble proteins³. This has led to improved bioavailability for certain protein-drugs [4].
- 4) PEGylated proteins have been reported to possess superior stability in comparison to their unmodified counterparts [10]. PEG-proteins are also believed to exhibit superior *in-vivo* stability with respect to proteolytic cleavage. This effect, which contributes to extending their plasma half-lives, is attributed to the steric hindrance offered by the PEG.

The advantages discussed above have led to the successful development of several PEGylated protein drugs that are FDA approved (Table 1) with more candidates in early and late stage development (Table 2).

The real impact of PEGylated protein therapeutics to patients' health and their quality of life can be illustrated with the help of four such drugs. In the early 1990s, Amgen (Thousand Oaks, CA) developed a novel protein - recombinant human methionyl

³ The hydrophobic properties of PEG also have been exploited to solubilize proteins in non-aqueous solvents in the field of non-aqueous enzymology [5]

Granulocyte Colony Stimulating Factor (rh-met-G-CSF) called NEUPOGEN® for the treatment of neutropenia resulting from myelosuppressive chemotherapy in cancer patients. The drug was successful in rapidly restoring neutrophil counts in patients post chemotherapy and consequently helping to minimize infection related complications. However, the dosing regimen of NEUPOGEN® requires a daily administration of the drug for a period of up to 2 weeks post each chemotherapy cycle [7]. In 2001 Amgen introduced NEULASTA®, a PEGylated form of rh-met-G-CSF which has facilitated a substantial improvement in the dosing regimen. With NEULASTA®, only a single injection is required per chemotherapy cycle in comparison to the potential fourteen that would be required with NEUPOGEN® [6, 7].

Table 1: FDA approved PEGylated protein drugs

Product	Company
ADAGEN®	Enzon, NJ
NEULASTA®	Amgen, CA
ONCASPAR®	Enzon, NJ
PEGasys®	Hoffman LaRoche, Switzerland
PEG-INTRON®	Schering Plough, NJ
Somavert®	Pfizer, NY

Table 2: PEGylated protein drug candidates in development

Product	Company	Stage
CDP-870	Pfizer, NY	Phase III
PEG-AXOKINE®	Wyeth, NJ	
CDP-860	Celltech, UK	Phase II
PEG-sTNF-R1	Amgen, CA	
PEG-Interferon-b-1a	Regeneron, CA	Phase I

Interferon alpha 2a, (IFN- α -2a) and Interferon alpha 2b (IFN- α -2b) have been demonstrated to be effective therapeutic agents for the treatment of Chronic Hepatitis C (CHC). However, both agents suffer from the drawback of a serum half-life of only 7-9

hours [8], which necessitates a thrice weekly, subcutaneous dose of either drug over a one-year treatment period. The PEGylated forms of these molecules - PEG-INTRON® (PEG-IFN- α -2b: Schering Plough, NJ) and PEGasys® (PEG-IFN- α -2a: Hoffman LaRoche, Switzerland) have been demonstrated to be equally effective and have facilitated a dramatic reduction in dosing frequency. Both PEG-INTRON® and PEGasys® require only a once weekly subcutaneous injection through the 1-year treatment period. This translates into 100 fewer injections per patient over one year of treatment!

The drug pegaspargase or ONCASPAR® (Enzon, NJ) is a PEGylated form of L-asparaginase developed for the treatment of acute lymphocytic leukemia. Two limiting factors to the unmodified L-asparaginase treatment are: (i) it has a short half-life due to a neutralizing immune response, and (ii) a sub-population of patients develops severe hypersensitivity to the drug. It has been demonstrated that ONCASPAR® elicits a dramatically reduced immune response and consequently has a longer in-vivo half-life. Further, most of the patients with hypersensitivity to the native asparaginase preparations tolerate pegaspargase without further clinical hypersensitivity [9].

1.1 Dissertation Objectives

The continued interest in PEGylated proteins for pharmaceutical use warrants an even greater need for an in-depth understanding of the molecular mechanisms in which PEGylation affects the physicochemical and pharmacokinetic properties of proteins. Although reports on PEG-proteins often state that PEG modification results in improved thermal stability of proteins [10, 11], there appears to be no clear mechanistic understanding of the phenomenon in reported literature. Also, PEGylated proteins are

believed to have prolonged half-lives due to reduced renal filtration. Again, there are few studies in literature that correlate their reduced renal clearance to molecular size, charge and shape; properties which have been shown to be the molecular determinants of the kidney filtration process [12].

The research presented herein had two objectives:

- 1) Gain mechanistic insights into the thermal stability of a PEGylated protein
- 2) Understand the hydrodynamic behavior of PEG and PEGylated proteins

Both aspects were researched using Hen Egg Lysozyme (HEL) as a model protein for reasons discussed later. Studies were designed not only to enhance our biophysical understanding of the two phenomena, but also to draw conclusions that would help towards a more rational molecular design of PEGylated proteins.

1.2 Thermal Stability of PEGylated Proteins

An increasing number of protein drugs entering the marketplace have led to an intense study of their stability in various product dosage forms. Such study has been critical to ensure quality and safety of the product over its entire shelf life. As with any drug, even small amounts of chemical degradation and physical instability can cause undesired, toxic reactions in patients. A protein therapeutic bears the added risk of inducing immunogenic and antigenic responses targeted directly towards it or its physical/chemical degradants. Thus, it is even more critical that the chemical, and conformational structure of a protein drug be preserved through its shelf life for quality and safety purposes.

Physical instability in protein formulations is a result of irreversible aggregation of the protein. Aggregation can be induced by thermal stress, agitation and/or by surface

effects at an interface (air-liquid, or liquid-container wall). These irreversible aggregates can be soluble and in extreme cases can also precipitate out of solution. Importantly, the result of aggregation is that the protein is often left with very little or with no therapeutic activity. Moreover, the aggregates can trigger an undesired immunological response in a patient.

The classical Eyring Lumry Model [13] has been successfully applied to explain the protein aggregation phenomenon. The model is represented by the following reaction scheme:



where N is the native form of the protein, D its denatured or unfolded form, and A represents the irreversible aggregate. T_m is the melting temperature governing the equilibrium between the native and denatured states, and k_a is the aggregation rate constant.

From the above scheme, it follows that protein denaturation or unfolding is a prerequisite for aggregation, and that the aggregation reaction proceeds only via the denatured form of the protein. One should bear in mind that there are more complex models reported in literature where it has been shown that aggregation can also proceed via a partially denatured or unfolded form [14]. However, these models can be considered as extensions of the fundamental proposal that protein unfolding - partial or complete is a pre-condition for protein aggregation, and this follows from the Eyring-Lumry model. The physical basis for the model is discussed below.

A protein assumes its three-dimensional tertiary structure such that the polar, hydrophilic residues of its polypeptide chain are on the surface exposed to the polar

aqueous environment, while its non-polar hydrophobic residues are buried in the interior, shielded from exposure to water. When the native or folded conformation of a protein is perturbed by various stresses (thermal, shear or interfacial) to cause unfolding, its hydrophobic residues are exposed to water, resulting in a thermodynamically unfavorable state. To minimize their exposure, a protein molecule can refold or, alternatively, reduce its hydrophobic surface area by associating with other unfolded molecules via hydrophobic interactions. These hydrophobic interactions are usually irreversible in nature and lead to aggregation.

Thermodynamically, the free energy of unfolding (ΔG_{unf}) is the true indicator of protein stability. However, the equilibrium between N and D in reaction scheme I is often studied in terms of the transition melting temperature or T_m . The T_m is the temperature at which half the protein is in its native conformation while the other half is unfolded or denatured. Although there is no defined relationship between T_m and the free energy of unfolding, it is generally accepted that any increase in T_m should lead to an increase in protein stability [15]. Importantly, an increase in T_m has been correlated to improved real time stability of proteins [16]. If T_m is mid-point of the $N \rightarrow D$ transition, the equilibrium governing this transition should increasingly favor the native state (N) when the storage temperature (T) of a protein becomes progressively lower than the T_m . Conversely, it would follow that if the solution conditions may be so manipulated such that the T_m of the protein is increased, then the N form of the protein will be more favored under these solution conditions at the storage temperature, T [17].

Changing solution conditions such as pH or the addition of excipients (additives) can modulate the T_m of a protein [16]. Sugars, polyols, amino acids & certain salts are known to increase the T_m of proteins, which is postulated to occur via the mechanism of preferential exclusion [18, 19]. Briefly, at sufficiently high concentrations, certain excipients are preferentially excluded or repelled from the protein surface. Because the denatured form (D) of the protein has a larger surface area as compared to its native (N) form, the exclusion of these molecules from a larger surface area (D form) becomes thermodynamically unfavorable. Hence, in an attempt to minimize the surface area of exposure, the equilibrium between the N and D forms shifts towards the more compact native, N conformation in the presence of these excipients (Figure 1). This leads to an increase in T_m , and to a consequent stabilization of the protein.

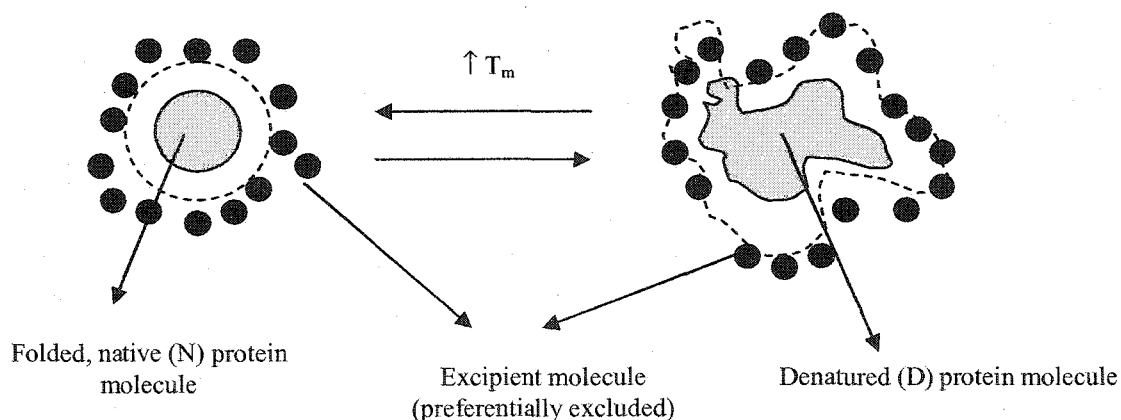


Figure 1: Schematic of the preferential exclusion mechanism. Preferential exclusion of certain excipients from the protein surface leads to an increase in the melting temperature (T_m) of the protein.

The latter half of the aggregation reaction scheme I, which proceeds primarily through the denatured form is governed by a kinetic aggregation rate constant (k_a). As with T_m , one can also modulate k_a by altering solution conditions [20]. Thus, there are

two components to the thermal stability of a protein with respect to aggregation; (i) a thermodynamic component which is controlled by the equilibrium between the native and denatured form of a protein, and (ii) a kinetic component controlled by an aggregation rate constant (k_a) and the concentration of the unfolded or denatured protein D .

In designing and optimizing protein formulations, researchers often perform screening experiments aimed at maximizing the T_m of the protein in the hope of stabilizing it. However, it is important to understand the mechanistic effects of excipients employed for stabilization. While sugars, polyols and amino acids are thermodynamic stabilizers that work by increasing the T_m of the protein, excipients such as polysorbates appear to be kinetic stabilizers that affect the aggregation rate constant. For example, in a study by Bam *et al.* [21], the researchers observed that although polysorbate 20 caused a decrease in the T_m of human Growth Hormone (hGH), the excipient greatly reduced agitation-induced aggregation in liquid hGH formulations. Therefore, in the presence of polysorbate 20 the aggregation of hGH appears to be kinetically controlled.

Although it is reported that PEGylation reduces protein aggregation, studies in literature provide no mechanistic insights into this observed effect. In studies with insulin and lipase, PEGylation has been observed to greatly reduce their aggregation rate in solution [10, 22]. In a study with PEGylated Brain Derived Neurotrophic Factor (PEG-BDNF), Callahan *et al.* conclude PEGylation has no effect on the thermal stability of the protein. They base their conclusion upon observing no change in the onset temperature of melting [24]. However, they do not comment on the effect of PEGylation on the aggregation of BDNF. In the case of PEG-G-CSF, it was observed that the physical instability or aggregation depended on the type of PEG used for conjugation [25].

Although the authors compare two types of PEG-G-CSF conjugates with respect to aggregation, they do not comment on the aggregation rate of either of the two conjugates in comparison to the unmodified G-CSF. The most interesting results are those with PEGylated Hen Egg Lysozyme (HEL), the model protein employed in the present research. Nodake *et al.* report an increase in thermal stability of PEGylated Lysozyme based on the residual activity of HEL or PEG-HEL after a 30-minute heat treatment at 98 °C [26] In contrast, So *et al.* [27] in their study conclude PEGylated HEL to be less stable than the unmodified HEL, based on denaturation experiments conducted with the chaotropic agent, guanidinium hydrochloride. Based on these studies, it is difficult to form a generalized, mechanistic understanding of the effect of PEGylation on the thermal stability and aggregation of proteins.

Given the interest in PEGylated protein therapeutics, it is critical that the effect of PEGylation on the stability of proteins be studied systematically. The questions that need to be addressed are - is the thermal stability of a PEG-protein thermodynamically controlled or is it kinetically controlled, or are both factors important? An even more important question is – can a PEG-protein be thermodynamically less stable, and yet possess superior stability with respect to aggregation? The basis for this question stems from the work of Lee *et al.* on the “Thermal Stability of Proteins in the Presence of Polyethylene Glycol” [28].

In their paper, Lee and co-workers studied the effect of highly concentrated PEG (MW: 400 – 4000) solutions on the thermal stability of four different proteins: β -Lactoglobulin (BLG), Hen Egg Lysozyme (HEL), Chymotrypsinogen (CTG), and Ribonuclease A (RNase). Consistent with previously reported results by Timmasheff *et*

al. [29], the researchers demonstrated that PEG was preferentially excluded from the protein surface. However they observed that in the presence of PEG, the T_m for three of the four proteins - BLG, HEL, and CTG decreased with increasing PEG concentration (10 – 30 %), while no change in the T_m of RNase was observed. To explain this, the authors conducted interaction parameter measurements between PEG and the unfolded forms of the proteins. Through these experiments, they demonstrated that the amphipathic PEG interacted with, and stabilized the unfolded form of the protein, which led to the decrease in T_m (Figure 2).

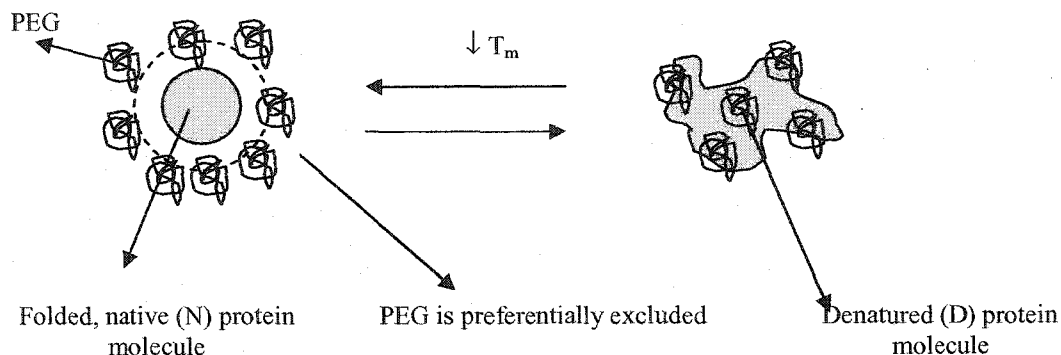


Figure 2: Preferential Exclusion and PEG. Although PEG is preferentially excluded, it can interact with the exposed hydrophobic patches and stabilize the D form, which leads to a decrease in T_m

Lee *et al.* [28] postulated that the magnitude of the drop in T_m depended on the intrinsic hydrophobicity of the protein i.e. the largest decrease in T_m was for the most hydrophobic protein –BLG followed by CTG, and HEL with the least change being observed for the relatively hydrophilic RNase.

A similar behavior should be observed in the case of PEGylated proteins. The covalently attached PEG in the immediate microenvironment of the protein will be available to interact with its hydrophobic interior upon unfolding, and consequently stabilize the denatured form. In terms of reaction scheme I, this should cause the

equilibrium between N and D to shift towards the D form resulting in a decrease in T_m . The magnitude of the decrease may be proportional to the PEG chain length, the degree of PEGylation, and on the intrinsic hydrophobicity of a protein. In effect, PEGylation would give rise to a very high local concentration of PEG in the vicinity of the protein, available to interact with and stabilize the hydrophobic core when exposed.

It is this author's hypothesis that although PEGylation may cause a decrease in T_m , the kinetic aggregation rate for a PEGylated protein will be significantly lower than its unmodified counterpart. As discussed earlier, the aggregation reaction occurs in order to minimize the exposure of the hydrophobic surface area of the unfolded protein to water. However, in the case of a PEGylated protein, the PEG will patch the exposed hydrophobic surface area upon protein unfolding, and inhibit protein-protein, hydrophobic interactions. Further the PEG chain(s) will present a significant steric hindrance to any protein-protein interactions. Both these effects would lead to a reduction in the number of productive collisions between two unfolded molecules to form aggregates and to a consequent lowering of the kinetic, aggregation rate constant. As depicted in reaction scheme II below, although a decrease in T_m may be observed for PEG-proteins implying thermodynamic instability, the aggregation rate constant will be dramatically lower leading to an increased stability with respect to aggregation. Overall, the aggregation of PEG-proteins will be kinetically controlled.



1.3 Hydrodynamic Behavior of PEGylated Proteins

A major advantage of protein PEGylation is that the resulting PEG-protein conjugates usually demonstrate prolonged in-vivo half-lives. This enhancement in residence time is attributed to (i) reduced in renal clearance (ii) decreased immunogenicity & antigenicity, and (iii) reduced proteolytic cleavage. In the absence of any immunogenic or antigenic issues with the unmodified protein, PEGylation is mainly employed to reduce the kidney filtration of smaller proteins, which would otherwise be cleared by this mechanism.

The renal clearance of a molecule depends upon its molecular size, shape and charge [12]. It is well understood that while smaller molecules are rapidly filtered through the glomerulus, there is a marked restriction for the passage of molecules around the size of serum albumin (36 Å) or larger [30]. Molecular shape has also been shown to be an important determinant of glomerular filtration, wherein elongated molecules are cleared more rapidly than spherical molecules of similar size and charge. A striking example is that of bikunin, a 16 kD polypeptide with an 8 kD chondroitin sulfate chain, and a 1 kD N-linked oligosaccharide and has a molecular size and surface charge similar to that of albumin but exhibits much faster clearance [31]. The glomerular filter is also charge selective as the trans-glomerular passage of anionic proteins has been shown to be more restrictive in comparison to neutral or cationic molecules of equivalent size and shape [32]. PEGylation can have a dramatic effect on the size, shape & charge of a protein and hence its effect on these properties must be systematically studied.

To date, the design of most PEGylated proteins appears to be empirical rather than fundamental. In most cases, the clearance of a PEGylated protein has been

correlated to the molecular weight of serum albumin of 69 kD rather than its molecular size of 36 Å [33, 34, 35]. Katre and co-workers [36] have correlated the systemic clearance of various PEGylated interleukin-2 (IL2) molecules to an “effective” molecular weight. The IL-2 was PEGylated with a varying number of 5-7 kD PEG chains IL-2 per molecule. The effective molecular weight was calculated based on the SE-HPLC retention times of the different PEGylated IL-2 molecules and was used as a measure of molecular size. The researchers observed that the systemic clearance of PEG-IL2 sharply decreased at an effective molecular weight of 69 kD, around that of serum albumin. This appears to be consistent with the renal clearance of globular proteins. However, a limitation of this study is that IL-2 also induced a neutralizing immunogenic response, which was significantly reduced upon PEGylation. Further, it has been shown that increasing the degree of PEGylation can similarly reduce the immunogenicity and antigenicity of proteins [37]. Thus, in the case of PEG-IL2, the systemic clearance is likely to be a composite of a reduced immuno/antigenicity, proteolytic cleavage & kidney clearance, and not a sole indicator of renal filtration. This is even more evident from a study by Koumenis *et. al* on the pharmacokinetics of a therapeutic, PEGylated Fab-dimer [35]. The authors observed increasing residence times for PEG-Fab₂ species up to “effective” molecular weights of 1.6 –1.9 Million Daltons, which clearly exceed the presumed effective molecular weight cut-off of 65-70 kD. It is unlikely that renal filtration is the major clearance pathway for such large molecules.

The Stokes or the hydrodynamic radius (R_h) is a fundamental measure of molecular size and has been effectively employed to study the glomerular filtration of globular proteins and linear polymers [30, 32, 38]. For PEG-proteins it would be more

appropriate to correlate renal clearance to their Stokes Radii rather than to effective molecular weights. Some important questions that need to be addressed are - what is the size of PEG that should be employed for PEGylation that would provide an adequate barrier towards glomerular filtration? How does the degree of PEGylation affect the hydrodynamic behavior of a protein?

Generally, the activity of a protein is inversely related to the degree of PEGylation. However, increasing the degree of PEGylation may prolong the half-life of a protein by increasing its hydrodynamic radius. Although a PEG-protein may have muted in-vitro activity it can still exhibit a superior in-vivo efficacy due to its enhanced plasma half-life. Thus, it is important to understand how much the degree of PEGylation contributes to increasing the hydrodynamic volume of a protein.

Another important aspect that needs discussion is solution conformation of a PEG-protein. Important questions include - is the PEG wrapped around the protein molecule? Or is it more like a random coil hanging freely in solution with its one end tethered to the protein? These questions are central to understanding its beneficial effects with respect to reduced immunogenicity and antigenicity. It is believed that the non-immunogenic, and non-antigenic effects of PEG are a result of its high degree of hydration and due to the steric hindrance offered by the polymer. It has been proposed that the covalently attached polymer chains provide steric protection as the PEG-protein moves through the crowded milieu in-vivo, and prevent antibodies from approaching the protein for binding [39]. A study of the hydrodynamic behavior of PEG and PEG-proteins in solution would provide better insight into the solution conformation of PEGylated proteins.

The hydrodynamic behavior of PEG-proteins can be studied using Dynamic Light Scattering and Sedimentation Velocity techniques. Both techniques provide information regarding hydrodynamic radii, and shapes of molecules from physical first principles. Previous work by this author on the Biophysical Characterization of PEGylated proteins demonstrates that PEG-proteins exhibit an anomalous sedimentation behavior [40]. The sedimentation coefficient (s) is a fundamental property of a molecule that is related to its mass, frictional coefficient, partial specific volume, and the solvent density. In studies with PEGylated recombinant human deoxyribonuclease I (rhDNase), and PEGylated horseradish peroxidase (HRP), it was observed that the sedimentation coefficients for both PEGylated proteins decreased with respect to those of the unmodified rhDNase and HRP. This is anomalous because the sedimentation coefficient of proteins usually increases with increasing protein molecular weight. Furthermore, a sedimentation pattern consistent with a single homogenous species was observed for a heterogeneous mixture of either PEG-HRP or PEG-rhDNase containing mono, di and triPEGylated DNase or HRP species. With respect to the latter observation it was hypothesized that with an increasing degree of PEGylation, the increase in molecular mass was almost exactly compensated by an increase in the frictional coefficient and consequently the sedimentation coefficient remained unchanged. This hypothesis was tested wherein sedimentation studies were conducted with purified mono, di, and triPEGylated HEL to study the effect of PEGylation on the sedimentation coefficient of lysozyme.

In sum, the hydrodynamic characterization studies were aimed at understanding the following:

- 1) Hydrodynamic behavior of PEG and the solution conformation of PEG-proteins

- 2) Effect of degree of PEGylation on the hydrodynamic radius of a protein
- 3) Effect of degree of PEGylation on the sedimentation properties of a protein.

1.4 Hen Egg Lysozyme as a Model Protein

Hen Egg Lysozyme (HEL) is a small, 14.3 kD enzyme comprised of 129 amino acids. It catalyzes the hydrolysis of the 1→4 glycosidic linkages of oligosaccharides present in the peptidoglycan cell wall of gram-positive bacteria [41]. The amino acid sequence of HEL was first published by Canfield in 1963 [42] and it was the first enzyme to have its crystal structure determined by X-ray diffraction techniques [43]. Hen Egg Lysozyme is one of the best characterized proteins with extensive information available in literature on its structural, spectral and biophysical properties. The amino acid composition of HEL is presented in Table 3, while a summary of its key properties is presented in Table 4.

Table 3: Amino acid composition of Hen Egg Lysozyme

Amino Acid	Frequency	Amino acid	Frequency
Alanine	12	Methionine	2
Cysteine	8	Asparagine	14
Aspartic acid	7	Proline	2
Glutamic acid	2	Glutamine	3
Phenyl alanine	3	Arginine	11
Glycine	12	Serine	10
Histidine	1	Threonine	7
Isoleucine	6	Valine	6
Lysine	6	Tryptophan	6
Leucine	8	Tyrosine	3

Table 4: Properties of Hen Egg Lysozyme

Property	Value
Primary structure	129 amino acids, 4 disulfide bonds [42]
Sequence molecular weight	14305 [42]
Isoelectric point (pI)	~11 [46, 66]
Extinction coefficient (ϵ)	2.635 mg/(mL-cm) at 281.5 nm [28]
Size	Stokes radius = 19.3 Å [47]

Hen Egg Lysozyme has been employed as a model protein in a wide array of studies. It has been used to study the kinetics and thermodynamics of protein unfolding and refolding [44]. It was one of the first proteins to be studied by NMR in applying this technique for secondary structure determination [45]. In addition, HEL has been used extensively as model protein in the advancement of applied scientific techniques and processes such as lyophilization [48], microencapsulation [49], and PEGylation [50, 51].

To meet the objectives outlined in the present research, HEL was an appropriate model protein given its small hydrodynamic radius of ~ 20 Å [47]. A therapeutic protein the size of HEL would be an ideal candidate for PEGylation. Further, it was particularly well suited to be utilized in the thermal stability studies, as it was one of the four proteins employed by Lee *et al* [28] in their investigation of the thermal stability of proteins in the presence of polyethylene glycol. This would allow one to study the effects of the covalently attached PEG on the thermal stability of HEL, and compare its effect on the thermal stability of the protein when present in high concentration as a solute. Further, the vast amount of characterization, and thermodynamic data available for HEL could be harnessed in conducting a comparative analysis while studying the effect of PEGylation on the structural, and thermodynamic unfolding properties of HEL.

Chapter 2

EXPERIMENTAL

2.1 Research Design

To meet the research objectives outlined in the previous chapter (Section 1.1), studies were designed, and conducted in three phases as described below:

1) Synthesis and characterization of PEG-HEL molecules

A linear, 20-kD PEG polymer was employed to PEGylate HEL. The synthesis and purification procedure is described later in this chapter (Section 2.2). Several different techniques were employed to examine the effect of PEGylation on the structural and solution properties of HEL. These are summarized below in Table 5.

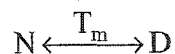
Table 5: Techniques employed to characterize PEG-HEL molecules

Effect/Property Studied	Technique(s)
Proof of modification & species purity	SDS-PAGE, MALDI-TOF
Molecular Weight	MALDI-TOF, Static Light Scattering, Sedimentation Velocity
Effect on secondary structure	Far-UV-CD
Effect of tertiary structure	Near-UV-CD, Fluorescence
Partial specific volume of PEG ⁴	Precision densitometry
Hydrodynamic behavior	Sedimentation Velocity, Dynamic Light scattering

⁴ The partial specific volume of PEG was measured to enable the sedimentation analysis of PEG-HEL.

2) Thermodynamic Denaturation or Unfolding Studies

The equilibrium between the native HEL or PEG-HEL and their respective denatured forms was studied in this phase.



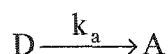
Two experimental techniques were employed to study this: (i) an optical, Difference Spectrum (DS) method and (ii) Differential Scanning Calorimetry (DSC). Experimental conditions were optimized to ensure reversibility of the unfolding reaction, which allowed for the estimation of thermodynamic parameters. The effects of high concentrations of PEG and of PEGylation on the melting or transition temperature of HEL were studied as outlined below in Table 6.

Table 6: Techniques employed to study the thermal denaturation of HEL and PEG-HEL

Effect Studied	Technique(s)
Thermal denaturation of HEL	DS Method & DSC
Effect of high concentration of PEG 400 (0 - 30 %) on the thermal denaturation of HEL	DS Method
Effect of high concentration of PEG 20 kD (0 - 30 %) on the thermal denaturation of HEL	DS Method
Effect of PEGylation on the thermal denaturation of HEL	DS Method & DSC

3) Kinetic Aggregation Experiments

Aggregation studies were conducted to study the latter half of reaction scheme I, wherein the aggregation reaction is controlled by the kinetic rate constant (k_a).



Experimental conditions were optimized to ensure that at least a substantial amount of the protein would be in its denatured form, D. A turbidimetric method was

developed to study the effect of free PEG and of PEGylation on the aggregation rate of HEL. The aggregation of HEL and of the various PEGylated HEL molecules also was studied using Size Exclusion HPLC (SE-HPLC) and digital photography. These experiments are summarized below in Table 7.

Table 7: Techniques employed to study the aggregation rate of HEL and PEG-HEL

Effect Studied	Technique(s)
Aggregation of HEL	Turbidimetry
Effect of ~ 30 fold molar excess of free PEG 20 kD on the aggregation rate of HEL	Turbidimetry
Effect of PEGylation on the aggregation rate of HEL	Turbidimetry, SE-HPLC, Digital photography

2.2 Synthesis and Purification of PEGylated Hen Egg Lysozyme

Hen Egg Lysozyme (HEL) was PEGylated by employing the reductive amination reaction between aldehydes and primary amines as described by Kinstler *et al.* [25]. Specifically, seven molar excess of methoxy-PEG-propionaldehyde, MW - 20 kD (Shearwater Polymers, Huntsville, AL 35801, Catalog # 052M0P01) was dissolved in 15 mL of a 10 mg/mL HEL (Sigma Chemical Co., MO., Cat # L-6876) solution prepared in 20 mM sodium acetate at pH 4.5. The reaction was conducted in the presence of 20 mM sodium cyanoborohydride (Sigma Chemical Company, MO) at 4 °C for 16 hours.

A Pharmacia FPLC® system was employed to purify the various PEGylated HEL molecules using Cation-Exchange chromatography. The reaction mixture was loaded on to a Pharmacia SP Sepharose®, HiLoad, 16/10 column, pre-equilibrated with a 20 mM sodium acetate, pH 4.0 buffer (Buffer A) at a flow rate of 1 mL/min. The column was washed with three column volumes (60 mL) of Buffer A prior to applying a linear gradient to 45 % Buffer B (Buffer A + 1 M NaCl) over 25 column volumes (500 mL).

The eluting solution (post column wash) was fractionated into 5 mL aliquots. Fractions with an A_{280} value > 0.1 were subjected to SDS-PAGE to determine the purity of each fraction with respect to monoPEGylated HEL (PEG1-HEL), diPEGylated HEL (PEG2-HEL), and triPEGylated HEL (PEG3-HEL).

Multiple fractions containing a particular PEGylated HEL species were pooled together, concentrated and de-salted into a 20 mM sodium acetate, pH 4.5 buffer using Ultrafree-15® centrifugal filters (Millipore Corporation, MA). The purified and concentrated PEG-HEL solutions were filtered through 0.22 micron, low protein binding syringe filters and transferred into 2 mL, Type I, glass vials. The vials were stoppered with 13 mm, Flurotec® coated, serum stoppers (Daikyo, Japan) and capped with aluminum flip-off overseals and stored at $-70\text{ }^{\circ}\text{C}$ until further use. The synthesis and purification process is represented pictorially in Figure 3.

2.3 Concentration Determination of HEL and PEGylated HEL molecules

The concentrations of HEL solutions were measured spectrophotometrically using a previously determined extinction coefficient of $2.635\text{ mL/mg}\cdot\text{cm}$ at 281 nm [28]. Importantly, the same extinction coefficient was used to determine the concentration of the three PEGylated HEL molecules. The rationale for this was that the absorbance peak maximum for all the three PEG-HEL molecules remained unchanged at 281 nm (Figure 4). In other words, the concentration of the PEGylated-HEL molecules was expressed in terms of the mg/mL of HEL. This allowed for appropriate comparative analysis of the effects of PEGylation on the hydrodynamic behavior and thermal stability of HEL.

Figure 3. Pictorial representation of the synthesis and purification of PEGylated HEL molecules

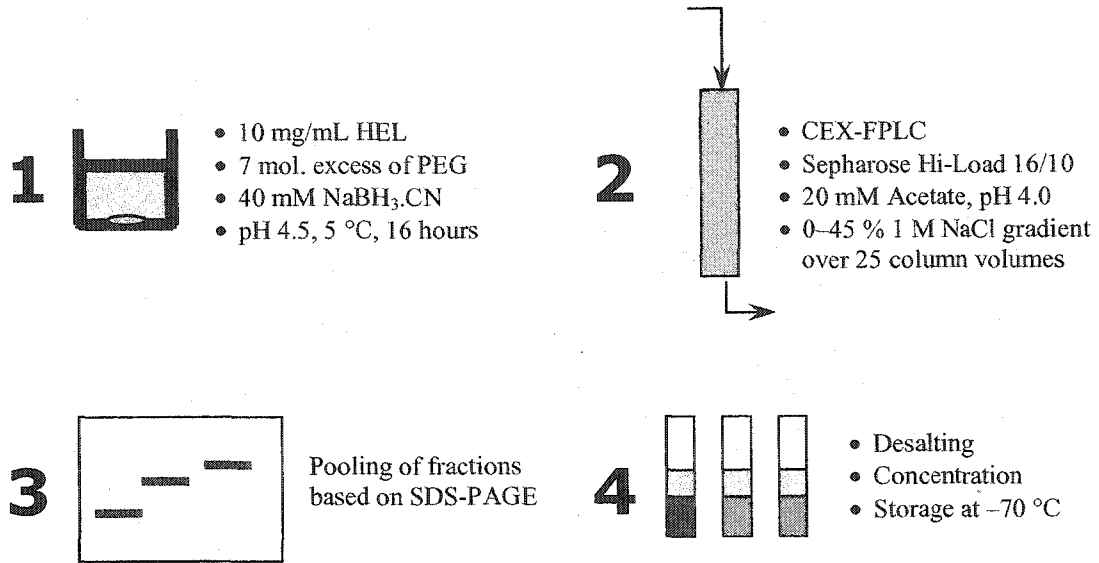
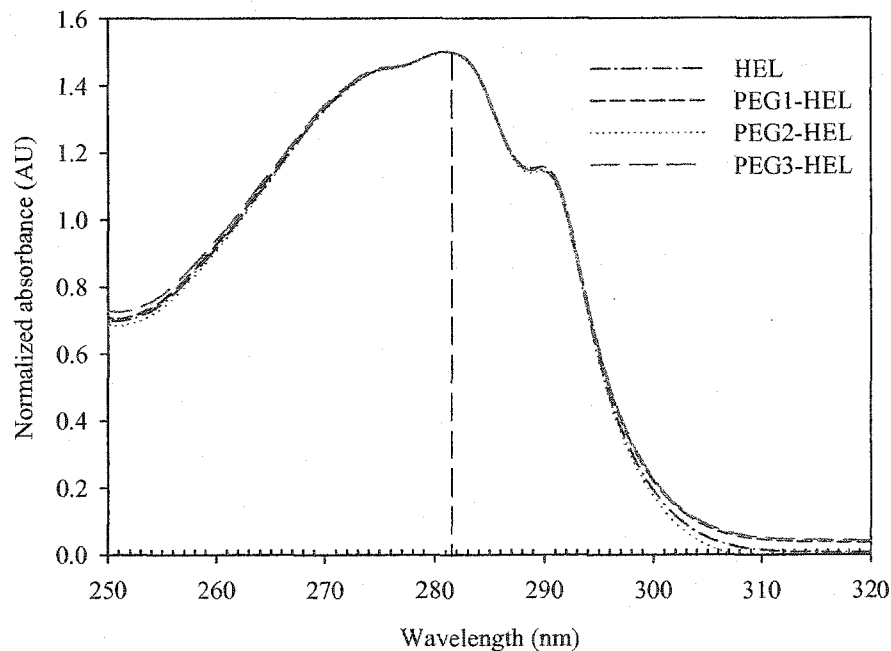


Figure 4. UV Spectra of HEL, PEG1-HEL, PEG2-HEL, and PEG3-HEL. Experiments conducted in 25 mM sodium phosphate, 125 mM NaCl, pH 7.5 at room. All spectra are normalized to an arbitrary absorbance value of 1.5 at 281 nm to facilitate comparison.



2.4 Sodium Dodecyl Sulfate-Polyacrylamide Gel Electrophoresis

Sodium Dodecyl Sulfate-Polyacrylamide Gel Electrophoresis or SDS-PAGE was conducted using the approach described by Laemmli [52]. Non-reducing and reducing SDS-PAGE experiments were conducted using either 12 % or 4-15 % pre-cast polyacrylamide, Tris-Glycine, Ready Gels® from Biorad (Hercules, CA). In non-reducing SDS-PAGE experiments, samples were prepared by mixing an equal volume of the test protein solution (~ 0.5 – 1 mg/mL) with a 2X sample treatment buffer containing 0.0625 M Tris, 10 % glycerol, 2 % SDS, and 0.05 % bromophenol blue (Biorad, CA). In reducing SDS-PAGE experiments, a 10X NuPAGE® sample reducing agent from Invitrogen (Carlsbad, CA) was added to the treated sample in a 1:10 ratio. Following this, in both cases, the treated samples were heated at 90 °C for 5 minutes.

After the heat treatment, samples were cooled to room temperature prior to conducting electrophoresis. All SDS-PAGE experiments were performed in a Mini-Protean II electrophoresis system (Biorad, Hercules, CA) connected to a Biorad Power Pac 1000 DC power supply at a constant voltage of 200 V. Post electrophoresis, the protein bands were visualized by using two types of stains: (i) Coomassie Blue stain - specific for the polypeptide chain, and (ii) a barium iodide (BaI_2) stain - specific for PEG [53].

The Colloidal Blue Staining Kit from Invitrogen, CA was used to stain gels with the Coomassie Blue Stain. Briefly, a staining solution was freshly prepared by mixing 110 mL of deionized water with 40 mL of methanol, 10 mL of a Stainer A and 40 mL of Stainer B solutions. The proprietary Stainer A and Stainer B solutions were provided as

part of the Colloidal Blue Staining Kit. Gels were soaked in the staining solution under gentle shaking for 3-12 hours. Following this, the gels were destained in distilled deionized water for a minimum of 7 hours or until a clear background was attained.

The recipe for the BaI₂ staining described below is for a single Tris-Glycine gel. The solution quantities were increased proportionally if multiple gels were stained at a given time. First, the gel was soaked in a 5% glutaraldehyde solution for 15 minutes, then, transferred into a suitable shallow dish containing 40 mL of 0.1 M perchloric acid and soaked for an additional 15 minutes. Following this, the gel was stained by adding 10 mL of a 5 % barium chloride solution followed by 4 mL of a 0.1 N Iodine solution under constant, gentle shaking. After the first staining, the gel was soaked in water for 15 minutes and the entire staining procedure was repeated. The gel was stained twice because significantly better results were obtained using this process. The gel was destained in distilled deionized water for up to two hours and then digitally imaged using a Hewlett Packard Scanjet® 6200C digital scanner.

The stock reagents; glutaraldehyde – 50 % in water (photographic grade) and 69-72 % Perchloric acid (ACS reagent) were from Sigma (St. Louis, MO), while the 0.1 N iodine and 10 % barium chloride solutions were from VWR (Plainfield, NJ).

Apparent molecular weights for HEL, and various PEG-HEL molecules also were determined using the Coomassie Blue stained gels. A calibration curve between natural log of the marker molecular weights versus their migration distances relative to the 10 kD marker was constructed. The migration distance for the 10 kD marker band was arbitrarily set to zero and distances of all other bands were measured relative to the 10 kD marker band. A calibration equation describing the marker molecular weight – distance

data was obtained by linear regression. Consequently, molecular weights of HEL & various HEL species were determined by substituting the respective migration distances into the calibration equation.

2.5 Matrix Assisted Laser Desorption & Ionization –Time of Flight (MALDI-TOF) Measurements

The molecular weights of purified PEG1-HEL, PEG2-HEL, and PEG3-HEL were determined using Matrix Assisted Laser Desorption & Ionization –Time of Flight (MALDI-TOF) measurements in Dr. Matthew McLean's Lab at Pfizer, Inc., Skokie, IL.

First, a C4 ZipTip (Millipore Corporation, Bedford MA, cat. # ZTC04S096) was conditioned with approximately 50 μ L of methanol and then washed with 20 - 30 μ L of water using repeated pipetting/aspiration cycles with a 10 μ L pipette. Ten microliters of a given PEG-HEL sample was then adsorbed on to the C4 ZipTip using 15 – 20 pipetting/aspiration cycles with the 10 μ L pipette. The pipette tip was then washed with water using 10 pipetting/aspiration cycles and eluted into a 10 μ L volume of 50/50 mixture of methanol/water again using 10 (or more) pipetting/aspiration cycles. One microliter of the eluant was then mixed with a saturated solution of sinapinic acid (in 50/49.5/0.5 acetonitrile/water/TFA) at a one-to-one ratio and spotted onto the MALDI target.

The MALDI mass spectrometer used was a Perseptive Biosystems DE STR time-of-flight mass spectrometer operated in the linear mode. The instrument parameters used to acquire the spectra were as follows; laser power, 2984; accelerating voltage, 25 kV; delay time, 1500 ns; grid voltage, 93%; mass acquisition range 5,000 – 100,000; low mass gate, 5000 Da; transient digitizer scan rate, 0.1 GHz (10 ns bin size); vertical scale, 50 mV; input bandwidth 25 MHz; and N2 laser repetition rate, 3 Hz;. The reported mass

spectra consist of the summation of between 60 and 100 individual laser shots per spectrum.

2.6 Molecular Weight Determination by Static Light Scattering

The weight average molecular weights of PEG 20kD, PEG1-HEL, & PEG2-HEL, were determined using a PD2000DLS static/dynamic light scattering & refractive index detector (Precision Detectors, Inc., Franklin, MA) equipped with an 800 nm, polarized, laser light source. The light scattering (LS) detector was built in within a 2410 Waters refractometer which was connected downstream to an HP-1100, HPLC system (Agilent Technologies, CA). This facilitated simultaneous detection of the RI and 90° light scattering signals along with the UV (280 nm) signal during the SE-HPLC analysis of the PEG-HEL molecules.

A Tskgel G3000SW_{XL} column (Tosohaas Corporation, Montgomeryville, PA) was used for the SE-HPLC analysis of PEG, PEG1-HEL and PEG2-HEL. The mobile phase consisted of a 50 mM Tris, 200 mM NaCl, pH 8.0 buffer pumped at a rate of 1 mL/min. Prior to any sample application (50 µL), the column was pre-equilibrated with at least 5 column volumes of the mobile phase. The UV Data collection was performed using the Chemstation® software package, while the RI and LS data was gathered using the PrecisionAcquire® software (provided by Precision Detectors, Inc.)

The Molecular weight determination using the PD2000 detector is similar to the two-detector method as described elsewhere [54]. Briefly, the light scattering signal (LS) from a point scatterer (a solute that is smaller than 10th the wavelength of incident light) can be mathematically related to its molecular weight (MW), concentration (C) in g/mL and to its refractive index increment (dn/dc) by the following equation:

$$LS = K \cdot MW \cdot C \cdot (dn/dc)^2 \quad (1)$$

where K , the instrument constant is a function of the angle of detection, wavelength of incident radiation, the scattering distance etc.

The refractive index detector can be used to determine the concentration C , of the solute in equation 1. The difference in refractive index between an eluting solute and its solvent is measured by passing a light beam through two cells, one of which contains the pure solvent, while the other contains the eluant as it passes through the cell downstream from the column. The cell with the pure solvent is filled with the solvent prior to the separation and maintained at the same temperature as the eluant. The observed signal (RI) that corresponds to the deviation of the light beam is proportional to the difference in the refractive index of the fluid in the two cells as shown in equation 2.

$$RI = B \times C \times \left(\frac{dn}{dc} \right) \quad (2)$$

where, B is the refractive index instrument constant, C is the concentration of the sample in the solvent, dn/dc , the change in the index of refraction of the solution as a function of concentration.

Substituting for C in equation 1 and rearranging, we get,

$$MW = \frac{1}{(dn/dc)} \left(\frac{LS}{RI} \right) \left(\frac{B}{K} \right) \quad (3)$$

Thus, the molecular weight of a solute can be determined from the measured LS & RI signals and knowing the refractive index increment (dn/dc) of the solute. The dn/dc for proteins can be considered to be a constant at a given wavelength and has previously been determined to be 0.167 at 800 nm [55].

A 2 mg/mL BSA standard from Sigma (St. Louis, MO, Cat #: P0839) was employed to determine the instrument constants K and B based on the light scattering and refractive index signals of the BSA monomer (66.5 kD). The instrument constants were determined at the start of each day's operation using a procedure provided by Precision Detectors, Inc.

For the PEGylated HEL molecules, a weighted average of the dn/dc for the unmodified HEL and the free PEG was used as presented in Equation 4 below,

$$(dn/dc)_{cp} = f_p (dn/dc)_p + \sum f_{np} (dn/dc)_{np} \quad (4)$$

where $(dn/dc)_{cp}$ is the refractive index increment of the conjugated protein, f_p & f_{np} , the weight fraction of protein and non-protein components and $(dn/dc)_p$ & $(dn/dc)_{np}$ are their respective refractive index increments. A previously determined value of 0.136 mL/g was used for the dn/dc of PEG [56]. The weighted average approximation has previously been shown to be valid in the case of PEG-proteins [57].

2.7 Fluorescence Spectroscopy

Fluorescence experiments were performed in a Fluoromax-2 ® fluorimeter (Jobin Yvon-Spex, Instrument, S.A. Edison NJ 08820) with 0.4 mg/mL HEL, PEG1-HEL, and PEG2-HEL respectively in a 25 mM sodium phosphate, 125 mM sodium chloride, pH 7.5 buffer. Measurements were made using a semi-micro, 1 cm path length, quartz cuvette at room temperature. Emission spectra were recorded between 305 nm and 400 nm using an excitation wavelength of 295 nm, which is selective for tryptophans. The band pass for the excitation beam was 2 nm. The emission was monitored using a band pass of 5 nm, an integration time of 0.1 sec and a step size of 1 nm.

2.8 Circular Dichroism Spectroscopic Studies

Two types of Circular Dichroism (CD) experiments were conducted with HEL, PEG1-HEL, and PEG2-HEL respectively: (i) Near-UV-CD measurements to examine the effect of PEGylation on the tertiary structure of HEL, and (ii) Far-UV-CD measurements to study the effect of PEGylation, if any, on the secondary structure of HEL. The experimental details for each type of measurement are presented below.

2.8.1 Near-UV-CD Experiments

Near-UV-CD experiments were performed in a Jasco 600 CD spectrometer between 250 and 320 nm. The data were gathered at room temperature using a 1 cm path length, quartz, semi-micro cuvette at protein concentrations of 0.4 mg/mL HEL, PEG1-HEL, and PEG2-HEL respectively in 25 mM sodium phosphate, 125 mM NaCl at pH 7.5. The spectra of the protein solutions and the buffer (blank) were obtained using a scan speed of 20 nm/min, a bandwidth of 1 nm, a response time of 1 sec, a step-size of 0.2 nm and were averaged over 5 replicates. Each protein spectrum was corrected by subtracting the respective buffer spectrum using the instrument software.

2.8.2 Far-UV-CD Experiments

Far-UV-CD experiments were performed using a Jasco 810 CD spectropolarimeter in the wavelength range of 260 nm to 190 nm. The data were gathered at room temperature using a 0.1 cm path length, quartz micro cuvette at protein concentrations of 0.2 mg/mL HEL, 0.17 mg/mL PEG1-HEL, and 0.2 mg/mL PEG2-HEL respectively, prepared in a 25 mM sodium phosphate, 125 mM NaCl, pH 7.5 buffer. Each protein spectrum was corrected by subtracting the respective buffer spectrum using the instrument software.

2.9 Determination of Partial Specific Volume

The partial specific volumes (\bar{v}) of various PEG molecules (MW 5000 – 40,000) were determined experimentally using precision densitometry in 25 mM sodium phosphate, 125 mM NaCl, pH 7.5 buffer.

Approximately 100 mg of a particular PEG was accurately weighed and analytically transferred into an empty 10 mL volumetric flask. Sufficient amount of the PBS buffer were added to the flask to adjust the volume to the 10 mL mark. The solution was mixed by inversion until the PEG was completely dissolved prior to any density measurements.

Density measurements of the various PEG solutions were made in a Mettler Toledo DE51 precision density meter at 20.00 °C. The density meter was equipped with a Peltier system capable of temperature control within ± 0.01 °C. Prior to any density measurements, the density meter was calibrated with double distilled water ($\rho = 0.99821$ g/mL) and dry air ($\rho = 0.00120$ g/mL).

Using the densitometric technique, the partial specific volume is calculated as,

$$\bar{v} = \frac{1}{d_0} \left(1 - \left(\frac{d - d_0}{c} \right) \right) \quad (5)$$

where d and d_0 are the solvent densities (g/mL), and c is the concentration of the solute (in this case PEG) in g/mL.

The partial specific volume of HEL was determined from its amino acid composition using the program SEDNTERP, which uses the Edsall and Cohn method for \bar{v} calculations as described elsewhere [58]. The amino acid sequence of HEL was obtained from literature [42]. The partial specific volume for PEG1-HEL, PEG2-HEL,

and PEG3-HEL were computed using SEDNTERP, which uses the following equation for estimating the partial specific volume of conjugated proteins.

$$\bar{v}_{cp} = f_p \bar{v}_p + \sum f_{np} \bar{v}_{np} \quad (6)$$

where \bar{v}_{cp} is the partial specific volume of the conjugated protein, f_p & f_{np} , the weight fraction of protein and non-protein components, and \bar{v}_p & \bar{v}_{np} are their respective partial specific volumes. The SEDNTERP database for conjugates was updated with the experimentally determined value of \bar{v} for PEG 20 kD.

2.10 Sedimentation Velocity Experiments

Sedimentation velocity studies were performed on HEL, PEG1-HEL, PEG2-HEL, and PEG3-HEL using the Beckman XL-I centrifuge, a eight-holed AN-50, titanium rotor, and sedimentation velocity cells assembled with 12-mm, double sector, charcoal or epon-filled centerpieces at 50,000 RPM and 20 °C. The online absorbance optical system was used to measure the concentration distribution of the sedimenting macromolecules. Experiments with PEG1-HEL and PEG2-HEL were conducted in a 25 mM sodium phosphate, 125 mM NaCl, pH 7.5 buffer, while a 50 mM Tris, 150 mM NaCl, pH 8.0 buffer was used in experiments with HEL, and PEG3-HEL.

Data were collected using the acquisition software provided with the Beckman XL-I centrifuge and analyzed using two software programs (i) DCDT+, and (ii) SVEDBERG. Both DCDT+ and SVEDBERG were purchased from Dr. John Philo (Alliance Protein Labs, CA). The DCDT+ program was used to represent the sedimentation velocity data in terms of the apparent sedimentation coefficient distribution function ($g(s^*)$) versus the sedimentation coefficient (s) [59]. The diffusion coefficients

and molecular weights for HEL and the various PEGylated HEL molecules were determined using SVEDBERG. The program calculates values for the sedimentation and diffusion coefficients by fitting the experimental data directly to the modified Fujita-MacCosham approximation of the transport equation [60].

A brief discussion on the sedimentation coefficient (s), its relationship to the frictional & diffusion coefficients, molecular weight, solvent properties, and the apparent sedimentation coefficient distribution function ($g(s^*)$) is presented below.

The sedimentation coefficient (s) is a hydrodynamic property, characteristic of each macromolecule. It is most useful for providing information about the shape of a macromolecule in solution. Along with the centrifugal force, a sedimenting particle experiences an opposing frictional drag. A force balance on the sedimenting particle results in the definition of the sedimentation coefficient as the ratio of the linear velocity of a macromolecule to the angular field strength. This can be mathematically represented as:

$$s = \frac{v}{\omega^2 \cdot r} \quad (7)$$

where v is the linear velocity (cm/s), ω is the angular velocity (s^{-1}), and r the radial distance (cm).

The sedimentation coefficient is related to the physical properties of the macromolecule and to the solvent properties as below

$$s = \frac{M_w (1 - \bar{v}\rho)RT}{N_a f} \quad (8)$$

where M_w is the molecular mass of the macromolecule, \bar{v} , the partial specific volume of the macromolecule (mL/g), ρ , the solvent density (g/mL), R , the universal gas constant

$(8.314 \times 10^7 \text{ g/mol-K})$, T , the temperature (K), N_a , the avogadro's number (6.023×10^{23}) and f the frictional coefficient of the macromolecule.

The frictional coefficient ' f ' is related to the diffusion coefficient ' D ' by the Stokes-Einstein equation as expressed below

$$f = \frac{RT}{N_a D} \quad (9)$$

Substituting equation 9 in equation 8, we get the Svedberg equation, which relates the sedimentation and diffusion coefficients of a macromolecule to its molecular mass.

$$\frac{s}{D} = \frac{M_w(1-\bar{v}\rho)}{RT} \quad (10)$$

For a particle in laminar flow, its frictional coefficient (f) is related to its Stokes or the hydrodynamic radius by the Stokes equation,

$$f = 6\pi\eta R_h \quad (11)$$

where η is the solvent viscosity. This equation allows one to calculate the radius of a sphere, which is hydrodynamically equivalent to a particle of any geometry but having the same frictional coefficient f as that of the sphere.

Substituting equation 11 in equation 9, the Stokes radius can be related to the particles' diffusion coefficient by

$$R_h = \frac{RT}{6\pi \cdot \eta \cdot N_a \cdot D} \quad (12)$$

Sedimentation velocity (SV) is a powerful technique that provides information on the hydrodynamic behavior of macromolecules. Particularly, two hydrodynamic properties can be determined using this technique - the sedimentation coefficient or ' s ' and the diffusion coefficient, D . Classically, only the sedimentation coefficient was

determined using sedimentation velocity. Hydrodynamic information on a molecule such as its frictional coefficient – f , its diffusion coefficient – D , and its Stokes radii was obtained using an independently determined molecular weight (from sedimentation equilibrium) and by employing Equations 8 – 12. However, recent advances have made it possible for simultaneous determination of s and D values directly from the sedimentation velocity patterns of macromolecules [60].

Since the sedimentation coefficient (s) is a function of buffer density, buffer viscosity, and temperature, it is usually reported as a value normalized to standard conditions. The standard conditions by convention are those of pure water and 20 °C. The equation used for normalization is,

$$s_{20,w} = s_{T,b} \frac{(1 - \bar{v}\rho)_{20,w} \cdot \eta_{T,b}}{(1 - \bar{v}\rho)_{T,b} \cdot \eta_{20,w}} \quad (13)$$

where $s_{20,w}$ is the normalized sedimentation coefficient, and $s_{T,b}$ is the measured sedimentation coefficient at a temperature T in buffer. The \bar{v} value in the numerator corresponds to the partial specific volume of the macromolecule in pure water at 20 °C, while the \bar{v} value in the denominator corresponds to the partial specific volume of the macromolecule at the experimental conditions. The density and viscosity of pure water are denoted by $\rho_{20,w}$ and $\eta_{20,w}$ respectively, while $\rho_{T,b}$ and $\eta_{T,b}$ are the density and viscosity of buffer at temperature T . Extrapolation of $s_{20,w}$ to zero macromolecule concentration yields $s_{20,w}^0$.

The diffusion coefficient values are reported at conditions of 20 °C and pure water. The normalization equation is,

$$D_{20,w} = \frac{D_{20,b} \cdot \eta_{20,b}}{\eta_{20,w}} \quad (14)$$

The apparent Sedimentation coefficient distribution is obtained from the time derivative of the sedimentation velocity concentration profile using,

$$g(s^*)_t = \frac{1}{c_0} \left(\frac{\partial c}{\partial t} \right) \left(\frac{\omega^2 \cdot t^2}{\ln(r_m/r)} \right) \left(\frac{r}{r_m} \right)^2 \quad (15)$$

where s is the sedimentation coefficient, r , the radial position of the sedimenting boundary, r_m the radial position of the meniscus, c_0 , the initial loading concentration, and $(\partial c / \partial t)$, the time partial differential of the concentration profile at a fixed radial position r . The time derivative, $\partial c / \partial t$ can be approximated as $\Delta c / \Delta t$ and computed from subtraction of two consecutive scans.

2.11 Dynamic Light Scattering Measurements

The PDEExpert® Dynamic Light Scattering Instrument (Precision Detectors, Inc., Waltham MA) equipped with an 800 nm, polarized, laser light source was employed to determine the hydrodynamic or Stokes radii of various molecules. In dynamic or quasi-elastic light scattering, the fundamental measurement is the fluctuation in the intensity of scattered light from a small volume element of the solution. The intensity fluctuations are a result of macromolecules moving in and out of the volume element due to Brownian motion and can be correlated to their diffusion coefficients. The Stokes or the hydrodynamic radii can be computed from the diffusion coefficients using equation 12.

DLS measurements were made with PEG (MW 5000 – 40,000), HEL, PEG1-HEL, PEG2-HEL and PEG3-HEL at 20 °C using a detection angle of 90°. Temperature control was achieved by a Peltier system within the PDEExpert® instrument. Experiments

with various PEG molecules (10 mg/mL) were performed in water, while those with HEL (2 mg/mL), PEG1-HEL (1 mg/mL), PEG2-HEL (1 mg/mL), and PEG3-HEL (0.5 mg/mL) were performed in a 25 mM sodium phosphate, 125 mM sodium chloride, pH 7.5 buffer.

2.12 Thermal Unfolding Studies Using UV Spectroscopy

The difference spectrum method as described by Lee *et al.* [28] was employed to study the effect of free PEG and of PEGylation on the thermal denaturation of HEL. Briefly, the method relies on the observation that the native and denatured states of a protein exhibit slightly different spectral properties. As a result, the thermal denaturation of a protein can be studied by monitoring the change in absorbance at the wavelength of maximum change as a function of temperature. For a given protein, one can determine the wavelength of maximum change by recording the absorption spectra of the protein at different elevated temperatures and subtracting them from a reference spectrum. In the case of HEL, the wavelength of maximum change has previously been determined to be 301 nm [28].

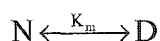
A Lambda 40 UV/Vis spectrophotometer (Perkin Elmer, Norwalk, CT), equipped with jacketed cuvette holders was employed to conduct equilibrium, thermal denaturation experiments. Studies were conducted with 0.5 – 1.25 mg/mL HEL, PEG1-HEL, PEG2-HEL, and PEG3-HEL respectively in a 40 mM glycine, pH 3.0 buffer. Experiments also were performed with 1 mg/mL HEL in the presence of 10, 20 & 30 % PEG 400 (Sigma, St. Louis, MO) and in the presence of 15 % and 30 % PEG 20 kD (Fluka, Germany) in the glycine buffer.

Prior to conducting an experiment, each sample solution was degassed and equilibrated at 30 °C using a Thermovac degassing instrument from Microcal, Inc. (Southampton, MA). Post degassing, approximately 3 mL of the sample was expressed through a 0.22 micron Durapore® syringe filter into a 3 mL capacity, 1 cm path-length, quartz cuvette. The cuvette was then placed in the spectrophotometer cell holder and equilibrated at 30 °C for at least 10 minutes. The sample temperature was monitored using a specialized temperature sensor (Perkin Elmer, part #: B018-5227) with a rated accuracy of ± 0.1 °C that could be inserted into the cuvette. It was ensured that the sensor tip was submerged in the sample solution, which allowed for the measurement of the actual sample temperature during an experiment. The base of the temperature sensor also served as a cuvette stopper.

After equilibration at 30 °C, the sample absorbance was zeroed using the 'Autozero' function. Following this, thermal unfolding was monitored in terms of the change in absorbance at a constant wavelength of 301 nm over a temperature range of 30 - 85 °C and at a ramping rate of either 0.5 °C/min or 1 °C/min. Controlled temperature ramping was achieved with a refrigerated, circulating water bath - Model RTE-111 from Neslab (Portsmouth, NH).

Data analysis was conducted using the software program DENFIT (Kindly provided by Dr. Les Holliday). The program employs nonlinear regression to fit thermal unfolding data (e.g., absorbance data) to a user's choice of models to estimate the enthalpy of unfolding (ΔH_m), the transition temperature (T_m) and the change in specific heat capacity during the unfolding reaction (ΔC_p). The models are based on the van't Hoff Equation and assume a two-state unfolding mechanism in which nearly all the

protein is present as either the native (N) or unfolded (D) state. The equilibrium between the native and the denatured state of a protein can be represented as:



where K_m is the equilibrium constant governing the unfolding reaction.

For any given temperature, the equilibrium-unfolding constant, K_m , can be related to an observable quantity that varies linearly with the fraction of native protein such as absorbance or ellipticity [61]. In the present case, the relationship between the measured absorbance and the thermodynamic parameters can be mathematically expressed as:

$$K_m = \left(\frac{A_N - A}{A - A_D} \right) = e^U \quad (16)$$

where the exponent U is,

$$U = \left\{ \frac{(\Delta C_p \cdot T_m - \Delta H_m)}{R} \left(\frac{1}{T} - \frac{1}{T_m} \right) + \frac{\Delta C_p}{R} \cdot \ln \left(\frac{T}{T_m} \right) \right\} \quad (17)$$

and, where A is the absorbance of the protein at a given temperature, T , and A_N & A_D are absorbance values corresponding to the native and denatured states of the protein at that temperature. R is the universal gas constant.

DENFIT also allows the user to choose appropriate models that account for a linear temperature dependence of A_N and/or A_D . Rearranging equation 16 & 17, one can express the measured absorbance explicitly in terms of the independent variable T and the sought thermodynamic parameters ΔC_p , T_m , and ΔH_m , by the following equation, which is the fitting form for non-linear regression analysis:

$$A = \left(\frac{A_N(T) + A_D(T) \cdot e^{U(T)}}{1 + e^{U(T)}} \right) \quad (18)$$

2.13 Differential Scanning Calorimetry

The thermal unfolding of HEL and PEGylated HEL molecules also was studied using Differential Scanning Calorimetry (DSC). Experiments were conducted at Microcal, Inc. (Southampton, MA) using two DSC instruments – the sensitive VP-DSC and the high-throughput Capillary-VP-DSC or Cap-DSC. Data analysis was performed by the author using the Origin ® software program modified with a DSC data analysis patch as provided by Microcal, Inc.

Studies were conducted with HEL (1 mg/mL), PEG1-HEL (1 mg/mL), and PEG2-HEL (0.8 mg/mL – VP-DSC, 0.4 mg/mL – Cap-DSC) in 40 mM glycine buffer at pH 3.0. A scanning rate of 60 °C/hr was used for VP-DSC, while a faster scanning rate of 220 °C/hr was utilized for experiments in the Cap-DSC. Each sample solution was degassed and equilibrated at 30 °C using a Thermovac degassing instrument from Microcal, Inc. (Southampton, MA). Prior to loading a protein sample, a thermogram for the matching buffer blank was obtained by ramping the VP-DSC from 25 °C to 90 °C and the Cap-DSC from 10 °C to 90 °C. The buffer thermograms were subtracted from the respective sample thermograms before any data analysis.

The reversibility of the unfolding reaction of HEL and the PEG-HEL molecules was studied by rapidly cooling the protein sample after the first heating to the initial temperature of either 10 °C (Cap-DSC) or 25 °C (VP-DSC) and then reheating it at the preset scanning rate to monitor the unfolding reaction again and obtain a second thermogram. The percentage reversibility was calculated as the ratio of the calorimetric enthalpy of unfolding measured during the 2nd heating (ΔH_2) to that observed during the 1st heating (ΔH_1) [62]. This is mathematically represented below in equation 19.

$$\% \text{ Reversibility} = \frac{\Delta H_2}{\Delta H_1} \times 100 \quad (19)$$

For all the molecules tested, a single transition peak was observed indicative of a two state transition. However, the data were fit to a model that accounted for non-two state transition with one peak. A non-two state model was chosen because this allowed for the calculation of the van't Hoff's enthalpy in addition to the calorimetric enthalpy. The calorimetric enthalpy or ΔH is simply the total enthalpy of unfolding measured during the unfolding process. The van't Hoff's enthalpy or ΔH_v on the other hand is defined as the enthalpy of unfolding per cooperative unit and depends on the shape of the transition peak. The ΔH_v can be calculated from a DSC thermogram using the following equation.

$$\Delta H_v = 4 \frac{R \cdot T_m^2 \cdot C_{p,m}}{\Delta H} \quad (20)$$

where T_m is the transition mid-point, $C_{p,m}$ is heat capacity at the transition mid-point, and ΔH is the calorimetric enthalpy of unfolding.

The ratio $\Delta H/\Delta H_v$ can provide insights into the mechanism of the unfolding process. For a purely two-state system, where the protein can exist in only the folded or the unfolded state, the ratio $\Delta H/\Delta H_v$ is 1. Values greater than 1 are indicative of intermediates playing a role in the unfolding process, while values less than 1 indicate intermolecular cooperativity [63]

2.14 Turbidity Measurements to Monitor Aggregation

A turbidimetric assay was developed to study the effect of PEGylation on the heat-induced aggregation of HEL. Aggregation in HEL or PEG-HEL solutions caused by

heating at a high temperature was monitored in terms of a turbidity increase at 320 nm as a function of time.

A Lambda 40 UV/Vis spectrophotometer (Perkin Elmer), equipped with jacketed cell-holders was employed for the turbidity experiments. Experiments were conducted with 1 mg/mL HEL, PEG1-HEL, & PEG2-HEL respectively in a 25 mM sodium phosphate, 125 mM NaCl, pH 7.5 buffer at 75 °C. Temperature control was achieved with the help of a refrigerated, circulating water bath - Model RTE-111 from Neslab (Portsmouth, NH). Studies also were conducted with 1 mg/mL HEL in the presence of 4 % PEG 20 kD (Fluka, Germany) to understand the effect of free PEG in solution on the aggregation rate of HEL.

Prior to conducting an experiment, each sample solution was degassed and equilibrated at 25 °C using a Thermovac degassing instrument (Microcal, Inc. Southhampton, MA). Post degassing, approximately 120 µL of the sample was transferred into a 125 µL capacity, 1 cm path-length, quartz cuvette. The cuvette was capped and then placed in the spectrophotometer cell holder pre-equilibrated at the experimental temperature of 75 °C. Immediately after this, the instrument was set to zero using the instrument 'Autozero' function and turbidity was monitored as % transmittance at 320 nm over a 25-minute period.

All turbidity studies were conducted in triplicate unless mentioned otherwise. The PEG1-HEL, and PEG2-HEL samples were subjected to reducing and non-reducing SDS-PAGE experiments after the turbidity experiments using the procedure described in section 2.4.

2.15 Aggregation Experiments Using Size Exclusion-High Performance Liquid Chromatography

The effect of PEGylation on the heat-induced aggregation of HEL also was studied using Size Exclusion-High Performance Liquid Chromatography. Briefly, samples of HEL, PEG1-HEL, and PEG2-HEL were heated at a constant, elevated temperature of 75 °C for 25 minutes and then analyzed by SE-HPLC to determine the amount of monomeric HEL, PEG1-HEL, or PEG2-HEL remaining after the heat treatment.

Experiments were conducted with 1 mg/mL HEL, PEG1-HEL, & PEG2-HEL in a 25 mM sodium phosphate, 125 mM NaCl, pH 7.5 buffer at 75 °C. Three sets of 500 µL aliquots of HEL and 100 µL aliquots of PEG1-HEL & PEG2-HEL respectively were transferred into 1.5 mL capacity centrifuge tubes. The tubes were placed in a 75 °C water bath for 25 minutes to induce aggregation and then immediately transferred to a 5 °C ice-water bath for another 25 minutes to quench the aggregation reaction. Following this, samples were subjected to SE-HPLC analysis in a HP-1100 HPLC system (Agilent Technologies, CA). The HEL samples were visibly cloudy after the heat treatment. Prior to HPLC analysis, these samples were centrifuged at 10000 RPM in an Eppendorf 5804 R centrifuge for 10 min. and the supernatant was passed through a 0.22-micron syringe filter before loading on the HPLC system. The PEG1-HEL, and PEG2-HEL samples were directly injected on to the HPLC without any further treatment.

A Tskgel G2000SW_{XL} column (Tosohaas Corporation, Montgomeryville, PA) was used for the SE-HPLC analysis of HEL, while the SE-HPLC of PEG1-HEL and PEG2-HEL was conducted using two SEC columns in series -Tskgel G4000SW_{XL} (1st) and G3000SW_{XL} (2nd). The mobile phase consisted of a 50 mM Tris, 200 mM NaCl, pH

8.0 buffer pumped at a rate of 1 mL/min for the SE-HPLC of HEL, and 0.9 mL/min for the SE-HPLC of the PEGylated HEL molecules. The eluting protein peaks were monitored using a detection wavelength of 280 nm. Prior to any sample application (20-50 μ L), the columns were pre-equilibrated with at least 5 column volumes of the mobile phase.

Data collection and analysis was performed using the Chemstation® or Turbochrome® software packages. The area of the peak corresponding to monomeric HEL, PEG1-HEL, or PEG2-HEL remaining after the aggregation reaction was calculated and expressed as a percentage relative to that of the respective, untreated control HEL, PEG1-HEL or PEG2-HEL sample.

2.16 Digital Visualization of Aggregation

The effect of PEGylation on the heat-induced turbidity of HEL also was captured photographically using a digital camera (Sony, model: Mavica). Four hundred microliters each of 0.9 mg/mL HEL, PEG1-HEL, and PEG2-HEL solutions in 25 mM sodium phosphate, 125 mM phosphate at pH 7.5 were transferred into three different clear, SEPCAP® vials (National Scientific Company, part # C4015-96). The vials were capped and placed in a 75 °C water bath with help of plastic buoys for 25 minutes. Immediately after this, the vials were cooled to room temperature by placing under running cold water and were digitally photographed.

Chapter 3

RESULTS AND DISCUSSION

3.1 Synthesis & Characterization of PEGylated Hen Egg Lysozyme

3.1.1 Choice of PEGylation Chemistry

Hen Egg Lysozyme was modified using linear, 20 kD, methoxyPEG-propionaldehyde chains by employing the reductive amination reaction of aldehydes and primary amines. There are two advantages to using this reaction chemistry:

- 1) It results in the formation of a secondary amine at the point of PEG attachment. A key outcome of this is that the net charge on the amine is preserved (Figure 5) [25].
- 2) Taking advantage of the difference in pK_a s of the α -amine and the ϵ -lysyl amines, selective PEGylation at the N-terminal, α -amine is possible. This is achieved by conducting the PEGylation reaction under fairly acidic conditions of pH 4.0 - 4.5 as employed in the present case.

Since a principal objective of this research was to examine the effect of the covalently attached PEG on the thermal stability of HEL, it was important to minimize any structural changes that could result from linker chemistry. Hence, the reductive

amination reaction chemistry was employed to preserve the charge on the PEGylated HEL molecules upon modification and eliminate any charge-related, confounding effects.

3.1.2 Heterogeneity in the PEGylated HEL Molecules

Three types of heterogeneity can exist in a given PEGylated protein:

- 1) Heterogeneity with respect to the number of PEG molecules attached per molecule (degree of PEGylation).
- 2) Heterogeneity arising out of the polydispersity in the PEG polymer
- 3) Heterogeneity with respect to positional isomers. This occurs when the PEG is attached to different amino acid residues on different molecules of a protein. For example, a given PEG-protein can be homogeneous with respect to the degree of PEGylation bearing just one PEG chain per molecule but can still exhibit positional isomerism with respect to the site of PEG attachment.

The degree of PEGylation of the different PEG HEL molecules was characterized using SDS-PAGE and MALDI-TOF analyses. The polydispersity within PEG or a particular PEG-HEL species was studied using MALDI-TOF and static light scattering (presented in Section 3.1.3.2). Discussion with respect to the positional heterogeneity in the PEG-HEL molecules is also presented in this section.

Figure 6a is a digital image of a Coomassie Blue stained, 4–15 % polyacrylamide gel post SDS-PAGE. The molecular weight standards (10 kD - 250 kD) are in lanes 1 and 8, while HEL, PEG1-HEL, PEG2-HEL, and PEG3-HEL are in lanes 3,4, 5, and 6 respectively. It should be noted that the lanes containing PEGylated HEL species have been overloaded to maximize the detection of impurities.

Figure 5. The reductive amination reaction of aldehydes and primary amines was employed for the PEGylation of HEL using methoxyPEG-propionaldehyde. The reaction was conducted at pH 4.5 in the presence of NaCNBH₃ to selectively target the N terminal α -amine.

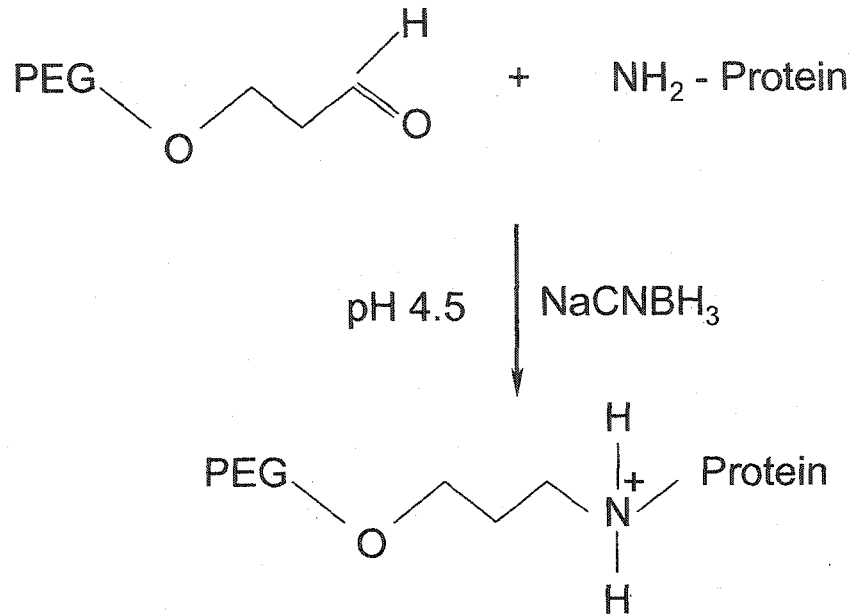
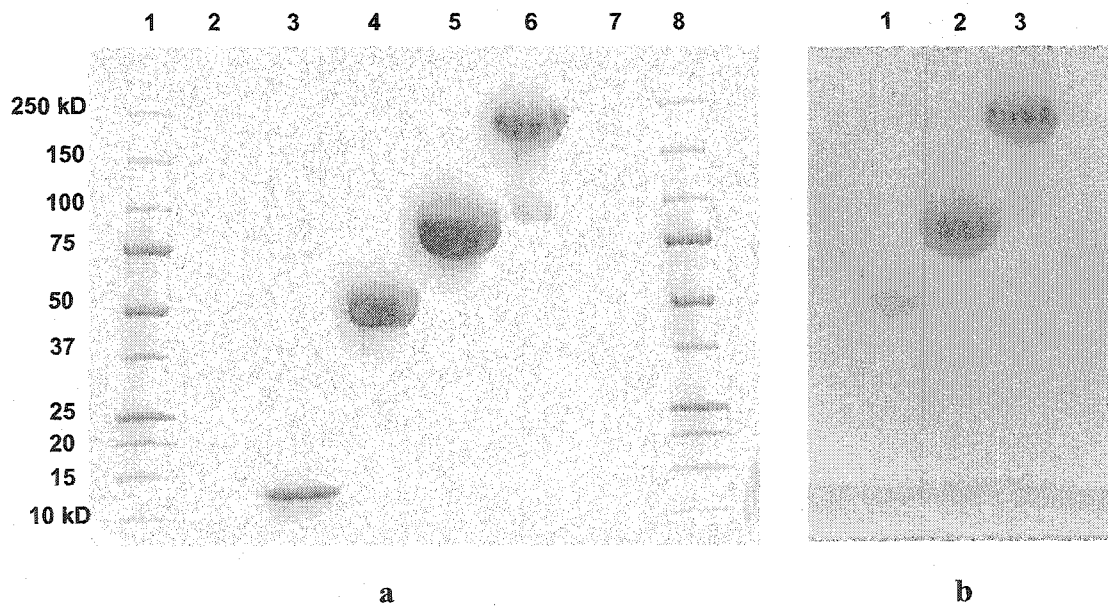


Figure 6a & b : SDS-PAGE analysis of HEL, and PEG-HEL (a) - Coomassie Blue stain. The molecular weight standards are in lanes 1 and 8, while HEL, PEG1-HEL, PEG2-HEL, and PEG3-HEL are in lanes 3-6 respectively. (b) - barium iodide stain. PEG1-HEL, PEG2-HEL, and PEG3-HEL are in lanes 1, 2, and 3 respectively

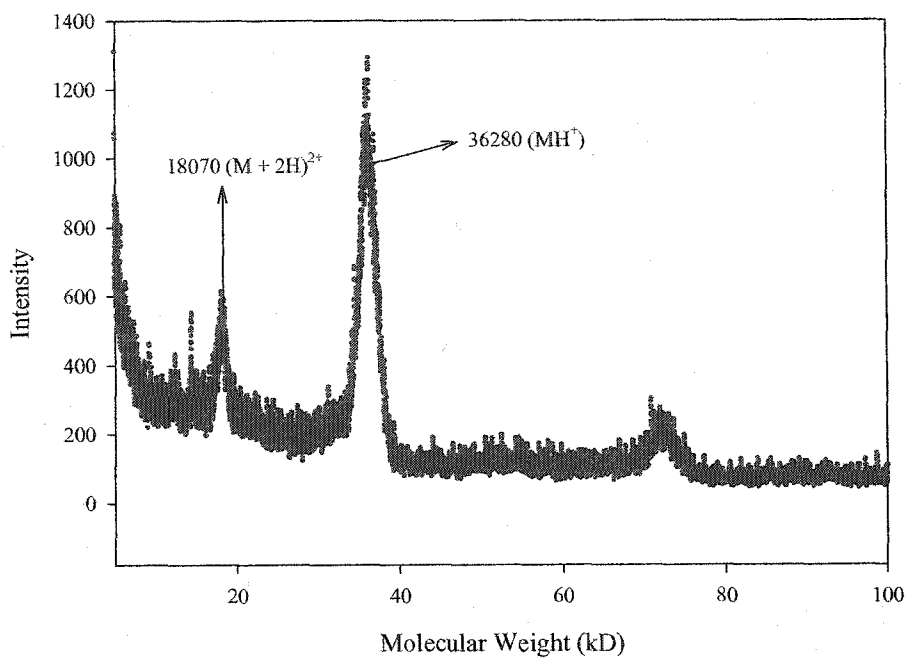


As seen from Figure 6, PEG1-HEL and PEG2-HEL (lanes 3 and 4) are free of any unreacted HEL. Further, both species are homogenous with respect to the degree of PEGylation (number of PEGs attached per HEL molecule). However, while no unreacted HEL is detected in the case of PEG3-HEL (lane 6), a trace amount of PEG2-HEL appears to be present in PEG3-HEL species. The same is observed in the barium iodide stained gel, which is specific for PEG detection (Figure 6b). In this case, PEG1-HEL, PEG2-HEL, and PEG3-HEL are in lanes 1, 2 and 3 respectively. As seen, PEG1-HEL & PEG2-HEL are observed to be homogenous, while the PEG3-HEL contains a small amount of PEG2-HEL.

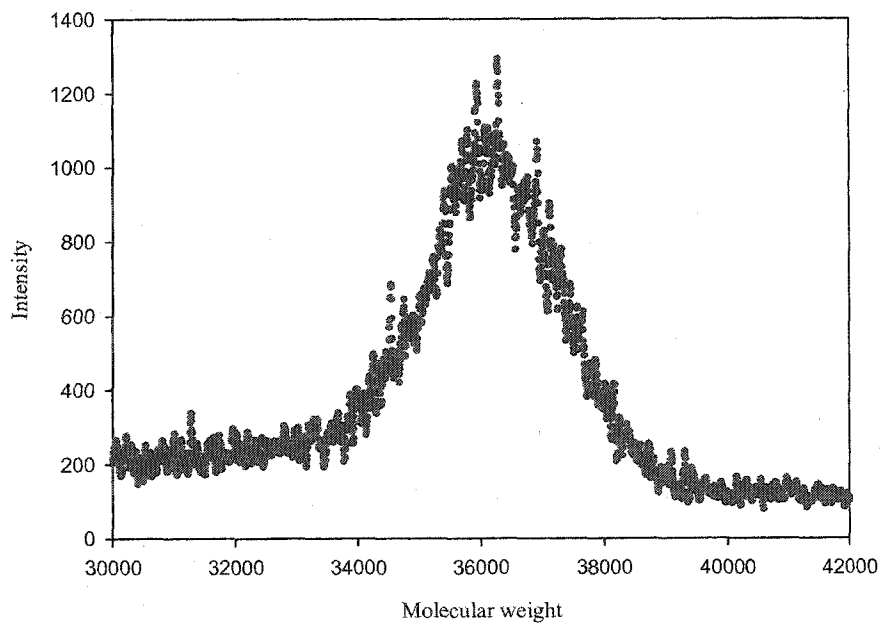
Importantly, the SDS-PAGE observations are in excellent agreement with the MALDI-TOF results (Figure 7 through Figure 9). As can be seen, while PEG1-HEL (Figure 7a) and PEG2-HEL (Figure 8) are homogenous with respect to the degree of PEGylation, PEG3-HEL (Figure 9) is observed to contain a small amount of PEG2-HEL. Another observation is that the polydispersity in PEG causes a peak broadening of the mass spectra (Figure 7b). This results in a range of molecular weights being obtained for a given PEG-HEL species and necessitates the use of weighted molecular weights for PEG-proteins as will be discussed in the following section.

There are seven possible sites of PEGylation per HEL molecule via the chosen reaction chemistry - the six, ϵ -amino groups of lysines and the α -amino group of the N terminal lysine. As mentioned earlier, the PEGylation reaction was conducted at pH 4.5 to selectively modify the α -amine and minimize the positional heterogeneity in the monoPEGylated HEL species.

Figure 7a & b: MALDI-TOF Spectra of PEG1-HEL. Experiments were conducted in a Perceptive Biosystems DE STR time-of-flight mass spectrometer with samples prepared in a sinapinic acid matrix. The broad peak (34–39 kD) presented in panel b represents the heterogeneity in mass within the purified PEG1-HEL resulting from the polydispersity of PEG.



(a)



(b)

Figure 8: MALDI-TOF Spectrum of PEG2-HEL. Experiments were conducted in a Perseptive Biosystems mass spectrometer with samples prepared in a sinapinic acid matrix.

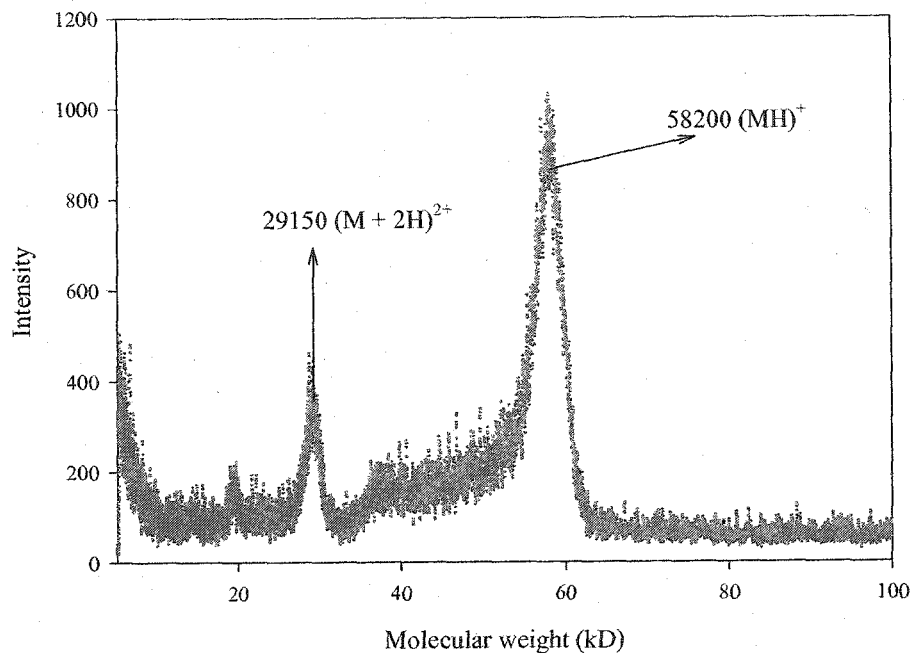
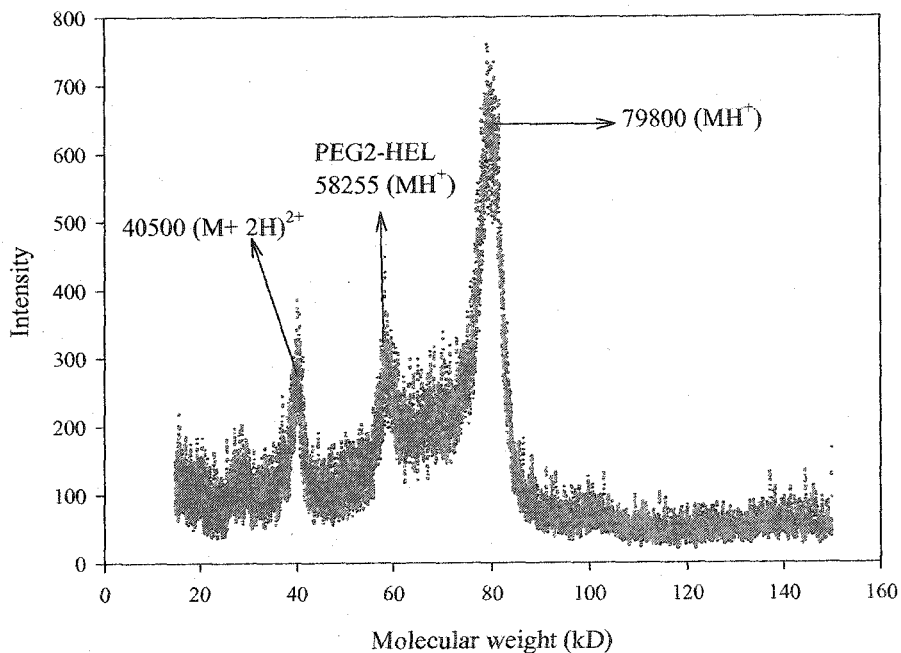


Figure 9: MALDI-TOF Spectrum of PEG3-HEL. Experiments were conducted in a Perseptive Biosystems mass spectrometer with samples prepared in a sinapinic acid matrix.



This was possible because of the large difference in pK_a s of the α -amine (5.2 – 7.8) versus ϵ -amines (11.1) in HEL [64 - 66]. Hence it is highly likely that the PEG is attached at the amino terminus in the case of PEG1-HEL. Studies to conclusively demonstrate N-terminal PEGylation were not conducted because this reaction has previously been shown to yield fairly homogenous (> 95 %), N-terminally modified products for several other proteins [67].

The positional homogeneity offered by the reductive amination reaction in the case of monoPEGylated species cannot be utilized to synthesize homogeneous, higher order PEGylated species. This is because differentiation between the ϵ -amines is not possible on the basis of their pK_a . Consequently, PEG attachment can occur on any of the available surface lysines. For the higher order species, the PEGylation reaction is governed by the inherent reactivity and steric availability of the surface lysines. Thus, positional isomers are likely to be present in the PEG2-HEL and PEG3-HEL species with the PEG attached to different lysines in different HEL molecules.

3.1.3 Determination of Molecular Weights

SDS-PAGE is an effective tool for the qualitative characterization of the homogeneity of PEGylated proteins as demonstrated in the previous section. However, the method cannot be applied to estimate molecular weights of PEG-proteins because gross overestimates are obtained using this technique. This can be illustrated using the SDS-PAGE analysis of the PEG-HEL molecules. The procedure for estimating apparent⁵ molecular weights (MW_{app}) using SDS-PAGE is as follows; first, a calibration curve is constructed by plotting the natural log of the molecular weight of the standards versus

⁵ The term apparent molecular weight is used because the MW is estimated relative to a set of MW standards.

their respective migration distances relative to a fixed point on the gel. Then the migration distance of an unknown sample from the fixed point is measured and its MW_{app} is estimated by interpolation of the calibration curve.

In the present case, a calibration line (Figure 10) was constructed using the migration distances of the molecular markers relative to the 10 kD molecular weight standard from the Coomassie Blue stained, SDS-PAGE gel (Figure 6a). The apparent molecular weights of HEL and the various PEG-HEL molecules were determined by substituting their respective migration distances (relative to the 10 kD standard) into the equation describing the calibration line. The numerical values of estimated molecular weights are presented below in Table 8. A graphical comparison of the expected (M_{exp}) and estimated (M_{est}) molecular weights is also presented in Figure 11. As seen from the figure, there is good agreement between the expected and predicted molecular weight for HEL. However, the molecular weights of all three PEGylated HEL molecules are grossly overestimated. Further, the error in the estimated values is observed to increase with increasing degree of PEGylation. In Figure 11, the extent of error in the estimation molecular weight can be measured in terms of the departure of the estimated value from the diagonal ($M_{est} = M_{exp}$).

Table 8: Apparent molecular weights of HEL, and PEGylated HEL determined from the Coomassie Blue stained SDS-PAGE gel

Molecule	Expected MW (kD)	SDS-PAGE (kD)
HEL	14.3	13
PEG1-HEL	34.3	53
PEG2-HEL	54.3	96
PEG3-HEL	74.3	210

Figure 10. Estimation of apparent molecular weight using SDS-PAGE-calibration curve constructed by plotting the natural log of the molecular weight of standards versus their migration distance (mm) relative to the 10 kD marker. Equation describing the calibration curve was obtained by linear regression.

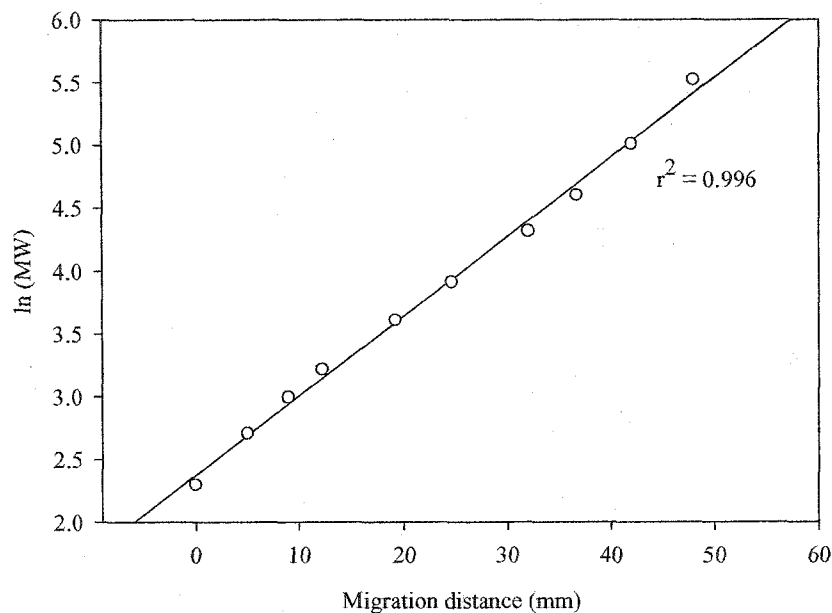
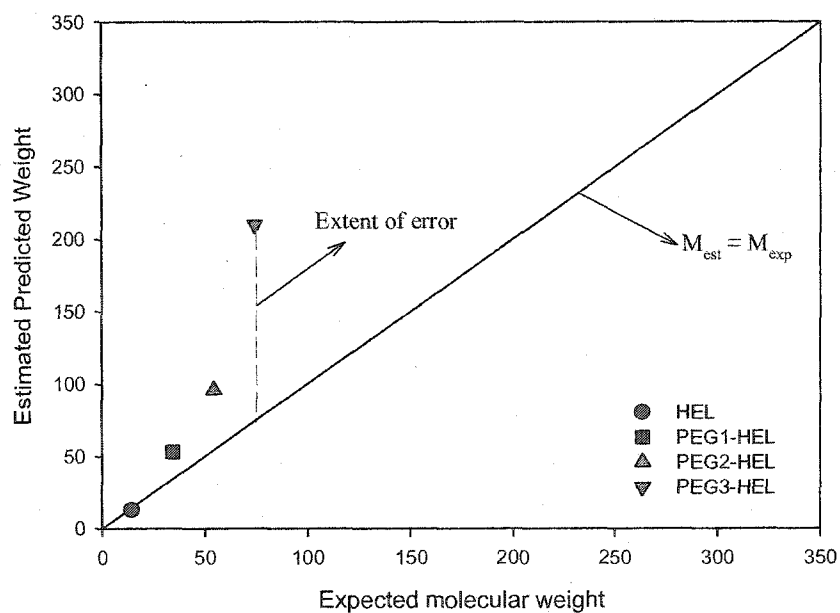


Figure 11. Comparison of estimated versus expected molecular weights for HEL, and various PEG-HEL molecules. The extent of error in estimation of the molecular weight is measured in terms of the departure from the $M_{est} - M_{exp}$ diagonal.



This discrepancy can be attributed to the anomalous electrophoresis of PEGylated proteins on a sieving matrix. In SDS-PAGE, a denatured protein is assumed to be in the form a single long polypeptide chain that is evenly coated with SDS molecules. This assumption is not valid for PEGylated proteins where there are branches and possibly an uneven distribution of SDS molecules. The anomalous, impeded migration of a PEG-protein through a polyacrylamide gel matrix is caused by three factors (i) the large hydrodynamic volume of PEG which slows diffusion, (ii) branching in the polypeptide chain caused by the covalently attached PEG, and (iii) an uneven distribution of SDS molecules surrounding the denatured PEG-polypeptide chain. In sum, while SDS-PAGE is an excellent tool for qualitative, purity analysis of PEG proteins, it not an appropriate method for molecular weight estimation.

Size exclusion chromatography is another technique that is used extensively for the determination of apparent molecular weights of proteins. Similar to SDS-PAGE, PEG-proteins have been shown to exhibit anomalous chromatographic behavior on size exclusion columns because of their large hydrodynamic volumes [36]. These proteins are observed to elute at much earlier retention times compared to molecular weight standards of equivalent mass resulting in an over-estimation of their molecular weight. For these reasons, absolute methods of molecular weight determination have to be employed in the case of PEGylated proteins.

The molecular weights of various PEG-HEL molecules were determined using three absolute techniques (i) Matrix Assisted Laser Desorption Ionization – Time of Flight (MALDI-TOF) measurements (ii) Static Light Scattering (SLS), and (iii) Sedimentation Velocity (SV) analysis. All three methods are based on

thermodynamic or physical first principles and do not rely on any standards for molecular weight determination.

3.1.3.1 MALDI-TOF Measurements

The molecular weights of PEG1-HEL, PEG2-HEL and PEG3-HEL determined using MALDI-TOF measurements are tabulated below in Table 9 and presented graphically in Figure 7-Figure 9.

Table 9: Molecular Weights of PEG1-HEL, PEG2-HEL, and PEG3-HEL determined using MALDI-TOF Measurements

Molecule	Molecular weight (Daltons)	
	Expected	MALDI-TOF
HEL	14305	ND
PEG	20000	ND
PEG1-HEL	34305	36280
PEG2-HEL	54305	58200
PEG3-HEL	74305	79800

ND – Not determined

As seen, the MALDI-TOF results are in excellent agreement with the respective, nominal molecular weight values of the three PEG-HEL molecules. Although the nominal molecular weight of the PEG reagent employed for PEGylation was 20 kD, its actual value appears to be higher at ~ 21900 as reflected in the masses of all three PEG-HEL molecules. This is in excellent agreement with its weight average molecular weight (M_w) of 21470 determined from static light scattering measurements (presented later). It should be noted that the molecular weight values reported from MALDI-TOF experiments are values at their respective intensity peaks. These measurements do not account for the polydispersity within a particular PEG-HEL species, which is reflected in the broadening of the mass spectrum (Figure 8b). The polydispersity is inherent to the PEG polymer, and is transferred over to the PEGylated protein upon modification.

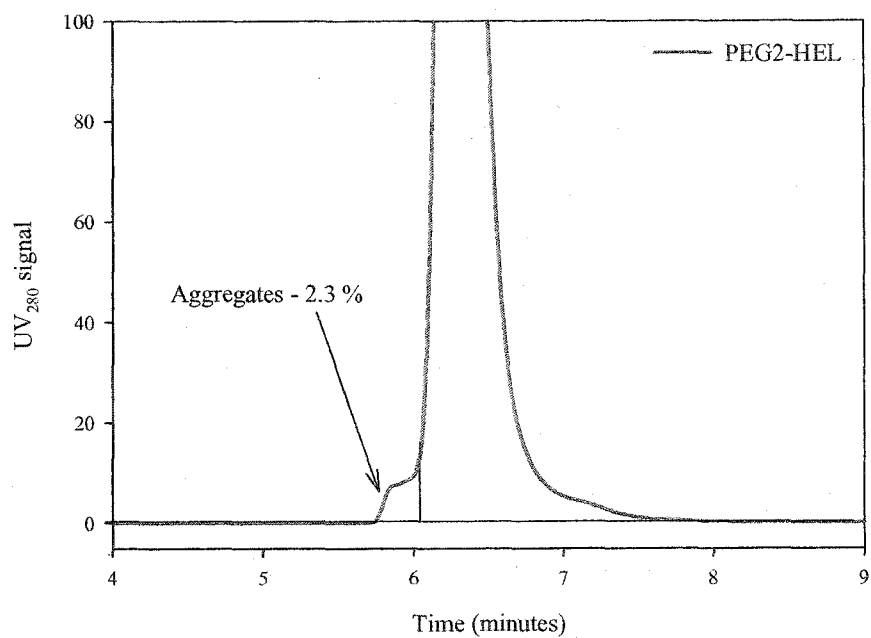
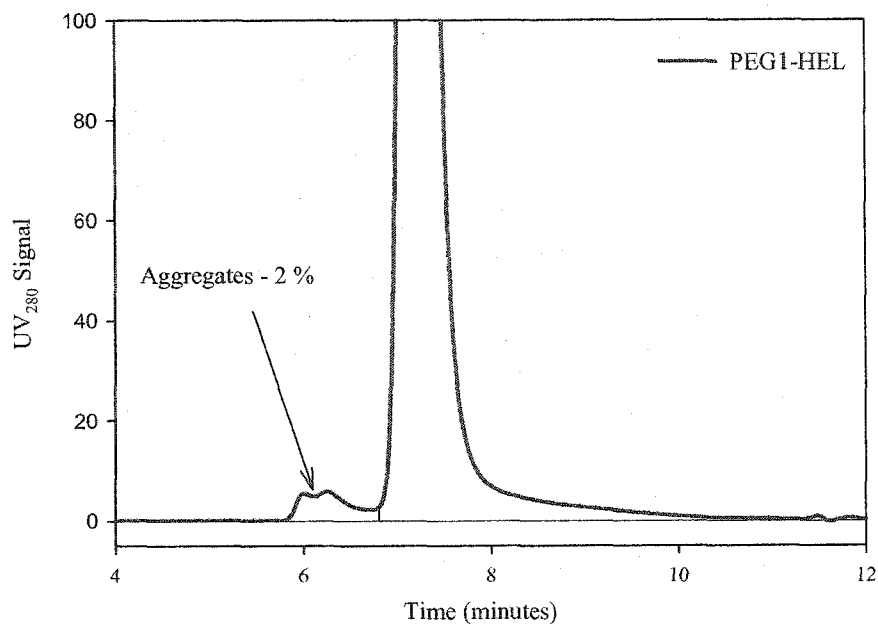
The MALDI-TOF measurements provide critical data on the molecular mass and degree of PEGylation of a PEG-protein; however, they do not provide any insight into the solution state of a molecule. For example, one cannot ascertain if a molecule self-associates in solution, or if non-covalent aggregates are present in a given sample. Solution molecular weights of macromolecules can be measured using Static Light Scattering (SLS) and Sedimentation methods. Both techniques were employed to study the PEG-HEL molecules, the results of which are discussed in the following sections.

3.1.3.2 Static Light Scattering Measurements

The static light scattering measurements (SLS) were made during the SE-HPLC analysis of PEG, PEG1-HEL, and PEG2-HEL as described previously in Section 2.6. PEG3-HEL was not studied due to limited sample availability. Three types of information were obtained from SE-HPLC coupled SLS measurements: (i) the presence of any non-covalent aggregates in a given sample (ii) weight average molecular weights of the monomer & aggregates, and (iii) the polydispersity index (PDI) in the monomer and aggregates of a particular species.

The relative amounts of non-covalent aggregates in PEG1-HEL and PEG2-HEL were quantified via size exclusion chromatographic separation using UV_{280 nm} detection. Both PEG1-HEL and PEG2-HEL are observed to contain small amounts of aggregates (Figure 12). Based on their relative peak areas, the aggregates were quantified to be 2.0 % and 2.3 % respectively.

Figure 12 Size Exclusion-HPLC analysis of PEG1-HEL and PEG2-HEL. Experiments were conducted in a HP 1100 HPLC system with simultaneous UV (shown below), RI and LS detection. PEG1-HEL and PEG2-HEL are observed to contain a small amount of non-covalent aggregates at 2 and 2.3 % respectively.



The aggregates are likely to be non-covalent in nature as no corresponding aggregate bands or peaks were observed in the SDS-PAGE (Figure 6) or MALDI-TOF (Figure 7 & Figure 8) studies. Importantly, these data demonstrate that both PEG1-HEL and PEG2-HEL are highly pure (~ 98 %) with respect to non-covalent aggregation. The SE-HPLC analysis of the PEG reagent (Figure 13) also revealed the presence of a high molecular weight impurity at ~ 2 %. This impurity is likely to be a covalent aggregate of the 20 kD monomer formed during its synthesis process.

The weight average molecular weights of PEG, PEG1-HEL, and PEG2-HEL were determined using the 90° light scattering (LS₉₀) and refractive index (RI) detection. The latter was employed to determine the sample concentration. A weighted average of the refractive increment (dn/dc) was used for both PEG-HEL molecules; the values were calculated using Equation 4 as described in Section 2.6.

The LS₉₀ and RI chromatograms for PEG, PEG1-HEL, and PEG2-HEL are presented in Figure 13 - Figure 15. The RI and LS₉₀ signals are superimposed for better visualization of the data. As shown, each chromatogram was sliced into two regions for integration and quantitative analysis. Region I was assigned to the major, monomer peak, while Region II was assigned to the aggregates or large impurities that had a detectable RI signal. The light scattering peaks in the third region – III will also be discussed.

The molecular weight distribution in a polydisperse system can be quantified in terms the polydispersity index or PDI. The PDI is defined as the ratio of the weight average molecular weight (M_w) of a sample to its number average molecular weight (M_n).

Figure 13. Size Exclusion-HPLC coupled Static Light Scattering analysis of mPEG propionaldehyde-20 kD. Experiments were conducted in a HP 1100 HPLC system with simultaneous RI and 90° LS detection. The weight average molecular weight of the PEG monomer (Region I) was determined to be 21470.

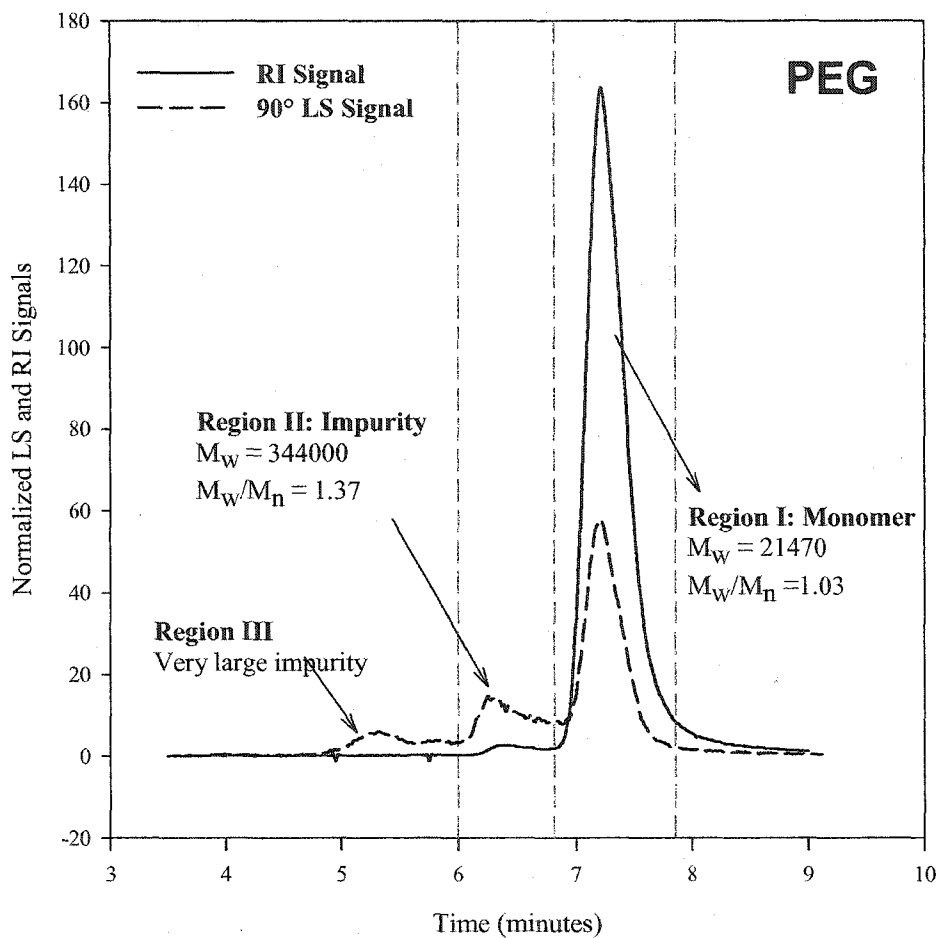


Figure 14. Size Exclusion-HPLC coupled Static Light Scattering analysis of PEG1-HEL. Experiments were conducted in a HP 1100 HPLC system with simultaneous RI and 90° LS detection. The weight average molecular weight of the PEG1-HEL monomer (Region I) was determined to be 34430.

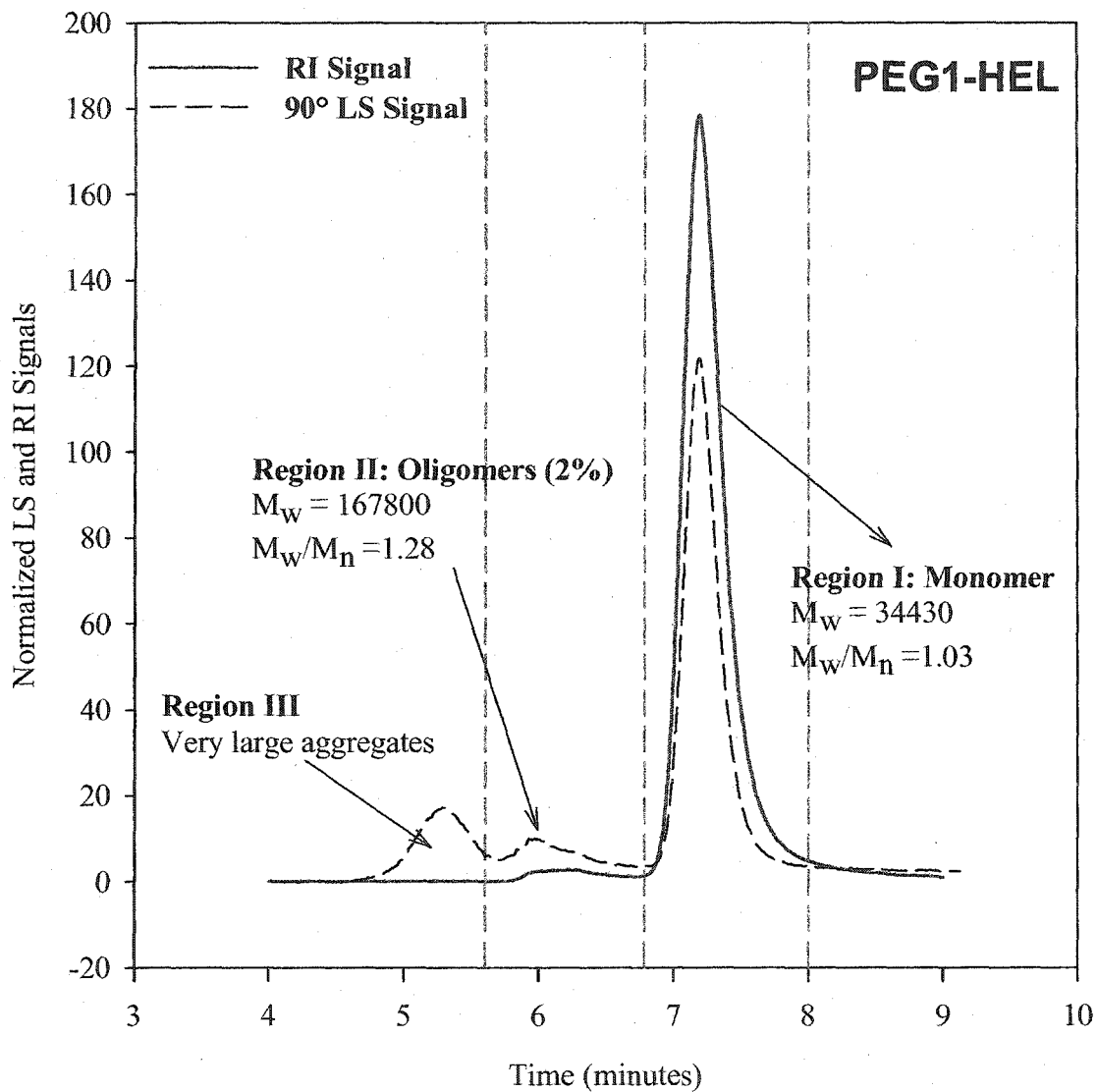
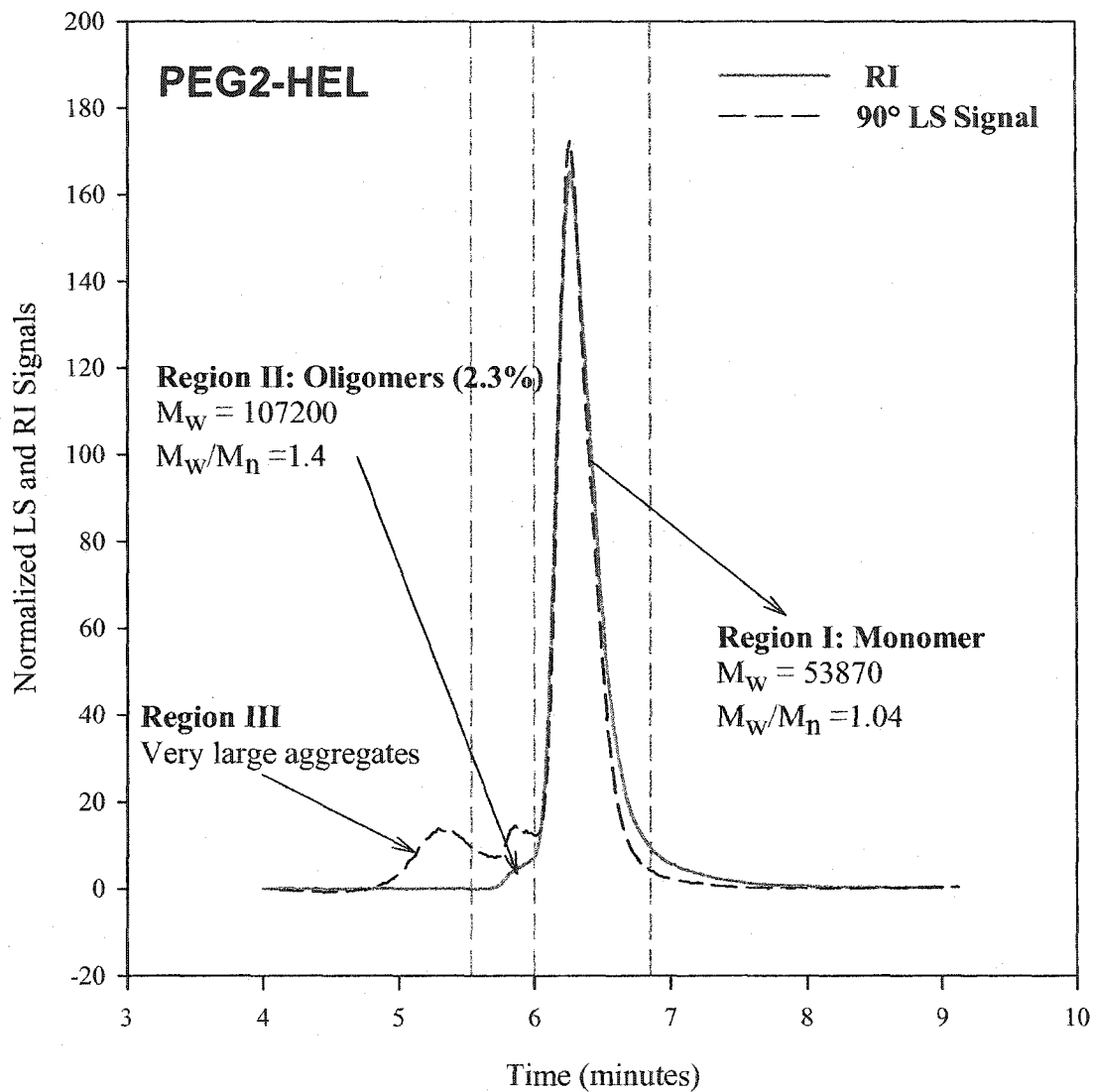


Figure 15. Size Exclusion-HPLC coupled Static Light Scattering analysis of PEG2-HEL.
 Experiments were conducted in a HP 1100 HPLC system with simultaneous RI and 90° LS detection.
 The weight average molecular weight of the PEG2-HEL monomer (Region I) was determined to be 53870.



For a truly monodisperse system, the PDI or the ratio M_w/M_n is equal to 1 and increases as the molecular weight distribution of a sample broadens. The polydispersity in the PEG and PEG-HEL samples was quantified by calculating the PDI in both chromatographic regions (I & II).

The weight average molecular weights of PEG, PEG1-HEL, PEG2-HEL, and their polydispersity indices (Region I) are presented in Table 10 along with the molecular weights of their aggregates and PDIs (Region II). The SLS molecular weights are also presented alongside the MALDI results below in Table 11 for comparison.

Table 10: Results from the static light scattering analysis of PEG, PEG1-HEL, and PEG2-HEL

Molecule	dn/dc	Expected molecular weight	Region I		Region II	
			M_w	M_w/M_n	M_w	M_w/M_n
PEG	0.136	20,000	21,470	1.03	344,000	1.37
PEG1-HEL	0.149	34,305	34,430	1.03	167,800	1.28
PEG2-HEL	0.142	54,305	53,870	1.04	107,200	1.40

Table 11: Comparison of the molecular weights of PEG, PEG1-HEL, and PEG2-HEL determined using MALDI-TOF and static light scattering measurements

Molecule	Molecular weight (Daltons)		
	Expected	MALDI-TOF	SLS
PEG	20,000	~21,900*	21,470
PEG1-HEL	34,305	36,280	34,430
PEG2-HEL	54,305	58,200	53,870
PEG3-HEL	74,305	79,800	ND

ND – Not determined

* - Molecular weight estimated by subtraction of the protein molecular weight in each of the three species

As seen from the above tables, the molecular weights of the PEG, PEG1-HEL and PEG2-HEL monomers are in excellent agreement with their respective expected, nominal molecular weights and with the MALDI-TOF results (within 5 – 8 %). Further, all three

monomeric species are observed to have a very narrow molecular weight distribution as demonstrated by their respective polydispersity indices, which are very close to 1.

The molecular weights of the aggregates in Region II of PEG1-HEL and PEG2-HEL suggest non-covalent oligomers (pentamers in PEG1-HEL and dimers in PEG2-HEL) to be present in the two samples. The aggregated species have a broader molecular weight distribution as indicated by their higher PDI values. The large impurity present in PEG reagent appears to be approximately a 16-mer based on its molecular weight of 344,000.

The light scattering signal is exquisitely sensitive to the presence of large aggregates as can be seen from Region III in each of the three chromatograms (Figure 13 - Figure 15). Although undetected by the UV and/or RI detectors, these aggregates contribute to a significant light scattering signal. It should be noted that while the UV and RI signals are directly proportional to the solute concentration in dilute solutions, the light scattering signal is directly proportional to the product of the concentration and the molecular weight of a species (Equation 1). This indicates that the aggregates in Region III are extremely large; the molecular weight of these species was approximated to be in excess of 10 million Daltons.

As demonstrated above, Static Light Scattering coupled Size Exclusion -HPLC (SLS-SE-HPLC) is a powerful technique that is very effective in the characterization of PEG-proteins.

3.1.3.3 Sedimentation Velocity Experiments

Sedimentation velocity is a classical technique employed for studying the hydrodynamic behavior of proteins. Useful information about the shape of a protein (or

macromolecule) in solution can be obtained by measuring its sedimentation (s) and diffusion (D) coefficients. The sedimentation behavior of PEGylated HEL molecules will be discussed in greater detail in Section 3.2. Here, the discussion will be limited to the determination of molecular weights using sedimentation velocity. As presented earlier in Section 2.10, the Svedberg Equation (Equation 10) relates the sedimentation and diffusion coefficients of a molecule to its molecular weight. This relationship was employed to determine the molecular weights for HEL and the various PEG-HEL molecules. Molecular weights were determined by simply substituting the respective experimentally determined 's' and 'D' values into the Svedberg equation.

$$\frac{s}{D} = \frac{M_w(1 - \bar{v}\rho)}{RT} \quad (10)$$

The partial specific volume of HEL, \bar{v} , was calculated based on its amino acid sequence. The \bar{v} values for the PEG-HEL molecules were calculated by employing the weighted approach described in Section 2.9. An experimentally determined value of the \bar{v} of 20 kD PEG was used in computing the weight averaged value. The partial specific volumes of various PEG molecules determined in 25 mM phosphate and 125 mM NaCl, pH 7.5 (Table 12).

Table 12: Partial specific volume of different PEG molecules with varying chain lengths and/or branching measured in 25 mM phosphate, 125 mM NaCl, pH 7.5.

Lot #	PEG Type	Linker chemistry	Nominal MW (kD)	Concentration (mg/mL)	\bar{v} (mL/g)
PT-088-01	Linear	Aldehyde	5	10.00	0.840
PT-03A-34	Branched	NHS ester	2 x 10	10.10	0.836
PT-089-24	Linear	Aldehyde	20	10.01	0.835
PT-079-02	Linear	Aldehyde	30	10.03	0.839
ZF-129-01	Branched	Aldehyde	2 x 20	9.99	0.831

The partial specific volume values of PEG in Table 12 are in excellent agreement (within 1 %) with previously published values of \bar{v} for the polymer. In particular, a \bar{v} value of 0.832 has been reported for the 20 kD PEG by Lepori *et al.* [68] which is in superb agreement with the values of 0.835 & 0.836 measured in the present study for two, different 20 kD PEG molecules.

An important point to note is that in the case of PEG-HEL molecules, both s and D were observed to exhibit a dependence on protein concentration, which is indicative of non-ideality effects. To account for this, the molecular weights of PEG1-HEL and PEG2-HEL were calculated using sedimentation and diffusion coefficient values extrapolated to infinite dilution (s° and D°). Unfortunately, s° and D° values could not be obtained for PEG3-HEL due to limited sample availability. As a result an accurate estimate of the molecular weight of PEG3-HEL could not be determined using this technique.

The relevant sedimentation data employed to determine the molecular weight of the various molecules is presented below in Table 13. The molecular weights determined using sedimentation velocity are presented in Table 14 along with the SLS and MALDI-TOF results to facilitate comparison.

Table 13: Summary of the sedimentation velocity data used to determine the molecular weights of HEL and various PEG-HEL molecules

Molecule	Sedimentation coefficient s or s°	Diffusion coefficient (D or $D^\circ \times 10^7 \text{ cm}^2/\text{s}$)	Partial specific volume	Molecular weight
HEL	1.81 (s)	10.9 (D)	0.718	14540
PEG1-HEL	1.18 (s°)	4.17 (D°)	0.785	32840**
PEG2-HEL	1.25 (s°)	3.00 (D°)	0.803	52940**
PEG3-HEL	1.00 (s)	1.59 (D)	0.811	(83840) _{0.6} ***

** - Molecular weights determined using s and D values extrapolated to infinite dilution

*** - Molecular weight determined at 0.6 mg/mL PEG-protein concentration

Table 14: Comparison of the molecular weights of HEL, PEG, and various PEG-HEL molecules determined using MALDI-TOF, static light scattering (SLS) and sedimentation velocity (SV) measurements

Molecule	Molecular weight (Daltons)			
	Expected	MALDI-TOF	SLS	SV
HEL	14305	ND	ND	14540
PEG	20000	~21900	21470	ND
PEG1-HEL	34305	36280	34430	32840**
PEG2-HEL	54305	58200	53870	52940**
PEG3-HEL	74305	79800	ND	(83840) _{0.6} ***

ND – Not determined

* - Molecular weight estimated by subtraction of the protein molecular weight in each of the three species

** - Molecular weights determined using s and D values extrapolated to infinite dilution

*** - Molecular weight determined at 0.5 mg/mL PEG-protein concentration

As seen from the above table, the molecular weight of HEL determined by sedimentation velocity is within 2 % of its sequence molecular weight. Further, the molecular weights of PEG1-HEL and PEG2-HEL are in excellent agreement with the values determined by MALDI-TOF (within 10 %) and static light scattering measurements (within 3 %). It should be noted that the molecular weight of PEG3-HEL has not been corrected for concentration effects as done in the case of PEG1-HEL and PEG2-HEL. The concentration dependence of the molecular weights of PEG1-HEL and PEG2-HEL determined using velocity experiments is presented in Figure 16. As seen from the figure, the concentration dependence appears to increase with increasing degree of PEGylation. For PEG1-HEL, the molecular weight decreases by ~ 10000 per mg/mL of the PEG-protein, while a much stronger dependence of ~ -30000/ mg/mL is observed in the case of PEG2-HEL. The cause of the observed concentration dependence is rooted in the non-ideality effects on the sedimentation and diffusion coefficients and is discussed in greater detail in Section 3.2. The point relevant to this discussion is that the molecular weight of 83850 for PEG3-HEL was determined at a protein concentration of 0.5 mg/mL and is most likely to be a over estimate by at least 10 %.

In general, the sedimentation coefficient of a molecule can be more reliably measured than its diffusion coefficient via sedimentation velocity experiments [60]. This is because the sedimentation coefficient is measured by following the mid-point of sedimentation boundary, while the diffusion coefficient is estimated from the shape of the sedimentation boundary. The boundary shape is very sensitive to sample heterogeneity and non-ideality effects, which can introduce a significant error in the determination of the diffusion coefficient. In the present case, the non-ideality effects were accounted for by extrapolating the s and D values to infinite sample dilution and by doing so excellent estimates of the molecular weights are obtained. Conversely, this suggests that the PEG1-HEL and PEG2-HEL samples are minimally heterogeneous and the diffusion coefficients measured for these molecules are fairly accurate, within 5 -10 % of their actual values.

3.1.4 Effect of PEGylation on the Secondary Structure of HEL

The effect of PEGylation on the secondary structure of HEL was examined using far-UV circular dichroism studies. The far-UV CD spectra of HEL, PEG1-HEL, and PEG2-HEL are presented in Figure 17. A spectrum of PEG3-HEL could not be obtained due to limited sample availability. As seen from Figure 17, the mean residual weight ellipticities (θ_{MRW}) of all three molecules are coincidental over the entire wavelength range of 195 nm to 260 nm. PEGylation appears to have no effect on the secondary structure of HEL.

Figure 16. The effect of sample concentration on the molecular weights of PEG1-HEL and PEG2-HEL determined by sedimentation velocity experiments. Experiments conducted at 20 °C in 25 mM phosphate, 125 mM NaCl, pH 7.5.

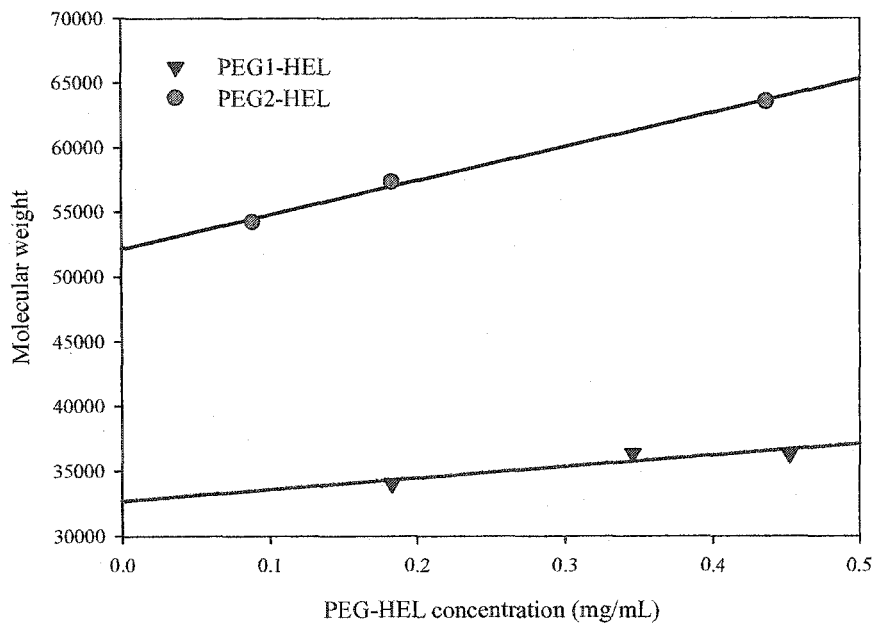
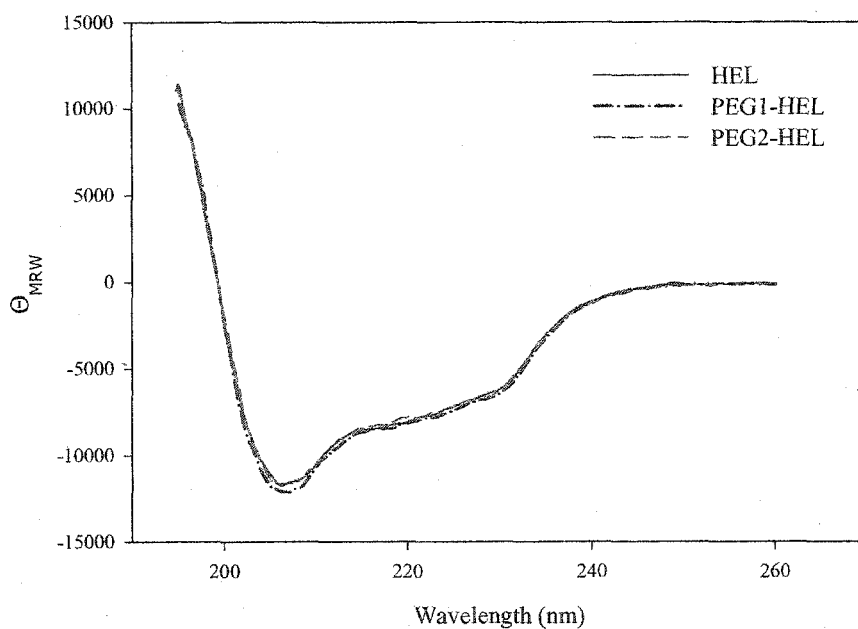


Figure 17. Far-UV CD Spectra of HEL, PEG1-HEL, and PEG2-HEL. Experiments were conducted with 0.2 mg/mL HEL, 0.17 mg/mL PEG1-HEL, 0.2 mg/mL PEG2-HEL respectively in 25 mM sodium phosphate, 125 mM NaCl, pH 7.5 at room temperature.



3.1.5 Effect of PEGylation on the Tertiary Structure of HEL

Fluorescence and near-UV CD spectroscopy were employed to study the effect of PEGylation on the tertiary structure of HEL. As with the far-UV CD studies, experiments could not be performed with PEG3-HEL due to limited sample availability. The near-UV CD and fluorescence spectra of HEL, PEG1-HEL, and PEG2-HEL are presented in Figure 18 & Figure 19 respectively.

The near-UV CD signature of HEL is comprised of three, positive peaks at 294, 288 & 282 nm, and by a negative plateau between 262 to 255 nm [69]. The three peaks are attributed to contributions from tryptophans and tyrosines, while the negative plateau is attributed to the disulfide bonds in the protein. The near-UV CD spectrum of HEL presented in Figure 18 is consistent with the above description.

However, as seen from Figure 18, a decrease in the intensity of all the three peaks in the 280–295 nm region is observed for PEG1-HEL and PEG2-HEL. This difference may suggest a subtle conformation change in the tertiary structure of the PEG-HEL molecules. Alternatively, the change could also be due to an interaction between the PEG and a hydrophobic patch on the protein surface containing tryptophans and/or tyrosines. Importantly, any gross conformational change such as protein unfolding can be ruled out based on these near-UV CD data. This is because HEL unfolding is accompanied by an increase in the intensity of the three positive peaks in its near-UV CD spectrum [69].

Figure 18. Near-UV-CD Spectra of HEL, PEG1-HEL, and PEG2-HEL. Experiments were conducted with 0.4 mg/mL HEL, PEG1-HEL, PEG2-HEL respectively in 25 mM sodium phosphate, 125 mM NaCl, pH 7.5 at room temperature.

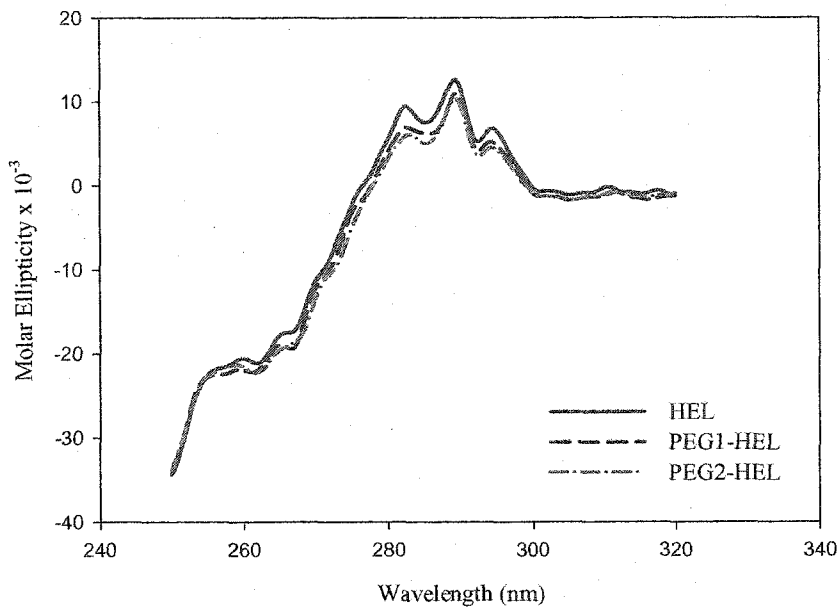
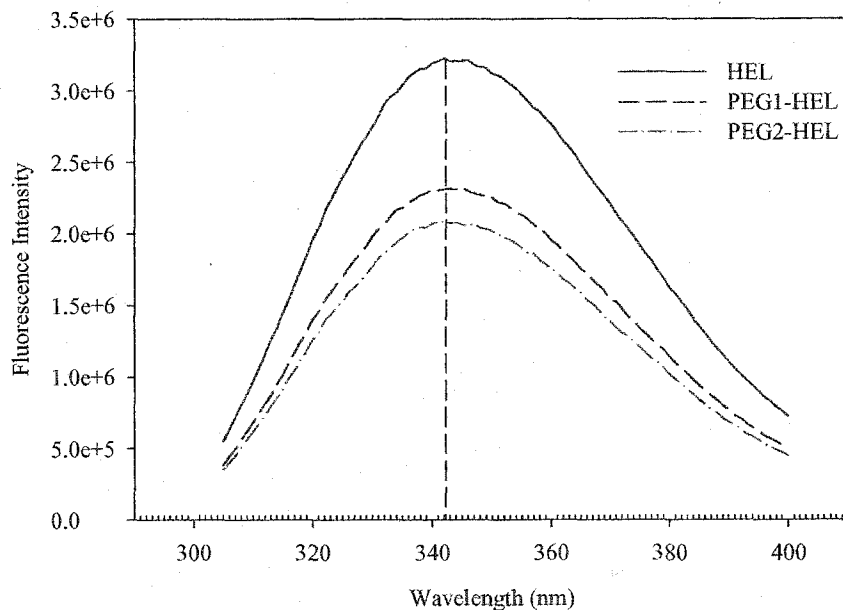


Figure 19. Fluorescence emission spectra of HEL, PEG1-HEL, and PEG2-HEL. Experiments were conducted with 0.4 mg/mL HEL, PEG1-HEL, & PEG2-HEL respectively in 25 mM sodium phosphate, 125 mM NaCl, pH 7.5 using an excitation wavelength of 295 nm.



The effect of PEGylation on the tertiary structure of HEL also was studied by determining the fluorescence emission of tryptophans. Fluorescence emission spectra of HEL, PEG1-HEL, and PEG2-HEL were recorded using an excitation wavelength of 295 nm, which is selective for tryptophans. As seen in Figure 19, HEL is observed to exhibit a broad emission spectrum with a peak maximum at 342 nm. This is consistent with previously published fluorescence data for HEL [70].

PEG1-HEL and PEG2-HEL are also observed to exhibit similar emission spectra with a λ_{max} of 342 nm, however, significant signal quenching is observed in the case of both PEGylated molecules. Further, the quenching appears to increase with increasing degree of PEGylation. It should be noted that the magnitude of change is highest between the native HEL and PEG1-HEL; a smaller change is observed between PEG1-HEL and PEG2-HEL. The λ_{max} of 342 nm, being unchanged for both PEG1-HEL and PEG2-HEL, suggests that there is no major change in the local environment of the tryptophans such as that caused by protein unfolding. For example, if the PEGylated molecules were partially unfolded, then one would expect a red shift of the λ_{max} in their emission spectra. The shift is caused by the exposure of buried tryptophans to the polar, bulk water. In fact, HEL unfolding has been routinely studied by monitoring the red shift of its emission maximum [71]. The fluorescence data in Figure 19, however, do suggest a possible subtle change in the local environment of the protein tryptophans.

Although HEL has a total of six tryptophans, only two - Trp₁₀₈ and Trp₆₂ have been shown to be the major contributors to its fluorescence signal [70]. The Trp₁₀₈, is caged beneath the protein surface and is partially solvent exposed with a λ_{max} of 342 nm, while Trp₆₂ is located in the active site and is completely solvent exposed with a λ_{max} of

350 nm. Thus, the possibilities for the observed quenching are limited to these two tryptophans. The quenching could be caused by: (i) a subtle, local conformational change near either one of the two tryptophans, (ii) a specific interaction involving PEG and the solvent exposed Trp₆₂, or (iii) slower tumbling times of the PEGylated molecules given their greatly enhanced hydrodynamic radii.

Interestingly, Furness *et al.* [72] have reported the presence of a weak, hydrophobic binding site for PEG on the HEL surface involving the solvent exposed tryptophan (Trp₆₂). Further, Kerwin *et al.* [73] have reported the ability of covalently attached PEG chains to modify the local surface structure of the Type I soluble tumor necrosis factor (sTNF – R1) that is away from the site of PEG attachment. Therefore, with respect to PEG-HEL, it is possible that the quenching is a result of PEG-Trp₆₂ interaction. However, such an interaction would be hydrophobic in nature and one would expect a blue shift in the fluorescence spectrum. An example of binding induced spectral shifts in HEL is that of N-acetyl-D-glucosamine trimer [(NAG)₃] binding to the HEL active site. In this case, a decrease in signal intensity was observed along with a blue shift of the emission spectrum [70].

Although improbable, the possibility of a PEG-binding induced fluorescence quenching cannot be eliminated based on the presented data. Additional experiments are required to better understand the observed fluorescence quenching. It should be noted that the near-UV CD and fluorescence studies were designed mainly to determine the presence of any PEGylation induced conformational changes in HEL. The results of these studies indicate that PEGylation does not cause any gross conformational changes in

HEL; however, the presence of subtle, localized conformational changes cannot be ruled out.

3.2 Hydrodynamic Behavior of PEG

Dynamic light scattering was employed to study the solution behavior of polyethylene glycol. The hydrodynamic or Stokes radii (R_h) of five PEG molecules with different chain lengths and/or branching are presented in Table 15. As mentioned earlier (Section 1.3), macromolecules of the size of serum albumin (36 Å) or larger are believed to be well retained by the glomerulus and hence can avoid elimination via renal filtration [31]. From Table 15 one can see that while the Stokes radius of the 5 kD PEG is ~ 20 Å and below the cut-off size of 36 Å, the Stokes radius of the 20 kD PEG is much larger ~ 43 Å and is well above the cut-off limit. This indicates that the attachment of a single, 20 kD PEG chain (or larger) should be sufficient to enhance the in-vivo half life of a small protein. In contrast, several 5 kD PEG chains may be required to achieve the same outcome.

Table 15: Hydrodynamic radii of PEG molecules of varying chain lengths

PEG Type	Linker chemistry	Nominal MW (kD)	Concentration (mg/mL)	Hydrodynamic radius (R_h) [*] (nm)	Calculated Mw (kD)
Linear	Aldehyde	5	5.3	2.2 ± 0.2	5,090 ± 530
Linear	Aldehyde	20	5.3	4.3 ± 0.1	19,020 ± 650
Branched	NHS ester ^{**}	2 x 10	7.2	4.3 ± 0.2	19,400 ± 1590
Linear	Aldehyde	30	5.3	5.3 ± 0.04	28,890 ± 840
Branched	Aldehyde	2 x 20	5.1	6.0 ± 0.2	38,180 ± 1520

* - Each value is an average of 10 measurements

** - Values calculated using the relationship $MW = k \times R^2$ for random coils

*** - Ester of N-hydroxysuccinimide

The covalently attached polymer chain(s) of a PEG-protein can interfere directly or sterically with its activity. In addition, the likelihood of a decrease in protein activity increases with an increasing degree of PEGylation. For this reason, PEGylation with a single large PEG chain of 20 kD or larger should be preferred over the attachment of multiple, smaller molecular weight PEG molecules. A single large PEG chain will provide the desired sustained duration effect in the circulatory system while minimizing the likelihood of reducing protein activity.

The hydrodynamic data presented in Table 15 were also employed to study the solution conformation of polyethylene glycol. The molecular weight of molecules with defined solution conformations such as rods, random coils, and spheres can be correlated to their Stokes radii by the following relationship

$$M_w = k \cdot R_h^n \quad (21)$$

where k is constant of proportionality, and the power n assumes a value of 1 for long rods, 2 for random coils, and is 3 in the case of spheres. Information about the conformation of a particular type of molecule can be obtained by determining the value of n for a set of such molecules. In the present case, the value of n for PEG was determined by constructing a plot of the natural log of R_h versus the natural log of the nominal molecular weights of the five PEG molecules. The slope of this plot was the reciprocal of the power - n in equation 21. The Stokes radii in Table 15 were utilized to construct such a log-log plot (Figure 20). As seen from Figure 20, a very good linear fit to the data is obtained ($r^2 = 0.999$). The value of n was determined to be 2.07, which demonstrates that PEG exhibits a near random coil behavior in solution.

The above result is supported by the molecular weight data presented in the sixth column of Table 15. The molecular weights were calculated by employing Equation 21, assuming a random coil behavior for PEG ($n = 2$) and using a pre-programmed value of k in the instrument software. As can be seen, the calculated molecular weights for all five PEGs are in excellent agreement with their respective nominal molecular weight values.

Another important observation is that the two 20 kD & 40 kD branched PEGs, each made up of two 10 kD PEG or 20 kD PEG chains, also exhibit a random coil behavior. In fact, the hydrodynamic radius of the 20 kD branched, bi-PEG is identical to that of its linear counterpart. This result is in contrast to previous suggestions by others [74, 75] who have proposed that a bi-PEG may possess a larger hydrodynamic radius (or volume) in comparison to its linear counterpart of equal molecular weight. For such a suggestion to be valid, one would expect a departure from the random coil behavior of the PEG as a result of branching. However, both branched bi-PEGs examined in this study were observed to exhibit random coil behavior. This suggests that any rigidity that may be introduced in the polymer backbone at the point of branching plays an insignificant role in the overall conformation of the polymer. The suggestion [74, 75] that a bi-PEG possesses a larger R_h in comparison to its linear counterpart is incorrect. Branching at a single point may have no effect on the overall solution conformation of polyethylene glycol.

3.3 Effect of PEGylation on the Hydrodynamic Behavior of HEL

Sedimentation Velocity (SV) and Dynamic Light Scattering (DLS) were employed to study the hydrodynamic behavior of HEL and the various PEGylated HEL molecules.

3.3.1 Effect of PEGylation on the Sedimentation Properties of HEL

Sedimentation velocity experiments were conducted with HEL, PEG1-HEL, PEG2-HEL, and PEG3-HEL at 50,000 rpm and 20 °C. The differential sedimentation coefficient distribution function – $g(s^*)$ versus the apparent sedimentation coefficient – s^{*6} plot for HEL and all three PEG-HEL molecules is presented in Figure 21. The sedimentation coefficients determined from the $g(s^*)$ versus s^* analysis at their respective protein concentrations are presented in Table 16.

Table 16. s^* values of HEL, and various PEG-HEL molecules determined using $g(s^*)$ versus s^* analysis

Molecule	Concentration (mg/mL)	s^* (svedberg)
HEL	0.73	1.83
PEG1-HEL	0.45	1.11
PEG2-HEL	0.45	1.02
PEG3-HEL	0.54	0.97

⁶ The term apparent sedimentation coefficient – s^* is used because the s value has not been corrected for concentration effects.

Figure 20. A plot between the natural log of the Stokes radii versus the molecular weights of the five PEG molecules for studying the solution behavior of PEG

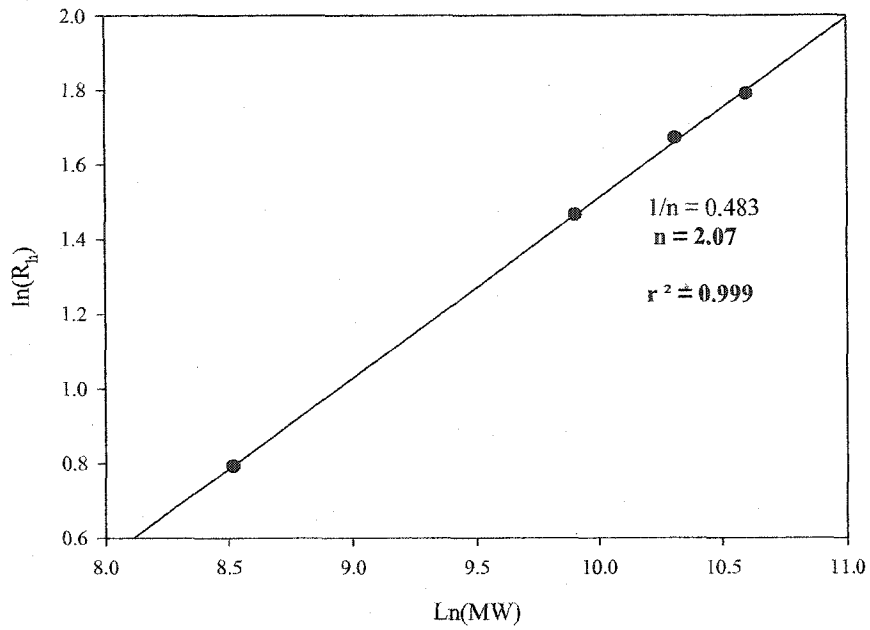
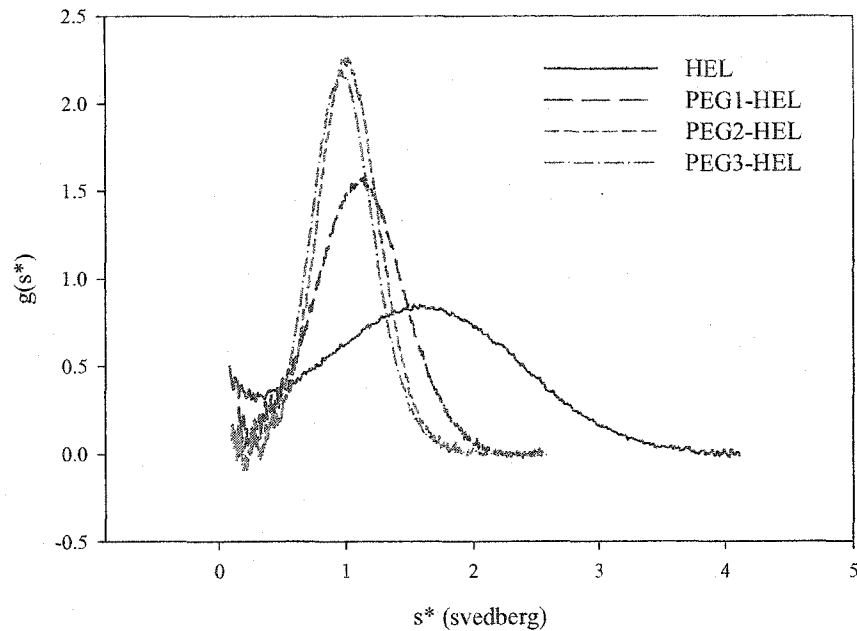


Figure 21. $g^*(s^*)$ analysis of HEL, PEG1-HEL, PEG2-HEL, and PEG3-HEL. Sedimentation velocity experiments were conducted at 50,000 RPM and 20 °C in a Beckman XL-I analytical ultracentrifuge using absorbance optics.



As seen from Table 16, the sedimentation coefficients of all three molecules are observed to decrease in comparison to the native HEL. Although the molecular weights of the three PEG-HEL molecules are significantly different, their sedimentation coefficient values are very close to each other (within 0.15 s units). The distribution functions of three PEG-HEL molecules also are almost coincident. It should be noted that the SV experiments with the three PEGylated HEL molecules were conducted at similar protein concentrations (within 0.1 mg/mL) as shown in Table 16 and hence the results are amenable to comparative analysis.

The above observations are consistent with those made in previously conducted SV studies with PEG-HRP and PEG-rhDNase-I (discussed in Section 1.3) [40]. Briefly, a similar decrease in the sedimentation coefficient was observed upon the PEGylation of both horseradish Peroxidase (HRP) and recombinant human deoxyribonuclease – I (rhDNase-I) [40]. Further, although both PEG-HRP and PEG-DNase-I samples were heterogeneous and contained a mixture of mono, di and tri-PEGylated species, a unimodal $g(s^*)$ pattern consistent with a pure, homogenous species was observed in both cases [40]. On this basis, it was hypothesized that the increase in molecular mass for the higher order PEGylated PEG-HRP and PEG-rhDNase-I species was almost exactly compensated by an increase in the frictional coefficient of these molecules. Consequently the sedimentation coefficient remained unchanged with an increasing degree of PEGylation.

The unimodal and coincidental $g(s^*)$ patterns observed in the case of the purified PEG1-HEL, PEG2-HEL, and PEG3-HEL molecules are consistent with this hypothesis. The increase in frictional drag due to the attachment of the first PEG molecule results in a

significant decrease in the sedimentation coefficient of HEL. For subsequent PEG attachments, the increase in frictional drag is canceled out by the increase in mass. The net result is a relatively invariant sedimentation coefficient. The coincidental $g(s^*)$ patterns also indicate that the heterogeneity within a given PEG-protein mixture will be poorly resolved by sedimentation velocity analysis.

Useful insights can be gained into the solution conformation of the PEGylated HEL molecules from the SV and DLS studies of the various PEG-HEL and PEG molecules. The hydrodynamic behavior of the PEGylated HEL molecules appears to be governed completely by the PEG as observed in the SV studies. The covalently attached PEG chains have a “parachute” like effect on the sedimentation of these molecules which causes an increase in their frictional drag. Thus, it is unlikely that a PEG-protein has a compact conformation in solution such as one in which the PEG chain(s) are wrapped around the protein molecule. Such a conformation would cause an increase in the sedimentation coefficient of the molecule. The hydrodynamic data of PEG suggest a random coil like conformation for the PEG-HEL molecules. The randomly coiled PEG chains can be imagined to be hanging freely in solution with one end covalently tethered to the protein.

3.3.2 Hydrodynamic Nonideality

Sedimentation velocity experiments also were conducted as a function of PEG1-HEL and PEG2-HEL concentration to detect any hydrodynamic non-ideality effects. Experiments as a function of PEG3-HEL concentration could not be performed because of limited sample availability. These studies revealed the presence of hydrodynamic non-ideality of both PEG1-HEL and PEG2-HEL. The effect of protein concentration on the

sedimentation and diffusion coefficients of PEG1-HEL and PEG2-HEL are presented in Figure 22 and Figure 23. The s and D values in these figures were determined using the program SVEDBERG. Both sedimentation and diffusion coefficients are observed to increase with decreasing concentration. The hydrodynamic non-ideality, which manifests itself in terms of the concentration dependence of s and D , is observed to increase with increasing degree of PEGylation. For PEG1-HEL the s and D values are observed to increase by $0.045 \text{ s}/(\text{mg}/\text{mL})$ and $1.11 \times 10^{-7} \text{ (cm}^2/\text{s})/(\text{mg}/\text{mL})$ respectively. In the case of PEG2-HEL, the rate of increase in s is 10-fold higher at $0.46 \text{ s}/(\text{mg}/\text{mL})$, while the rate of increase in D is almost two-fold higher at $2.1 \times 10^{-7} \text{ (cm}^2/\text{s})/(\text{mg}/\text{mL})$. The non-ideality is caused by weak, repulsive interactions between molecules resulting from a concentration polarization at the sedimentation boundary. These repulsive interactions lead to retardation and sharpening of the sedimentation profiles [76]

Even in the presence of these non-ideality effects, very good estimates of both sedimentation and diffusion coefficients were obtained by extrapolation of S & D to infinite dilution. The numerical values of s and D at different protein concentrations and at infinite dilution determined using two different software programs –SVEDBERG and DCDT + are presented in Table 17. As can be seen, the s values determined from both programs are nearly identical, while the diffusion coefficient values are within 5 % of each other.

Figure 22. Effect of concentration on the sedimentation coefficient of PEG1-HEL and PEG2-HEL. Sedimentation velocity experiments were conducted in 25 mM phosphate, 125 mM NaCl, pH 7.5 at 50,000 RPM and 20 °C in a Beckman XL-I analytical ultracentrifuge using absorbance optics.

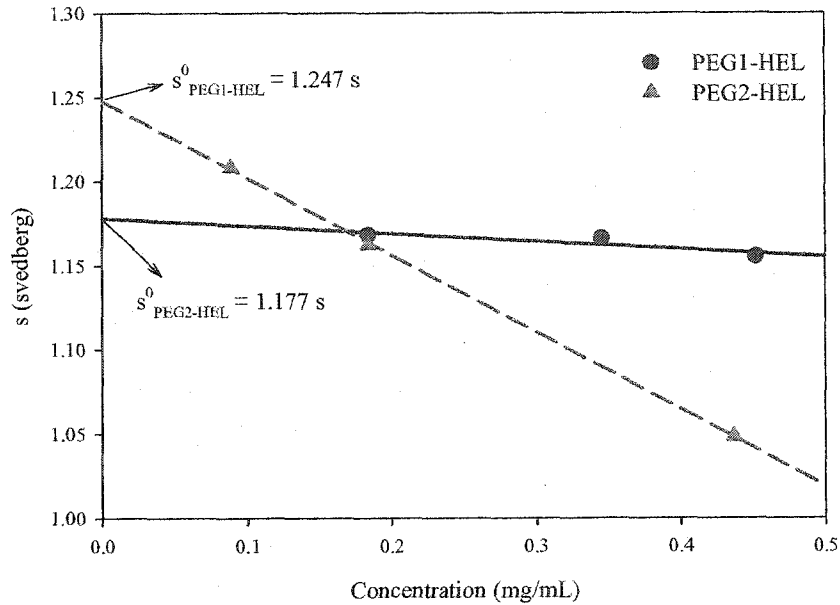
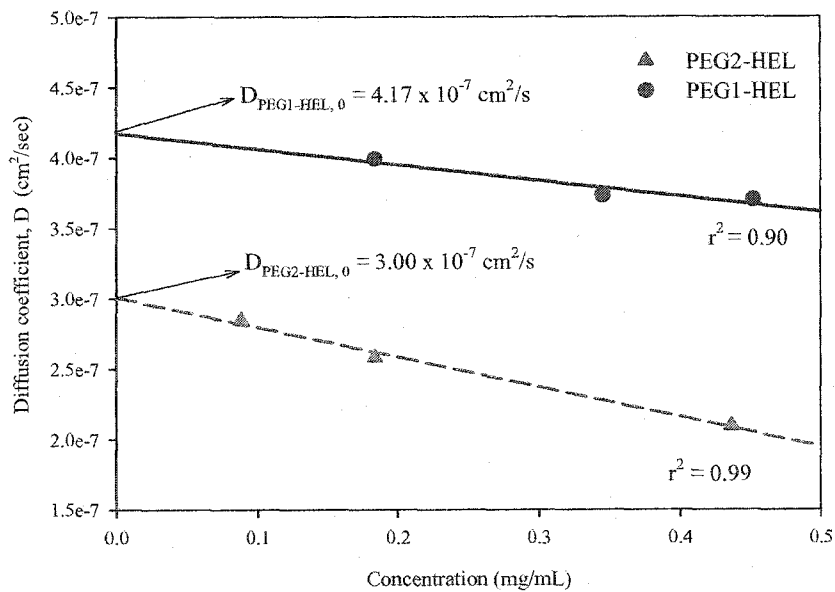


Figure 23. Effect of concentration on the diffusion coefficient of PEG1-HEL and PEG2-HEL. Sedimentation velocity experiments were conducted in 25 mM phosphate, 125 mM NaCl, pH 7.5 at 50,000 RPM and 20 °C in a Beckman XL-I analytical ultracentrifuge using absorbance optics.



In sedimentation velocity, the diffusion coefficient is determined from the shape of the sedimentation velocity profiles, which can be skewed even by small amount of heterogeneity. Hence, the estimation of D via SV analysis is prone to a greater error. Even so, there is excellent agreement between the D values from the two methods. The accuracy of s and D values can be independently validated by calculating the molecular weights using the extrapolated values of s and D and the Svedberg equation (Equation 10) as demonstrated in Section 3.1.3.3.

Table 17. s and D values of PEG1-HEL and PEG2-HEL determined at different protein concentrations using the software programs SVEDBERG and DCDT+

Molecule	Concentration (mg/mL)	s (Svedberg)		D x 10 ⁷ (cm ² /sec)	
		SVEDBERG	DCDT+	SVEDBERG	DCDT+
PEG1-HEL	0.45	1.16	1.15	3.70	3.81
	0.35	1.17	1.16	3.73	4.00
	0.18	1.17	1.17	3.99	4.16
	1/∞	1.18	1.18	4.17	4.41
PEG2-HEL	0.44	1.05	1.04	2.09	2.15
	0.18	1.16	1.15	2.58	2.69
	0.09	1.21	1.21	2.84	2.97
	1/∞	1.25	1.25	3.00	3.15

3.3.3 Hydrodynamic Radii of HEL and PEGylated HEL Molecules

The diffusion coefficients of HEL, PEG1-HEL and PEG2-HEL also were used to calculate the Stokes radii of these molecules using Equations 11 and 12. These R_h values are presented in Table 18. It should be noted that extrapolated D^o values were used in the case of PEG1-HEL and PEG2-HEL to calculate R_h. Dynamic light scattering was also

employed as an orthogonal technique to determine the Stokes radii of the various molecules. The DLS data are also presented in Table 18.

Table 18. Stokes radii of HEL and various PEG-HEL molecules determined from sedimentation velocity and DLS experiments

Molecule	Sedimentation Velocity		Dynamic Light Scattering		
	Conc. (mg/mL)	R_h (Å)		Conc. (mg/mL)	R_h (n) [*] (Å)
		SVEDBERG	DCDT [†]		
HEL	0.73	19.7	19.2	2	20.7 ± 1 (8)
PEG1-HEL	1/∞	50.1	47.4	1	48.0 ± 1 (18)
PEG2-HEL	1/∞	69.7	66.3	1	66.3 ± 2 (22)
PEG3-HEL	Not determined			0.5	73.8 ± 2 (6)

* n = number of measurements

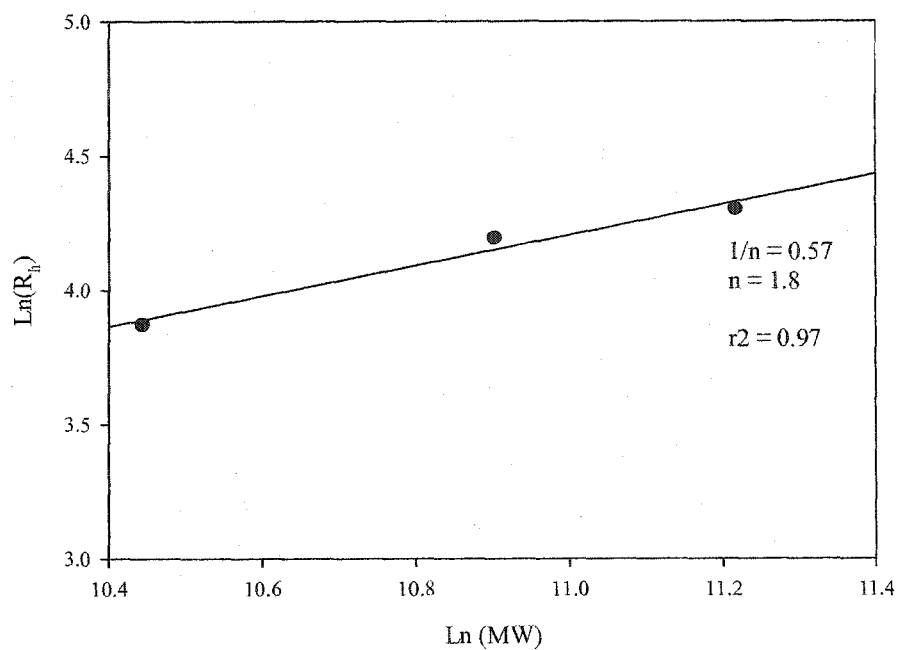
The Stokes radii values for each molecule as determined from SV and DLS methods are in excellent agreement (within 5 %) with each other. In addition, the Stokes radius of HEL determined in the present study is consistent with its previously published value of 19.3 Å based on DLS measurements [47]. Interestingly, while the DLS measurements for PEG1-HEL and PEG2-HEL were made at a concentration of 1 mg/mL for both molecules, the values computed from SV results are those at infinite dilution. Still, there is excellent agreement between the values determined from the two orthogonal methods. This demonstrates that the hydrodynamic non-ideality observed in the SV studies in terms of the concentration dependence of D is particular to this method of measurement. No thermodynamic non-ideality effect can be discerned at these concentrations.

As seen in Table 18, the R_h of HEL increases by 2.5-fold upon modification with a single 20 kD PEG chain (from ~ 20 Å to ~ 50 Å). The R_h of the triPEGylated species is

even greater at $\sim 75 \text{ \AA}$. However, the attachment of a single PEG chain appears to be sufficient for avoiding renal filtration. The Stokes radii of the PEGylated HEL molecules also shed light on their solution conformation. In comparing the Stokes radii of the 20-kD PEG polymer and the monoPEGylated HEL molecule, one can observe that the R_h of the PEG1-HEL ($48 - 50 \text{ \AA}$) is only marginally greater than that of the 20-kD PEG polymer (43 \AA). Similarly, the Stokes radius of PEG2-HEL of $\sim 67 - 70 \text{ \AA}$ is only about 10 % greater than the 40 kD branched bi-PEG. The diPEGylated, PEG2-HEL species can be imagined to be PEGylated with a 40-kD bi-PEG consisting of two 20-kD branches. These data provide further evidence that the covalently tethered PEG predominantly governs the solution conformation of a PEGylated protein, and that the PEG remains a random coil.

Additional evidence for a random-coil like conformation of the PEG-HEL molecules is obtained by plotting the natural log of the molecular weights of the three PEG-HEL molecules versus their respective Stokes radii to obtain a value for the exponent - n in Equation 21. Such a plot is presented in Figure 24. The nominal molecular weights of the three species and the R_h values from the DLS data were used to construct this plot. This was done because a good estimate of the weight average molecular weight of PEG3-HEL could not be obtained and the weight average molecular weights of PEG1-HEL and PEG2-HEL are within 5 % of the nominal weights values. The value of n was determined to be 1.8 from the slope of the plot, and as discussed earlier (Section 3.2), the value of n is 2 for a perfect random coil behavior. This provides additional support for the random coil like behavior for PEG-proteins.

Figure 24. A plot between the natural log of the Stokes radii versus the natural log of the nominal molecular weights of the three PEG-HEL molecules



3.4 Equilibrium Thermal Unfolding Studies

The thermal unfolding studies were geared towards understanding the thermodynamic component of the aggregation reaction presented in Reaction Scheme I (Section 1.2).



The principal objective was to determine the effect of PEGylation on the melting or transition temperature of the unfolding reaction. To achieve this, the thermal unfolding studies were conducted in three stages.

In the first stage of study, the thermal unfolding of native HEL was studied using two different methods: (i) the spectroscopic Difference Spectrum (DS) method, and (ii) Differential Scanning Calorimetry (DSC). Here, the focus was on establishing appropriate study conditions and comparing the thermodynamic parameters determined from the two methods. These studies formed the ‘control’ experiments for the second and third stages of study.

The thermal unfolding of HEL was studied in the presence of high concentrations of PEG (10 –30 % w/v) in the second stage. Studies were conducted with PEG 400 and PEG 20000. Polyethylene glycol 400 was employed to reproduce the thermal unfolding experiments conducted by Lee *et al* [28] as their work provided the framework for the hypothesis tested in the present research. PEG 20000 was employed to facilitate comparative analysis; its effect on HEL unfolding when present as a component of the solvent would be directly compared to its effect when covalently attached to the protein.

In the third stage, the effect of PEGylation on the unfolding thermodynamics of HEL was studied. Both DSC and the DS method were employed to study the unfolding of

PEG1-HEL and PEG2-HEL. The thermal unfolding of PEG3-HEL was studied using only the DS method due to limited sample availability.

3.4.1 Thermal Unfolding Studies of Hen Egg Lysozyme

The results of the thermal unfolding of HEL, studied using the DS method and DSC are discussed below.

3.4.1.1 Difference Spectrum Method

The thermal unfolding studies were conducted at three different concentrations of HEL (0.5 – 1.25 mg/mL) and using two different temperature ramp rates (0.5 °C/min and 1 °C/min) in a 40 mM glycine-HCl, pH 3.0 buffer. The unfolding reaction was monitored spectrophotometrically at 301 nm. The buffer conditions were those of Lee *et al.* [28] where it was shown that the thermal unfolding of HEL is reversible and exhibits a two-state (N → D) unfolding behavior under these conditions.

A representative plot of the unfolding reaction using the difference spectrum technique is presented in Figure 25. The experimental data were fit to a two-state model to obtain values for the melting temperature (T_m), the enthalpy of unfolding (ΔH_m), and the heat capacity change of unfolding (ΔC_p). As seen in Figure 25, an excellent fit to the data is obtained (residuals of the fit are randomly distributed). The thermodynamic parameters for HEL unfolding from the DS method are presented in Table 19.

Figure 25. Panel a –A representative plot depicting the thermal unfolding of HEL in 40 mM glycine-HCl, pH 3.0 buffer. Experiments were conducted with 1 mg/mL HEL using a temperature ramp rate of 60 °C/hr. The unfolding was monitored spectrophotometrically at 301 nm. The residuals of the fit are presented as solid circles in panel b.

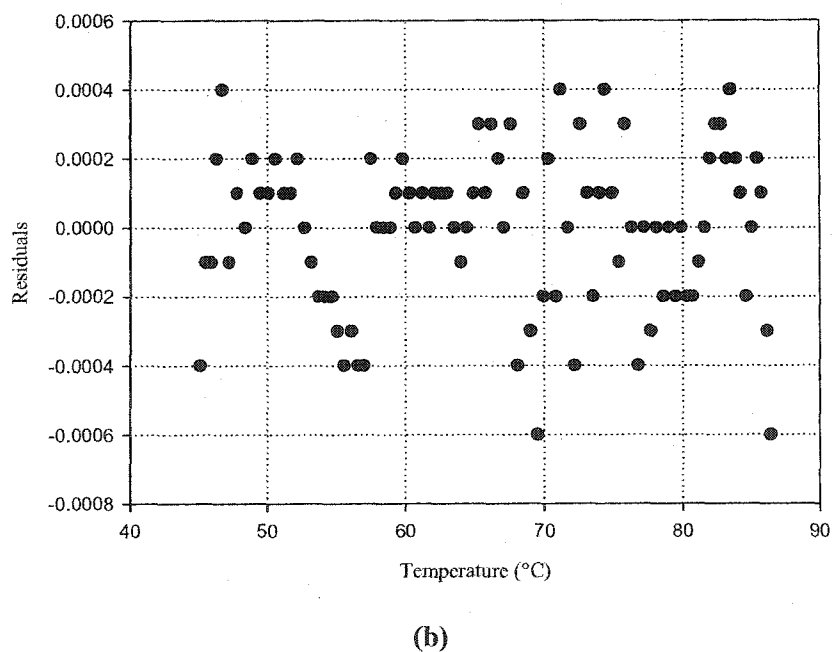
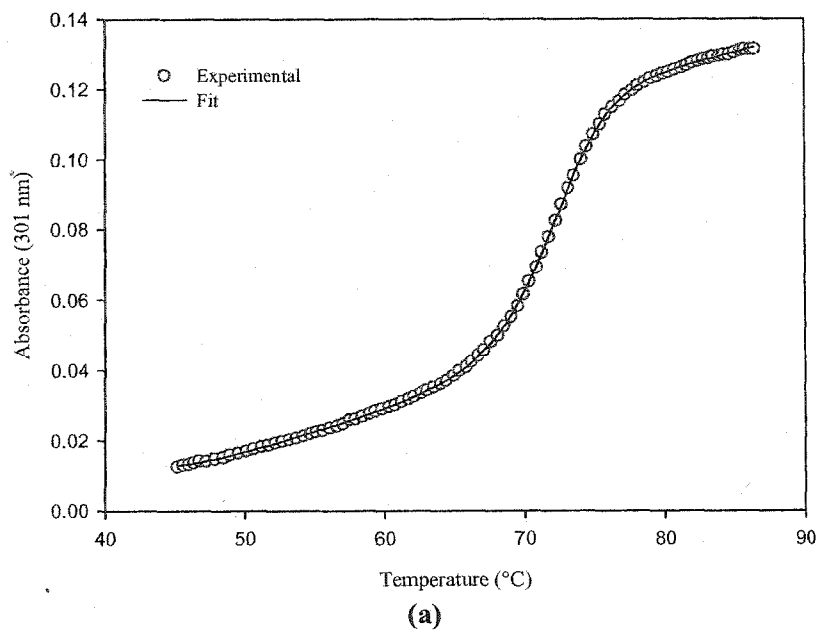


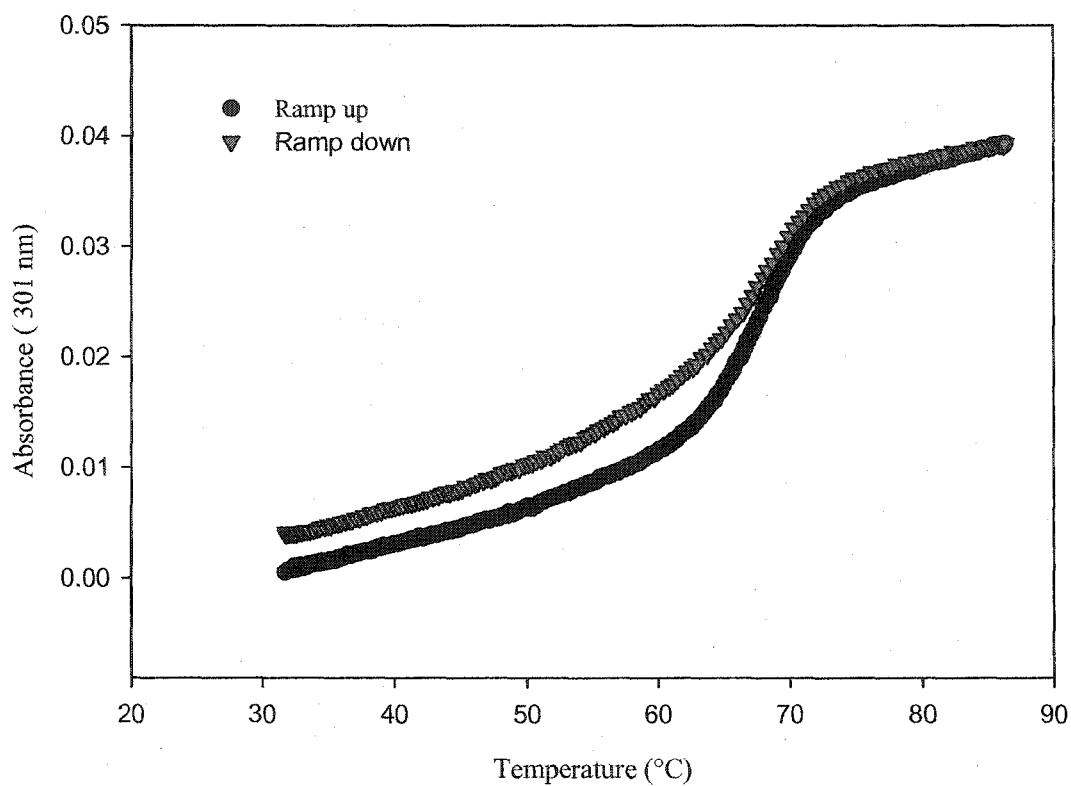
Table 19. Thermodynamic parameters governing the thermal unfolding of HEL: values determined using the difference spectrum method

Concentration (mg/mL)	Ramping rate (°C/hr)	T _m (°C)	ΔH _m (kcal/mol)	ΔC _p (kcal/mol-°C)
1.25	30	70.8	107	5.7
0.5	30	70.9	109	5.8
1	60	71.9	110	6.2
Average		71.2 ± 0.6	109 ± 2	5.9 ± 0.3

When studying an equilibrium thermal unfolding reaction, a key requirement is that the parameters governing the process should be independent of protein concentration and temperature ramp rate. When this occurs, the parameters are considered to truly represent the unfolding equilibrium. As seen from Table 19, the thermodynamic parameters remain constant with varying concentrations and ramp rates. The accuracy of these parameters is discussed along with DSC results.

Reversibility is another indicator employed to determine if a reaction is thermodynamically controlled. In most cases, the reversibility of HEL or PEG-HEL unfolding was ensured by checking that the Δ absorbance value had returned approximately to its initial value (prior to starting the experiment). A formal experiment to demonstrate the reversibility of the unfolding was conducted using PEG3-HEL, the results of which are presented here in order to validate the DS method. After completion of the unfolding reaction, the absorbance of the sample was monitored as it cooled to room temperature (Figure 26).

Figure 26. Panel a: Reversibility of the thermal unfolding of PEG3-HEL monitored spectrophotometrically at 301 nm. Experiment conducted with 0.3 mg/mL PEG3-HEL in 40 mM glycine, pH 3.0 buffer at a temperature ramping rate of 60°C/hr. The data gathered during the ramp-up cycle of the experiment are represented by closed circles, and data gathered during the ramp down cycle are represented by inverted triangles. The reversibility of thermal unfolding of PEG3-HEL was calculated to be 74 % based on the ratio of the $\Delta H_{\text{down}}/\Delta H_{\text{up}}$.



The reversibility of the unfolding reaction was quantified by calculating the reversibility factor $-\Delta H_{\text{down}}/\Delta H_{\text{up}}$, where ΔH_{down} & ΔH_{up} are the enthalpies of unfolding measured during the down and up ramps of the unfolding experiment. The thermodynamic parameters for the reversibility experiment are presented in Table 20. As can be seen, the melting temperature calculated from the two cycles is identical and the unfolding reaction is observed to be 74 % reversible.

Table 20. Reversibility of the thermal unfolding of PEG3-HEL monitored via the difference spectrum method

Ramping cycle	T_m (°C)	ΔH_m (kcal/mol)	Reversibility (%)
Up	67.6	102	74
Down	67.7	76	

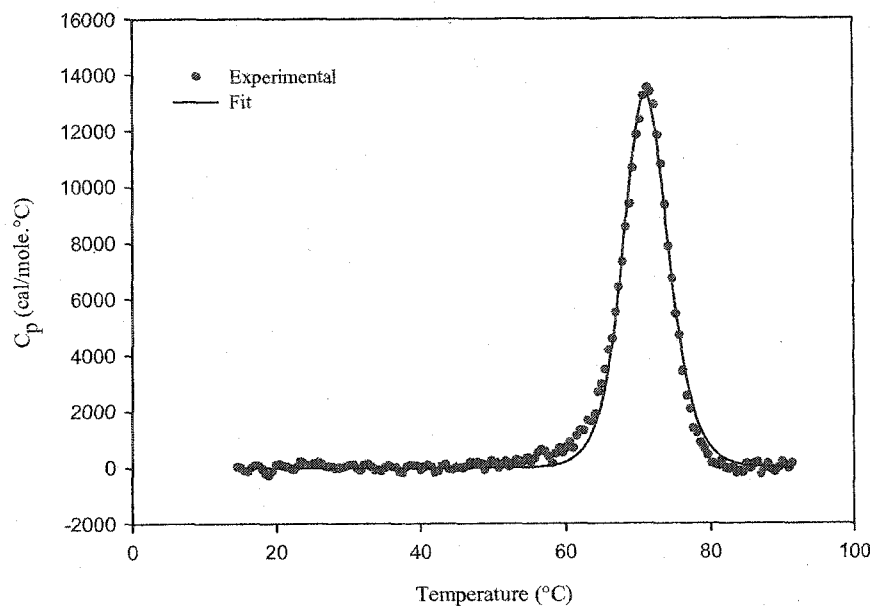
3.4.2 Differential Scanning Calorimetry Results

The thermal unfolding of HEL was monitored using two DSC instruments – VP-DSC and the Capillary or Cap-DSC. Experiments were conducted in the same 40 mM glycine, pH 3.0 buffer used in the Difference Spectrum method to facilitate comparison. A ramp rate of 60 °C/hr was used in the VP-DSC. A much faster ramping rate of 220 °C/hr was possible and was used in the capillary DSC. The DSC data were fit to a non-two state model⁷. This enabled the estimation of the vant-Hoff's enthalpy of unfolding (ΔH_v) in addition to the calorimetric enthalpy (ΔH_{cal}).

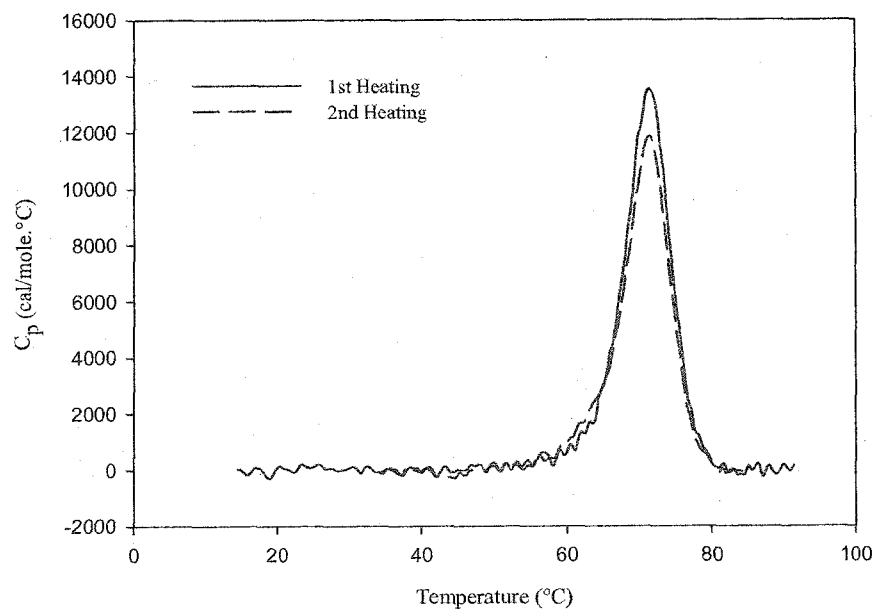
The thermograms depicting the thermal unfolding of HEL from the Cap-DSC and VP-DSC are presented in Figure 27 and Figure 28 respectively. The reversibility of the unfolding reaction in the two DSC instruments is presented in panel b of each figure.

⁷ A non 2-state model with one transition peak was chosen. If $\Delta H_{\text{cal}} = \Delta H_v$, then the model collapses to a two state model.

Figure 27. Panel a: Thermogram depicting the thermal unfolding of HEL in the Cap-DSC. Experiment conducted with 1 mg/mL HEL in 40 mM glycine, pH 3.0 buffer using a temperature ramp rate of 220°C/hr. Panel b: Thermogram depicting the reversibility in the thermal unfolding of HEL. The % reversibility ($\Delta H_2/\Delta H_1$) was calculated to be 88.6 %.

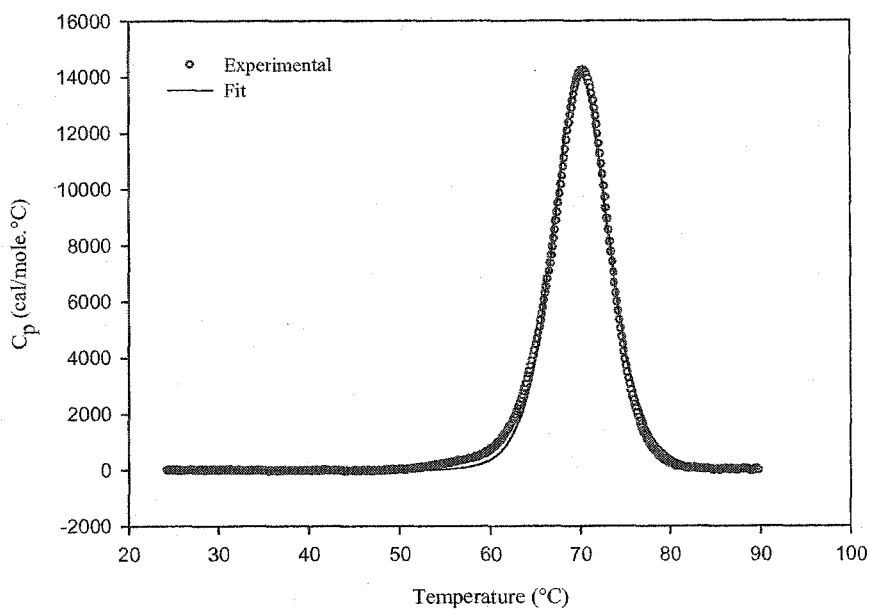


(a)

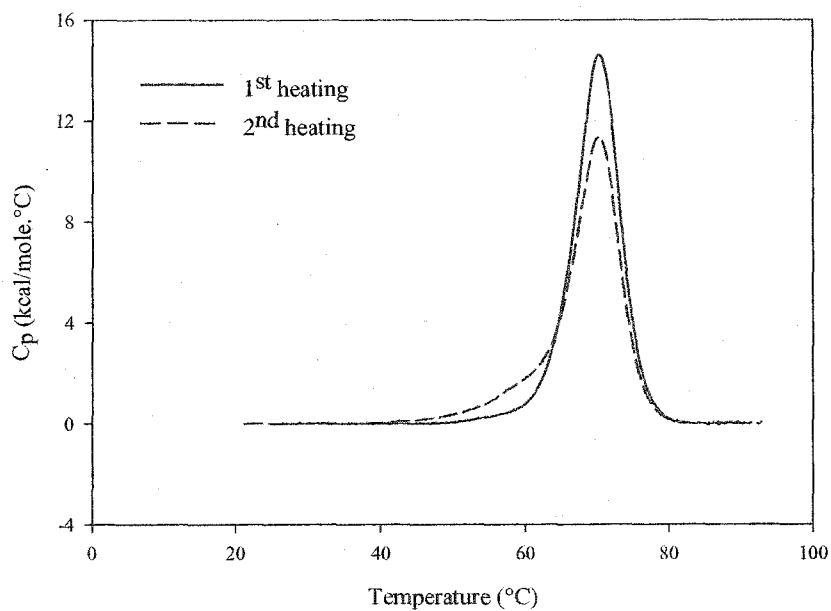


(b)

Figure 28. Panel a: Thermogram depicting the thermal unfolding of HEL in the VP-DSC. Experiment conducted with 1 mg/mL HEL in 40 mM glycine, pH 3.0 buffer using a ramp rate of 60 °C/hr. Panel b: Thermogram depicting the reversibility in the thermal unfolding of HEL. The % reversibility was calculated to be 75 %.



(a)



(b)

The thermal unfolding of HEL is characterized by a single, cooperative, endothermic peak, which is indicative of a two state transition (Figure 27a & Figure 28a). Further, very good fits to the experimental data are obtained with the chosen model. The thermodynamic parameters obtained from these fits are presented in Table 21. In the DSC experiments, the ΔC_p of unfolding was determined using the baseline subtraction method [77]. The thermodynamic parameters determined from the difference spectrum method are also presented in Table 21 for comparison.

Table 21. Thermodynamic parameters for thermal unfolding of HEL determined from the Cap-DSC, VP-DSC, and the difference spectrum method

Method	Conc (mg/mL)	Ramp rate (°C/hr)	T_m (°C)	ΔH_{cal} (kcal/mol)	ΔC_p^*	$\Delta H_{cal}/\Delta H_v$	$\Delta H_2/\Delta H_1$
Cap-DSC	1	220	71.2	112	1.9	0.96	89
VP-DSC	1	60	70.2	117	1.1	1.02	75
DS**	0.5 - 1.25	30 - 60	71.2	109 (ΔH_m)	5.9	ND***	ND

* The units of ΔC_p are kcal/mol-°C

** Average values presented

** ND - Not determined

The T_m and ΔH values from the DSC measurements and the DS method are in excellent agreement with each other (within 7 %). The T_m values are within 1 °C while the enthalpies are within 7 kcal/mol of each other. Several points can be made on the basis of these data about the mechanism of HEL unfolding.

The DS and DSC methods monitor two completely different properties during the unfolding process. The former monitors the loss in the tertiary structure of the protein, which is accompanied by a change in the extinction coefficient. The latter simply measures the heat required to cause protein unfolding. It should be noted that in the DS method, the experimental data were fit to a two state-model whereas a more general, non 2-state model was assumed for the DSC analysis. Still, the values from the two methods are almost identical. Such good agreement of the T_m and ΔH values between the

two methods demonstrates that HEL unfolding occurs via a two-state process. The assumption of a non-state model in the DSC experiments enabled the calculation of the vant-Hoff's enthalpy (ΔH_v). Information about the unfolding mechanism can be gained from the ratio of the calorimetric enthalpy to the vant-Hoff's enthalpy ($\Delta H_{cal}/\Delta H_v$). For a purely two state system, the ratio $\Delta H_{cal}/\Delta H_v$ assumes a value of 1. Values of less than 1 are indicative of inter-molecular cooperativity, while values greater than 1 indicate the presence of intermediates playing a role in the unfolding process [63]. As seen from Table 21, the $\Delta H_{cal}/\Delta H_v$ for HEL is 0.96 for the Cap-DSC and 1.02 for the VP-DSC. This demonstrates that HEL follows a two state ($N \leftrightarrow D$) unfolding process under the chosen solution conditions.

The reversibility of the unfolding process was determined from the ratio $\Delta H_2/\Delta H_1$. The reversibility of HEL unfolding in the Cap-DSC was calculated to be 89 %. However, a lower value of 75 % was observed in the VP-DSC. The VP-DSC value is comparable to the reversibility measured for PEG3-HEL via the DS method. Interestingly, the same ramp rate of 60 °C/hr was employed in both VP-DSC and DS experiments, while a much faster ramp rate of 220 °C/hr was employed in the Cap-DSC experiments. Consequently, reversibility may be dependent on the ramp rate of the two DSCs.

Although the solution conditions were chosen to minimize any kinetic, aggregation processes, such reactions cannot be eliminated completely. The reversibility in the VP-DSC indicates that about 25 % of the HEL molecules are lost due to kinetic processes (aggregation) between the 1st heating and cool-down. Only the remaining 75 % of HEL molecules are available to participate in the unfolding reaction a second time. It

should be noted that the sample heating and cooling processes in the Cap-DSC are approximately three times faster as compared to the VP-DSC. Once the unfolding reaction is complete, the sample is cooled to its initial temperature at much faster rate in the Cap-DSC. This may reduce the number of protein molecules that are inactivated between the 1st heating and the 2nd heating, thus leading to a greater reversibility in the Cap-DSC.

Another aspect of the HEL unfolding reaction worth noting is the ΔC_p of unfolding. The ΔC_p values measured in the two DSC experiments are in good agreement with each other and with those reported in literature. Liu and Sturtevant [78] and Lee *et al.* [28] have reported values in the range of 1.5 - 2.4 kcal/mol-°C. The ΔC_p values determined from the DS method reported here (Table 19) appear to be over-estimated. It should be recognized that in the DS method, the unfolding curve is measured in terms of the difference in extinction coefficients of the native and unfolded states of the protein. While T_m can be obtained directly from the experimental data, other parameters are estimated by fitting the curve to the Gibbs-Helmholtz Equation (Equation 17). Simplistically, the ΔH_m and ΔC_p can be viewed as being estimated from the first and second derivatives of the unfolding curve. Based on this, accurate determination of T_m can be expected using the method. However, the estimation of ΔH will be prone to greater error and the ΔC_p values will be estimated with the least accuracy. Thus, larger errors in the ΔC_p values from the DS method can be expected.

Importantly, although the ΔH values estimated from the DS method are consistent with their corresponding DSC values, caution should be exercised in attempting trend analysis using ΔH values determined from the DS method. On the other hand, the

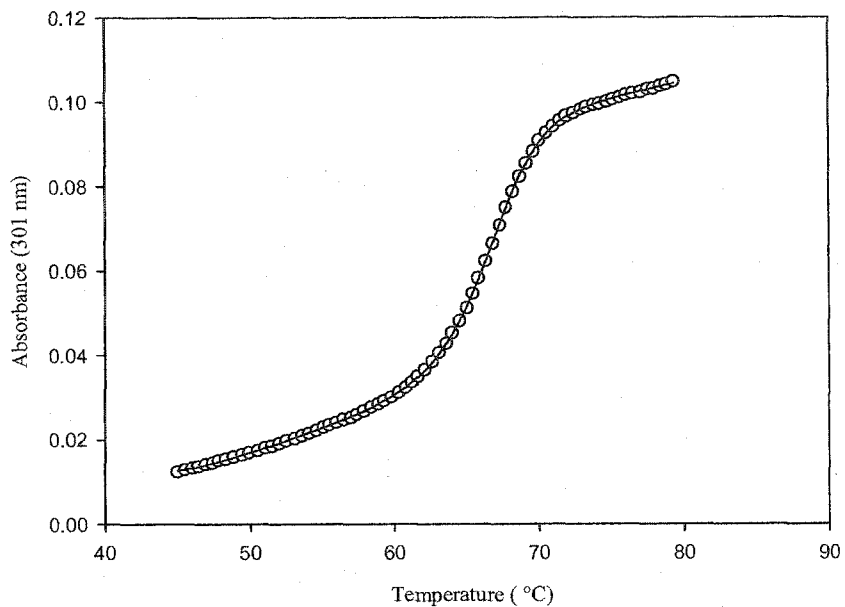
enthalpies in DSC experiments are measured directly as differential heats and are more amenable for use in trend analysis. Hence, in the present case analyses pertaining to ΔH only used DSC data.

3.4.3 Effect of Free PEG on the T_m of Hen Egg Lysozyme

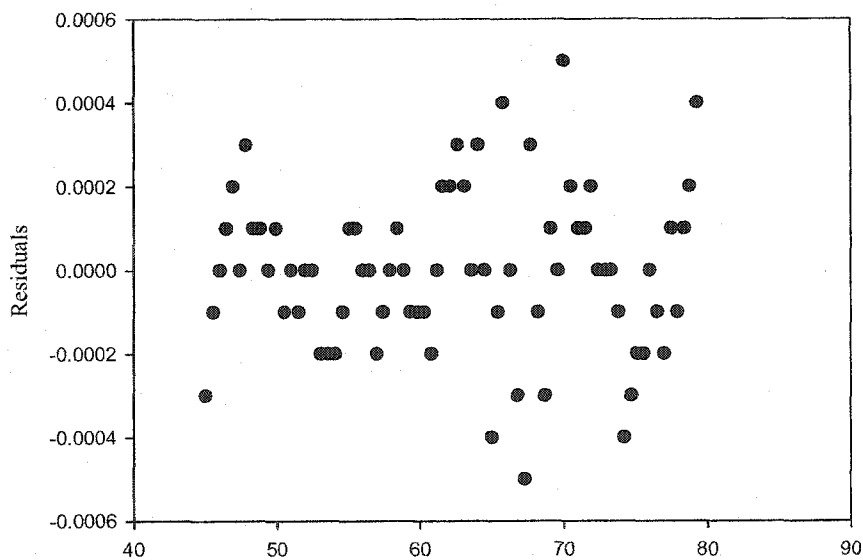
The effect of high concentrations of PEG 400 and PEG 20000 on the melting temperature of HEL was studied using the Difference Spectrum method. Representative plots of HEL unfolding in the presence of the two PEGs are presented in Figure 29 (30 % (w/v) PEG 400) and Figure 30 (30 % PEG 20 kD). Normalized unfolding curves representing HEL unfolding in the presence of 0, 10, 20, and 30 % (w/v) PEG 400, and in the presence of 0, 15 % and 30 % PEG 20 kD are presented in Figure 31 and Figure 32 respectively. The unfolding curves were normalized to facilitate visual comparison. There no change in the T_m post normalization, while the ΔH and ΔC_p values changed slightly in some cases. The thermodynamic data reported here (Table 22) is based on the fits to the original raw data.

As seen from Figures 29 and 30, excellent fits to the data are obtained. Importantly, Figure 31 and Figure 32 reveal the effect of the two PEGs on the T_m of HEL unfolding. As can be seen, the T_m of HEL unfolding decreases with increasing PEG concentration.

Figure 29. Panel (a): A representative plot depicting the thermal unfolding of HEL in the presence of 30 % PEG 400 monitored spectrophotometrically at 301 nm (a). Experiment conducted with 1 mg/mL HEL in 40 mM glycine, pH 3.0 buffer in the presence of 30 % (w/v) PEG 400 at a temperature ramping rate of 60°C/hr. The experimental data are represented as open circles (○) while the fit to the experimental data is represented as a solid line (—). The residuals of the fit are presented as solid circles (●) in Panel (b).

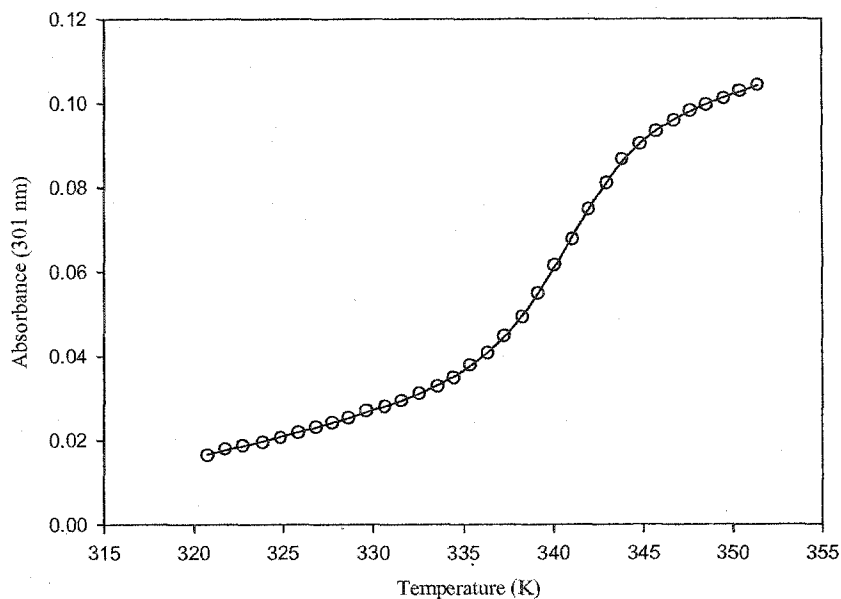


(a)

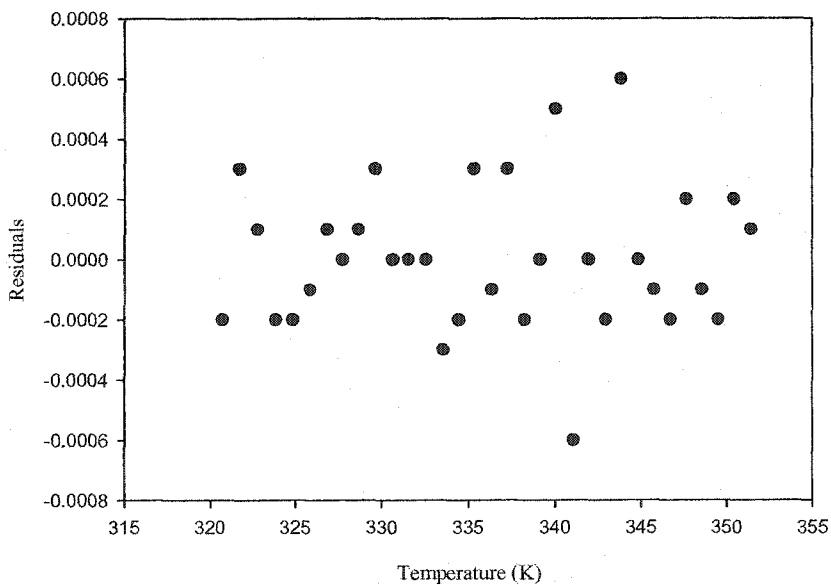


(b)

Figure 30. Panel a: A representative plot depicting the thermal Unfolding of HEL in the presence of 30 % PEG 20000 monitored spectrophotometrically at 301 nm. Experiment conducted with 1 mg/mL HEL in 40 mM glycine, pH 3.0 buffer in the presence of 30 % (w/v) PEG 20,000 at a temperature ramping rate of 60°C/hr. The experimental data are represented as open circles (○) while the fit to the experimental data is represented as a solid line (—). The residuals of the fit are presented as solid circles (●) in panel b.



(a)



(b)

Figure 31. Thermal unfolding of HEL in the Presence of 0, 10, 20 and 30 % (w/v) PEG 400. Experiments were conducted with 1 mg/mL HEL in 40 mM glycine, pH 3.0 buffer at temperature ramp rate of 60 ° C/hr.

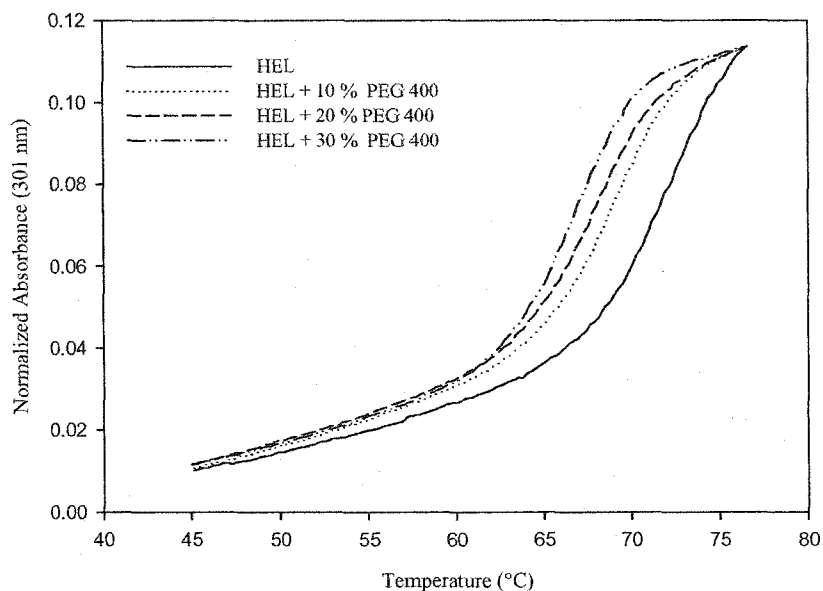
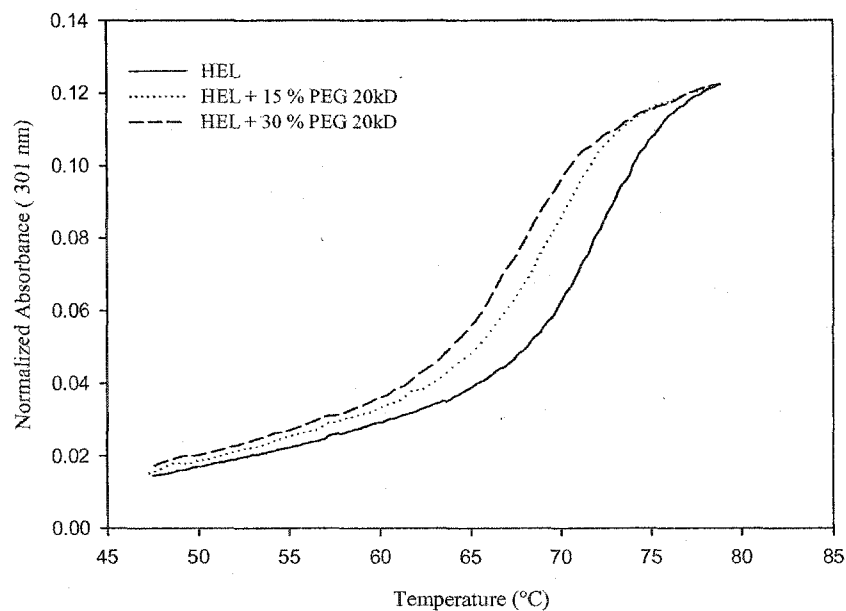


Figure 32. Thermal Unfolding of Hen Egg Lysozyme in the Presence of 15% and 30 % (w/v) PEG 20 kD. Experiments were conducted with 1 mg/mL lysozyme in 40 mM glycine, pH 3.0 buffer in the presence of 0, 15 % and 30 % (w/v) PEG 20 kD respectively at a temperature ramp rate of 60 ° C/hr



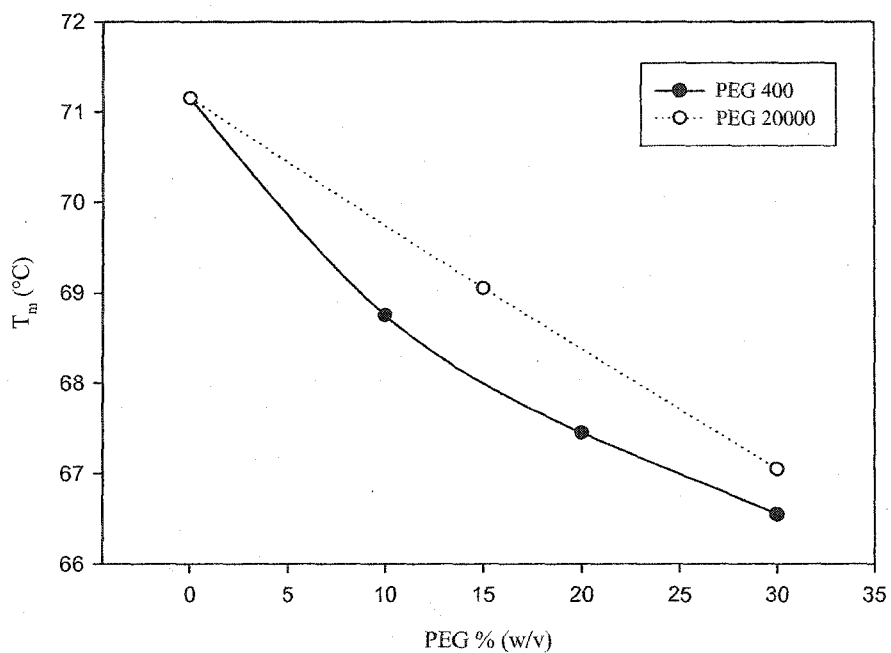
A plot of the T_m versus PEG concentration is presented in Figure 33. As seen from the Figure & Table 22, the T_m of HEL in the presence of 30 % (w/v) PEG 400 is 4.6 °C lower than the control (without PEG 400). These results are consistent with those reported by Lee and Lee [28]. In fact, the experiments with PEG 400 were repeated from Lee *et al.* as a 'bridge' to the present research. A similar trend is observed in the case of PEG 20 kD. The T_m in the presence of 30 % PEG 20 kD decreases to 67 °C, approximately 4 °C lower than in the control. Lee *et al.* [28] concluded that the amphipathic PEG interacts with the exposed hydrophobic core of the unfolded form of the protein and consequently stabilizes it. This shifts the unfolding equilibrium towards the D form, which is manifested in the form of a decrease in T_m . The results observed in this study are consistent with their conclusion.

Table 22. Thermodynamic parameters for the thermal unfolding of HEL in the presence of PEG 400 and PEG 20 kD

PEG (% w/v)	T_m (K)	ΔH_m (kJ/mol)	ΔC_p (kJ/mol-°C)
PEG 400			
0	71.2	107	5.7
10	68.8	116	7.2
20	67.4	115	7.4
30 - I*	66.6	123.9	8.3
30 - II*	66.6	119	7.4
PEG 20000			
0	71.2	107	5.7
15	69.0	106	6.3
30	67.0	105	6.8

* - I and II denote two separate experiments performed in the presence of 30 % PEG 400

Figure 33. The Effect of high concentrations of PEG 400 and PEG 20 kD on the melting temperature of HEL. Experiments were conducted with 1 mg/mL Lysozyme in 40 mM glycine, pH 3.0 buffer in the Presence of 0, 15 & 30 % (w/v) PEG 400, and 15 % & 30 % (w/v) PEG 20kD respectively at a temperature ramp rate of 60 ° C/hr.



No changes in the ΔH_m values were observed in the presence of the two PEGs. Because of the inherent uncertainty associated with the ΔH_m estimation using the DS method, no trend analysis was done. The ΔC_p values are over-estimated using the difference spectrum method. The reasons for this were discussed in section 3.4.2.

3.4.4 Effect of PEGylation on HEL unfolding

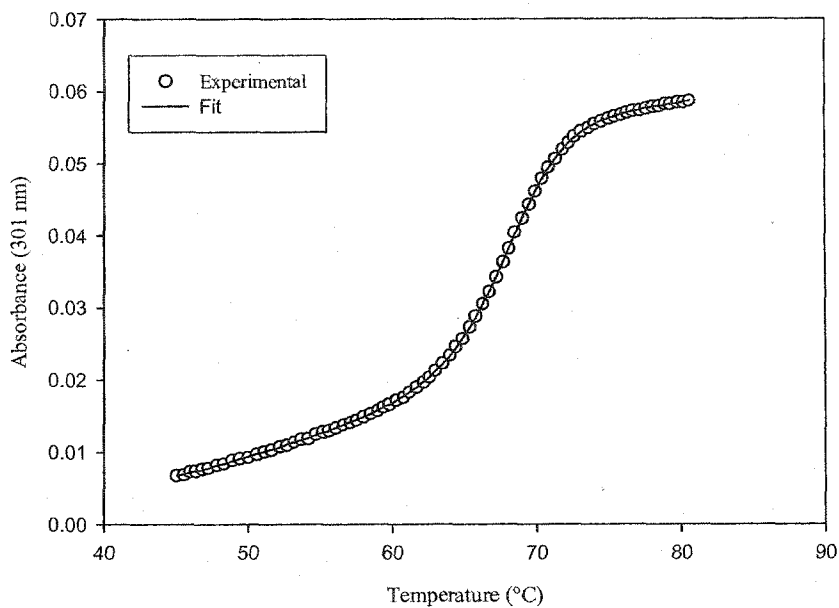
The effect of PEGylation on the melting temperature of HEL was studied using both DSC and the Difference Spectrum method. The DS method experiments were conducted with all three PEG-HEL molecules, while DSC studies were possible only with PEG1-HEL and PEG2-HEL due to limited availability of the PEG3-HEL sample. In addition, the DSC studies were conducted with both the Cap-DSC and the VP-DSC. Representative unfolding curves & thermograms for the various PEG-HEL molecules are presented in Figure 34 (DS method: PEG2-HEL), Figure 35 (Cap-DSC -PEG1-HEL), and Figure 36 (VP-DSC - PEG1-HEL). Normalized unfolding curves for the various PEG-HEL molecules are presented in Figure 37. The unfolding curves were normalized to facilitate visual comparison. It should be noted that the thermodynamic parameters were estimated based on the fits to the original raw data. The thermodynamic parameters estimated from the DS method and the two DSCs are presented in Table 23. The thermograms comparing HEL, PEG1-HEL and PEG2-HEL unfolding are presented in Figure 38 and Figure 39.

Table 23. Thermodynamic parameters for thermal unfolding of PEG-HEL molecules determined from the Cap-DSC, VP-DSC, and the Difference Spectrum method

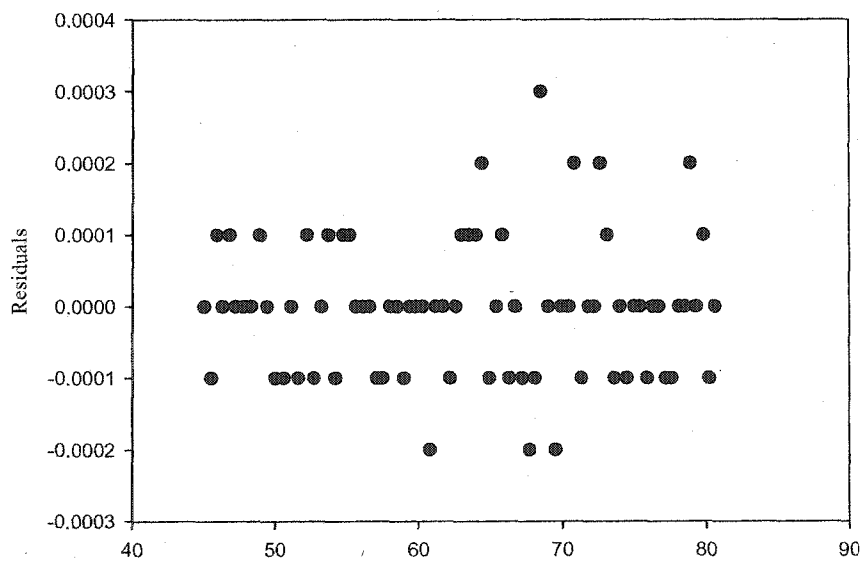
Molecule,	Rate (°C/hr)	T _m (°C)	ΔH _{cal} (kcal/mol)	ΔCp (kcal/mol-°C)	ΔH _{cal} /ΔH _v	ΔH ₂ /ΔH ₁ (%)
DS Method (PEG1-HEL: n = 3, PEG2-HEL: n = 3, PEG3-HEL: n = 1)						
HEL	60	71.2 ± 0.6	107 ± 2	5.9 ± 0.3	ND	ND*
PEG1-HEL		68.8 ± 0.3	95 ± 15	5.6 ± 0.4		ND
PEG2-HEL		67.5 ± 0.5	107 ± 3	6.2 ± 0.1		ND
PEG3-HEL		67.6	102	5.8		74
Cap-DSC (n = 1)						
HEL	220	71.2	112	1.9	0.96	89
PEG1-HEL		70.3	104	1.8	0.89	85
PEG2-HEL		68.9	94.3	1.6	0.80	90
VP-DSC (n = 1)						
HEL	60	70.1	116	1.1	1.02	75
PEG1-HEL		68.6	111	0.8	0.97	ND
PEG2-HEL		67.8	96	0.5	0.83	ND

* - Not determined

Figure 34. Panel a: A representative plot depicting the thermal unfolding of PEG2-HEL monitored spectrophotometrically at 301 nm. Experiment conducted with 0.5 mg/mL PEG2-HEL in 40 mM glycine, pH 3.0 buffer at a temperature ramping rate of 60°C/hr. The experimental data are represented as open circles (○) while the fit to the experimental data is represented as a solid line (—). The residuals of the fit are presented as solid circles (●) in panel b.



(a)



(b)

3.4.4.1 Effect on T_m

As seen from Figure 37 through Figure 39, the T_m of HEL is observed to decrease with increasing degree of PEGylation. A 2.3 °C decrease is observed for the PEG2-HEL by DSC measurements, while a slightly greater decrease of ~ 3.5 °C is observed in the Difference Spectrum method (Table 23). These results support the hypothesis proposed in this dissertation that similar to the experiments with free PEG, a drop in T_m should be observed for the PEGylated HEL molecules. In this case, the covalently attached amphipathic PEG chain(s) can interact with the exposed hydrophobic patches and stabilize the unfolded D form of HEL. The stabilization causes a shift in the unfolding equilibrium towards the D form and is manifested as a T_m drop.

Although the molar concentration of PEG in the PEG-HEL solutions is low, being covalently tethered, its local concentration in the immediate microenvironment of the protein is very high. Hence an effect similar to that observed with the free high-PEG concentration is seen. A comparison between the T_m drop for the PEG-HEL molecules and the T_m drop observed as a function of free PEG 20,000 reveals that the local concentration of PEG in the PEGylated molecules is equivalent to about 15-25 % (w/v) free PEG (Figure 40).

Interestingly, the data from all three methods suggest that the largest T_m drop occurs between the native and the mono PEGylated HEL species. The magnitude of the change decreases with increasing degree of PEGylation, with no change in T_m being observed between PEG2-HEL and PEG3-HEL (Figure 41).

Figure 35. Panel a: Thermogram depicting the thermal unfolding of PEG1-HEL monitored calorimetrically in the VP-Cap-DSC. Experiment conducted with 1 mg/mL HEL in 40 mM glycine, pH 3.0 buffer at a temperature ramping rate of 220°C/hr. The experimental data are represented as open circles (○) while the fit to the experimental data is represented as a solid line (—).

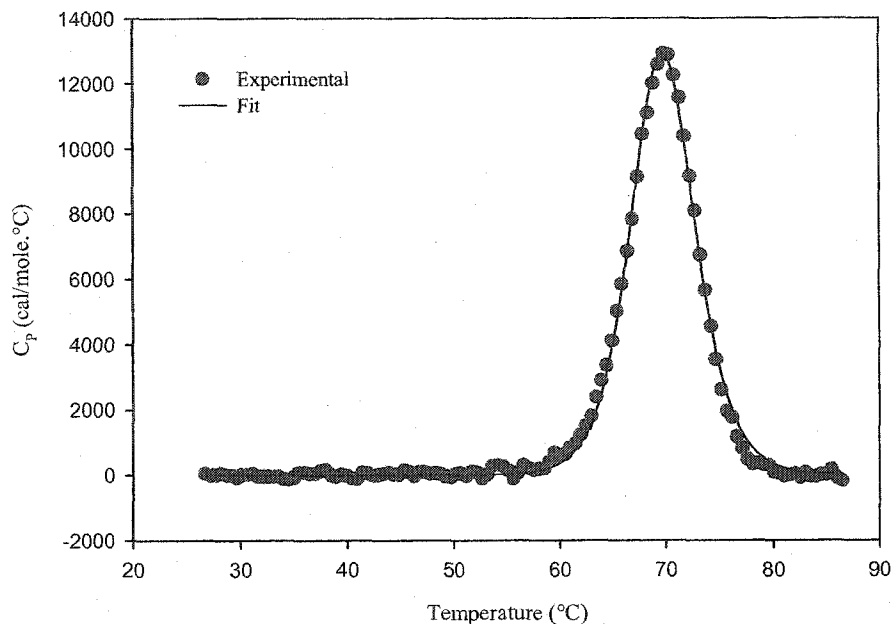


Figure 36. Panel a: Thermogram depicting the thermal unfolding of PEG1-HEL monitored calorimetrically in the VP-DSC. Experiment conducted with 1 mg/mL HEL in 40 mM glycine, pH 3.0 buffer at a temperature ramping rate of 60 °C/hr. The experimental data are in open circles (○), while the fit to the experimental data is represented by the solid line (—).

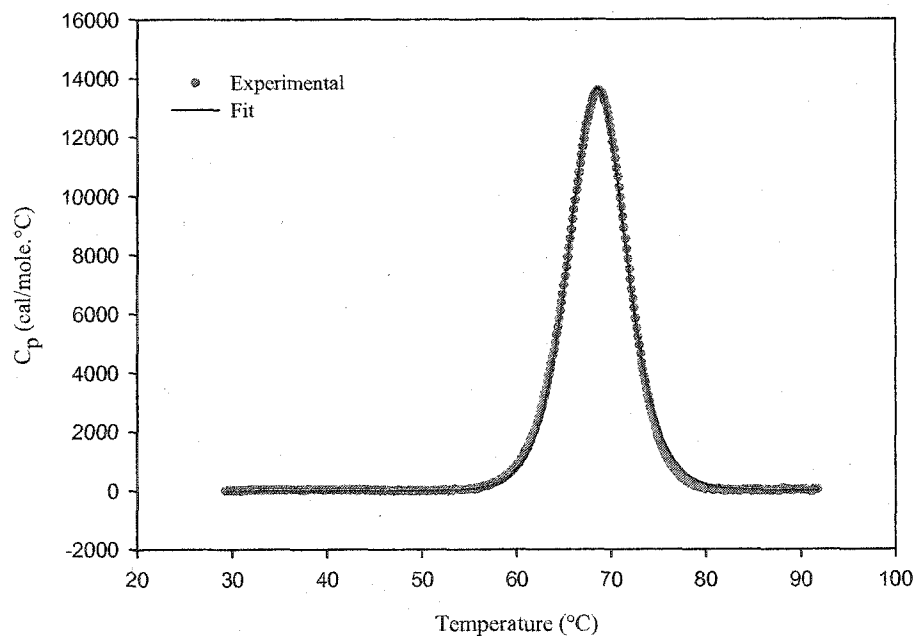


Figure 37. Comparison of the thermal unfolding of HEL, PEG1-HEL, PEG2-HEL & PEG3-HEL. Experiments conducted in a 40 mM glycine, pH 3.0 buffer Thermal unfolding monitored via the Difference Spectrum method using a ramp rate of 60 °C/hr

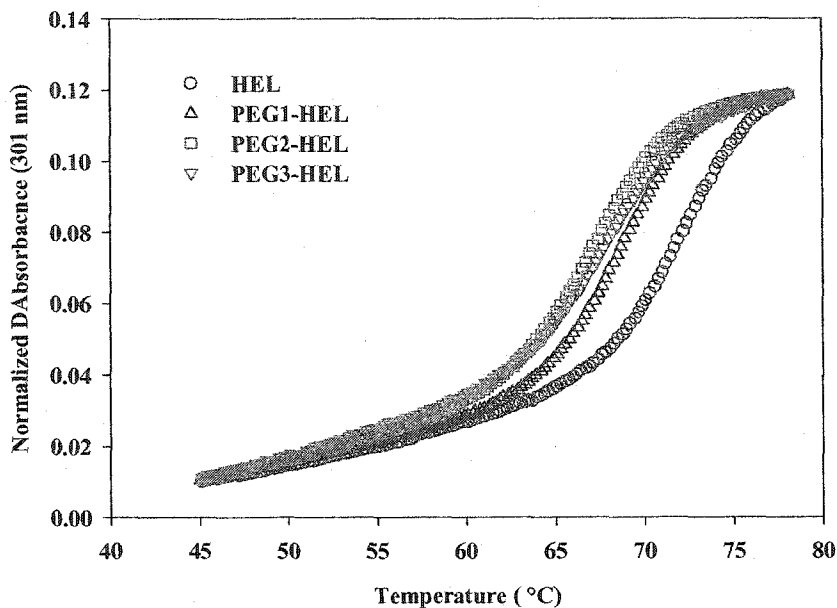


Figure 38. Comparison of the thermal unfolding of HEL, PEG1-HEL and PEG2-HEL. Experiments conducted with 1 mg/mL HEL, 1 mg/mL PEG1-HEL, and 0.8 mg/mL PEG2-HEL respectively in 40 mM glycine, pH 3.0 buffer in a Cap-VP-DSC at a temperature scan rate of 220 °C/hr.

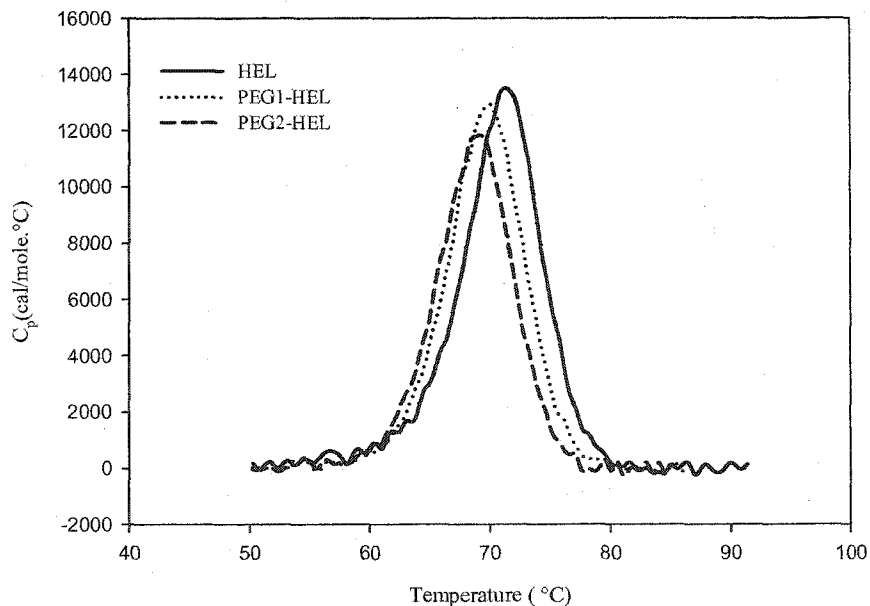


Figure 39. Comparison of the thermal unfolding of HEL, PEG1-HEL and PEG2-HEL. Experiments conducted with 1 mg/mL HEL, 1 mg/mL PEG1-HEL, and 0.4 mg/mL PEG2-HEL respectively in 40 mM glycine, pH 3.0 buffer in a VP-DSC at a temperature scan rate of 60 °C/hr.

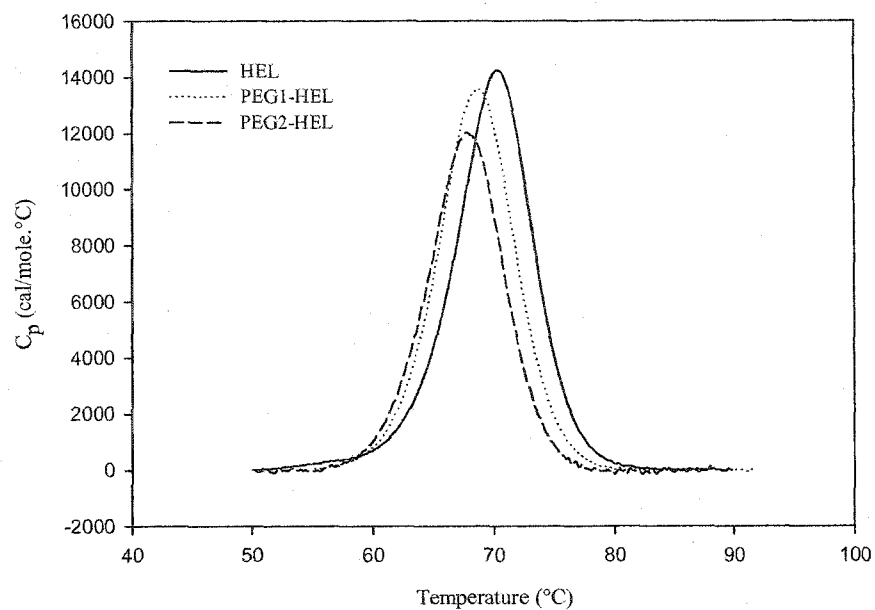


Figure 40. Comparison between the effects of free PEG 20 kD and of PEGylation with PEG 20kD on the melting temperature (T_m) of HEL. Experiments were conducted in 40 mM glycine, pH 3.0 buffer at a temperature ramp rate of 60 °C/hr. The thermal unfolding was spectrophotometrically monitored at 301 nm.

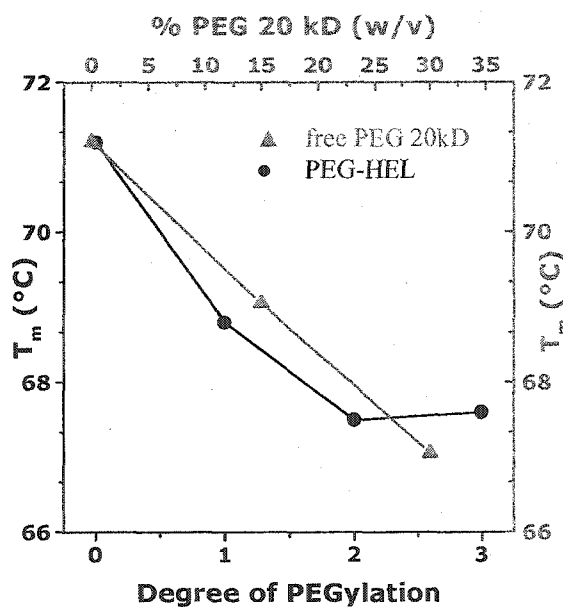
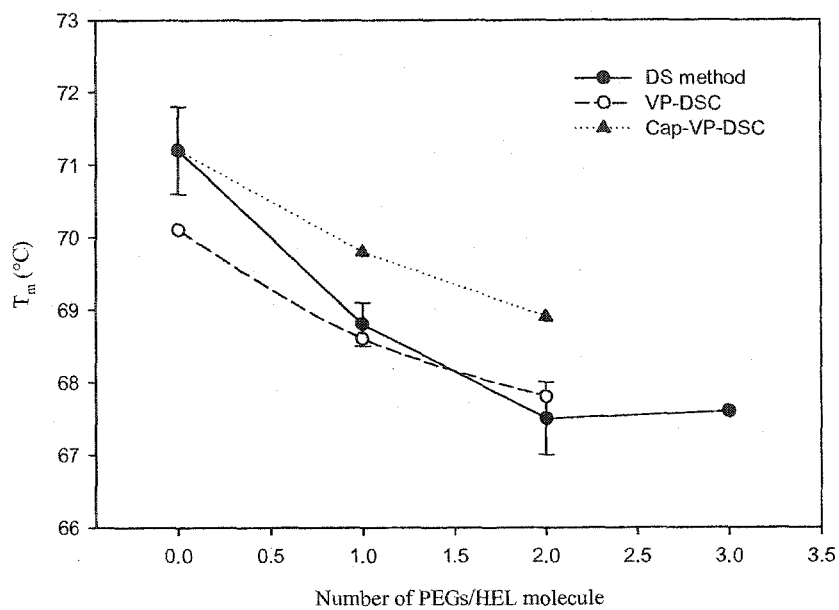


Figure 41. The Effect of PEGylation on the melting temperature (T_m) of HEL. Experiments were conducted with HEL, PEG1-HEL, PEG2-HEL, and PEG3-HEL in 40 mM glycine, pH 3.0 buffer at a temperature ramp rate of 60 °C/hr. The thermal unfolding was monitored spectrophotometrically at 301 nm.



One should bear in mind that any HEL-PEG interaction would be limited by the amount of the exposed hydrophobic surface area within the protein. Thus, when the amount of PEG available for interaction is in large excess compared to the available surface area for interaction, the T_m will become insensitive to further increases in PEG concentration.

3.4.4.2 Effect on the Unfolding Mechanism

Similar to the HEL unfolding, a single, cooperative, endothermic peak is observed during the unfolding of the PEG-HEL molecules (Figure 35 & Figure 36), which is indicative of a two state unfolding process. For the native HEL, the $\Delta H_{cal}/\Delta H_v$ ratio is close to 1 (0.96 – 1.02) supporting a nearly perfect two state transition. However, as seen from Table 23, the $\Delta H_{cal}/\Delta H_v$ ratio for the PEGylated HEL molecules decreases progressively with increasing degree of PEGylation, and is 0.8 for PEG2-HEL. This may be indicative of intermolecular cooperativity that is introduced in the unfolding process as a result of PEGylation. The PEG chains may chaperone the HEL through its unfolding process by progressively patching the hydrophobic interior as the protein unfolds.

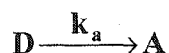
3.4.4.3 Effect on ΔH and ΔC_p

The ΔH_m values of the PEGylated HEL molecules estimated from the difference spectrum method are in good agreement with those measured with the DSC method (ΔH_{cal}). However, on close examination of the DSC-based ΔH_{cal} data, one can observe that the values decrease with increasing degree of PEGylation (Table 23). This may be due to the weak, exothermic hydrophobic interaction of PEG with the HEL interior. Branchu *et al* [79] have observed a similar decrease in ΔH_{cal} of HEL unfolding in the presence of amphipathic cyclodextrins.

A downward trend in the ΔC_p values with an increasing degree of PEGylation also can be seen from the DSC data (Table 23). The ΔC_p accompanying an unfolding reaction is believed to result from the clustering of the water molecules around the hydrophobic residues, which become solvent exposed as the protein unfolds. In the presence of PEG, the hydrophobic residues can preferentially interact with the PEG molecules and thus disrupt such water ordering [80]. The decrease in ΔC_p observed for the PEG-HEL molecules is consistent with this argument.

3.5 Kinetic Aggregation Studies

The aggregation studies were designed to study the latter half of the Reaction Scheme-I. Experiments were aimed at understanding the effect of PEGylation on the irreversible aggregation rate of hen egg lysozyme.



In contrast to the equilibrium unfolding studies, the kinetic studies were performed under conditions that were designed to accelerate the aggregation reaction. For example, the aggregation was monitored at an elevated temperature of 75 °C. This temperature was chosen so that a substantial amount of the native protein (N) would be converted to its D form. Also, the solution pH for these studies was increased from pH 3.0 to pH 7.5, which is closer to the pI of HEL (~ 11). The rationale was that reducing surface charge (by being near the pI) would minimize electrostatic repulsions between HEL molecules and this would help facilitate aggregation. Sodium chloride was also included at a concentration of 125 mM to aid in the precipitation of hydrophobic aggregates (salting out). Employing these reaction conditions, the aggregation of HEL, PEG1-HEL and PEG2-HEL was studied using turbidimetry, size- exclusion-HPLC, and

digital photography. Experiments with PEG3-HEL were not possible due to limited sample availability.

3.5.1 Aggregation Studies Using Turbidimetry

The turbidity studies were conducted in three phases. First, a suitable aggregation assay was developed and characterized. Then, the effect of free PEG on the aggregation rate of HEL was examined. In the third stage, the effect of PEGylation on the aggregation rate of HEL was studied.

3.5.1.1 Aggregation Assay

The heat-induced aggregation of HEL was monitored at 75 °C using the decrease in % transmittance at 320 nm over a 15 - 30 minute period. Experiments were conducted with 1 mg/mL HEL prepared in a 25 mM sodium phosphate, 125 mM NaCl buffer at pH 7.5. A representative plot of the HEL aggregation monitored via the turbidity assay is presented in Figure 42. As can be seen, the HEL solution becomes progressively turbid with time and by the end of the reaction period, almost no light passes through the solution. Importantly, the aggregation reaction curve is observed to be composed of three distinct phases: (i) a nucleation phase, (ii) a rapid, propagation phase, and (iii) a termination phase. Such aggregation behavior is typical of amyloid fibril formation [82]. In fact, the ability of HEL to form amyloid fibrils under similar reaction conditions has recently been reported by Yonezawa *et al* [81]. Although rapid and dramatic, nucleation-propagation type aggregation reactions are prone to considerable variability and often exhibit different lag times and propagation rates. Even minute changes in the initial protein concentration, buffer composition, and differences in the cuvette surface structure can lead to variable reaction rates. Hence, when performing comparative

analyses, the buffer and all protein solutions were prepared fresh using the same protocol. Care was also taken to use the same set of cuvettes, which were subjected to identical cleaning procedures. Even after these precautions, some variability in the rate of HEL aggregation persisted. The four reaction curves in Figure 43 represent aggregation experiments conducted on four different days with different, freshly prepared buffer and HEL solutions each day. Each curve in turn is an average of three experiments conducted on a given day. As can be seen (Figure 43), the assay variability within a given day is minimal, however, some day-to-day variability is observed. The day-to-day variability was quantified and the t_{50} value ranged from 4.5 – 8.5 minutes.

3.5.2 Effect of Free PEG on the Aggregation Rate of HEL

Prior to examining the effects of PEGylation on the heat-induced aggregation of HEL, the effect of a low concentration (4 % w/v) of free PEG on the aggregation rate of HEL was evaluated. A high PEG concentration was not employed in order to minimize any confounding effects. For example, an increase in solvent viscosity resulting from a high PEG concentration potentially might inhibit the aggregation reaction. Alternatively, a high PEG concentration might accelerate the aggregation reaction due to macromolecular crowding effects, as observed in the case of α -synuclein [82]. For these reasons, the concentration of PEG 20 kD was fixed at 4 % (w/v). At this level, the 20 kD PEG was approximately a 30-fold molar excess over the 1 mg/mL HEL. Three sets of experiments were conducted on three different days (Figure 44 - Figure 46).

Figure 42. A representative plot depicting the aggregation of HEL monitored turbidimetrically at 320 nm. Experiment conducted with 1 mg/mL HEL in a 25 mM sodium phosphate, 125 mM NaCl, pH 7.5 buffer at 75 °C.

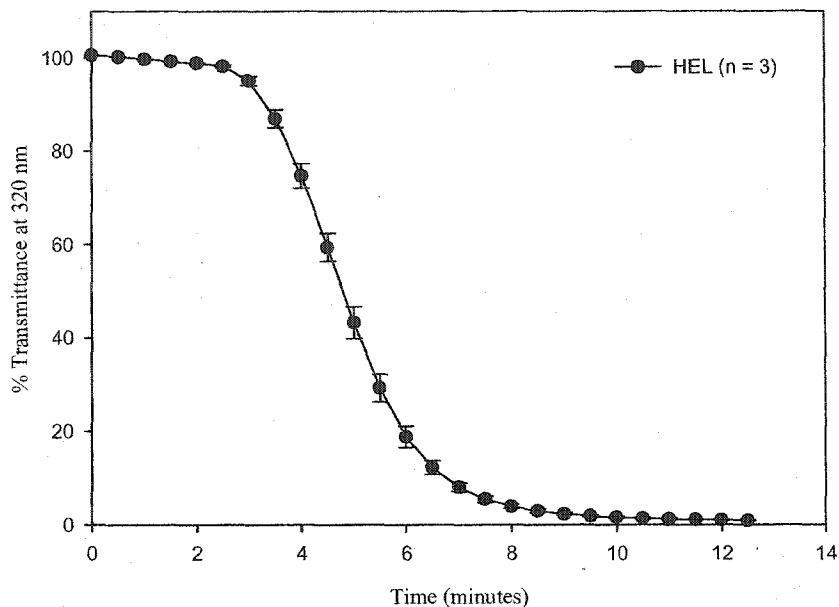


Figure 43. A plot depicting the variation in the turbidimetric assay for monitoring the heat induced aggregation of HEL. Experiments conducted with freshly prepared 1 mg/mL HEL solutions in a 25 mM sodium phosphate, 125 mM NaCl, pH 7.5 buffer on four different days (I-IV). The aggregation reaction was monitored turbidimetrically at 320 nm at 75 °C.

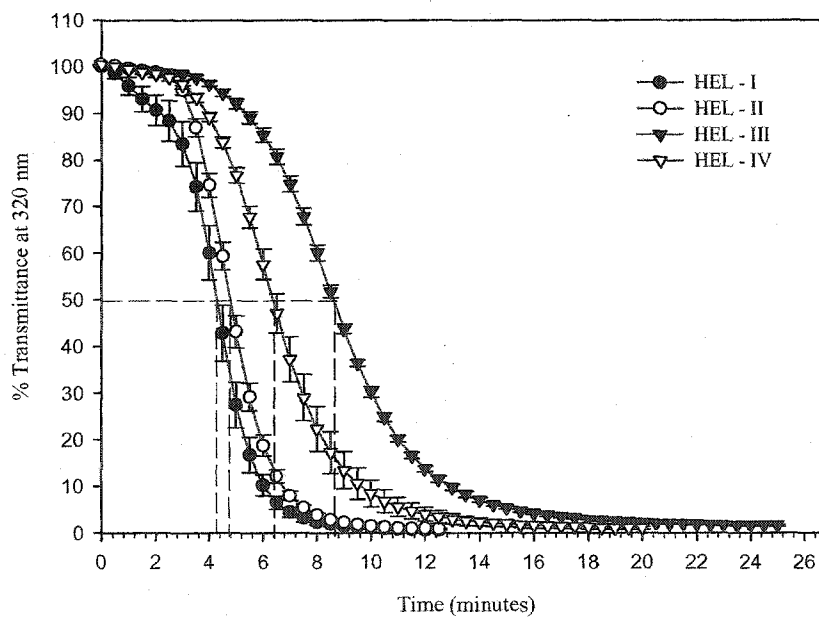


Figure 44. A plot depicting the effect of 4% PEG 20 kD on the heat induced aggregation of HEL: Set I. The aggregation reaction was monitored turbidimetrically at 320 nm at 75 °C.

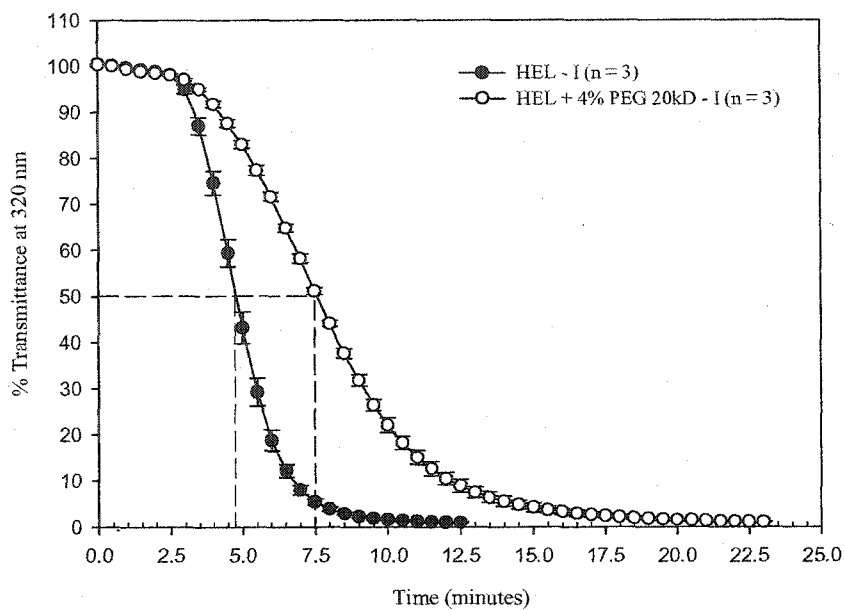
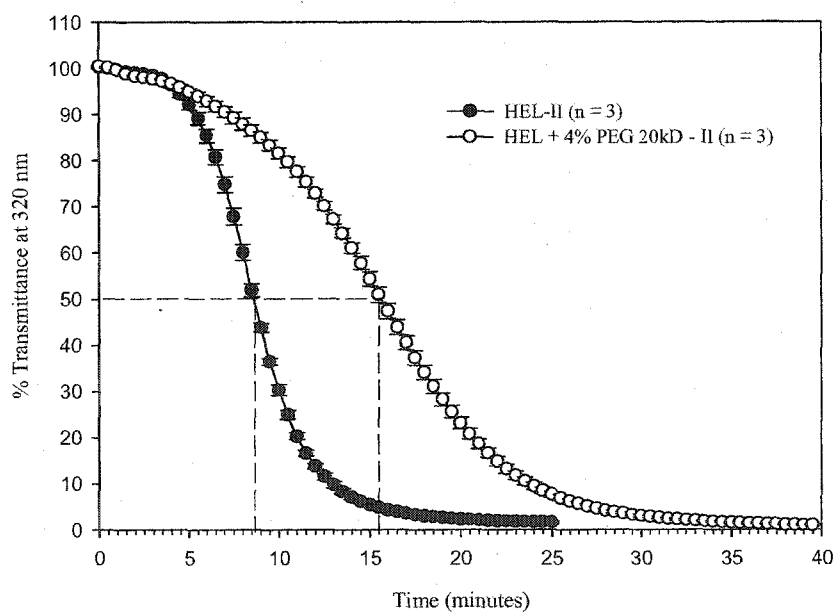


Figure 45. A plot depicting the effect of 4% PEG 20 kD on the heat induced aggregation of HEL: Set II. The aggregation reaction was monitored turbidimetrically at 320 nm at 75 °C.



As seen from Figure 44 through Figure 46, the aggregation reaction is inhibited in the presence of PEG 20 kD. Although the PEG does not eliminate aggregate formation, it appears to retard the propagation phase of the aggregation reaction. Similar lag phases are observed for both the control and test solutions in all three sets.

Importantly, the inhibition of the aggregation reaction in the presence of PEG supports the hypothesis that the PEG interacts with the exposed hydrophobic patches of the denatured HEL and inhibits any aggregate formation via the denatured, D form of the protein.

3.5.3 Effect of PEGylation on the Aggregation of HEL

The effect of PEGylation on the heat-induced aggregation of HEL was also studied using the turbidimetric aggregation assay. Experiments with PEG3-HEL were not possible due to limited sample availability. To facilitate comparison with the HEL and HEL + 4 % (w/v) PEG 20 kD results, experiments were conducted with 1 mg/mL PEG1-HEL and PEG2-HEL solutions prepared in the 25 mM phosphate, 125 mM NaCl buffer. The results of these studies are presented in Figure 47 and Figure 48. There was only a 5 % decrease in the % transmittance is observed for both PEG1-HEL and PEG2-HEL over a 25-minute period. This is indicative of some aggregation. The dramatic effect of PEGylation in reducing the HEL aggregation can be better observed when the PEG1-HEL and PEG2-HEL data are compared with the earlier, HEL and HEL + 4 % (w/v) PEG 20 kD results (Figure 49).

Figure 46. A plot depicting the effect of 4% (w/v) PEG 20 kD on the heat induced aggregation of HEL: Set III. The aggregation reaction was monitored turbidimetrically at 320 nm at 75 °C.

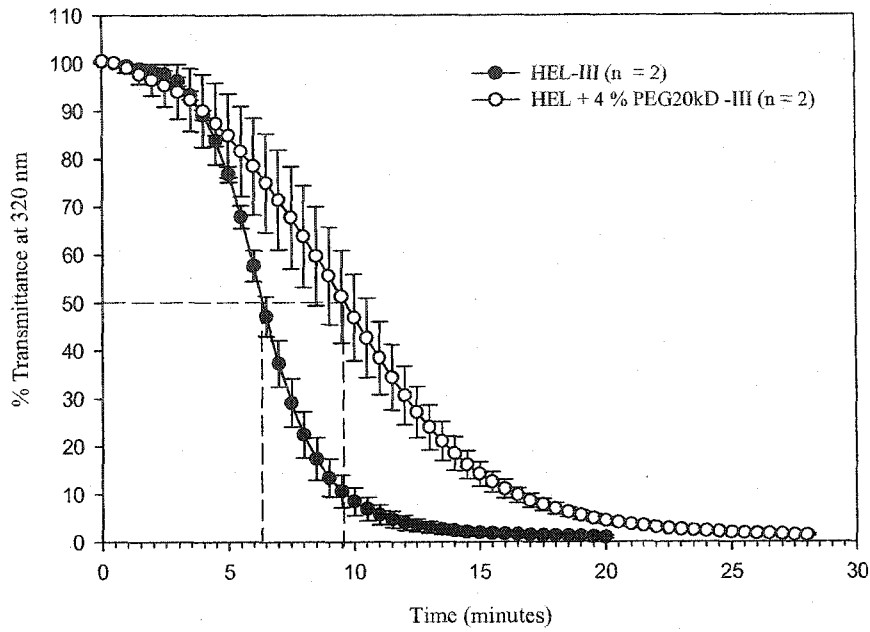


Figure 47. A plot depicting the aggregation of PEG1-HEL monitored turbidimetrically at 320 nm. Experiments (n = 4) conducted with 1 mg/mL PEG1-HEL in a 25 mM sodium phosphate, 125 mM NaCl, pH 7.5 buffer at 75 °C.

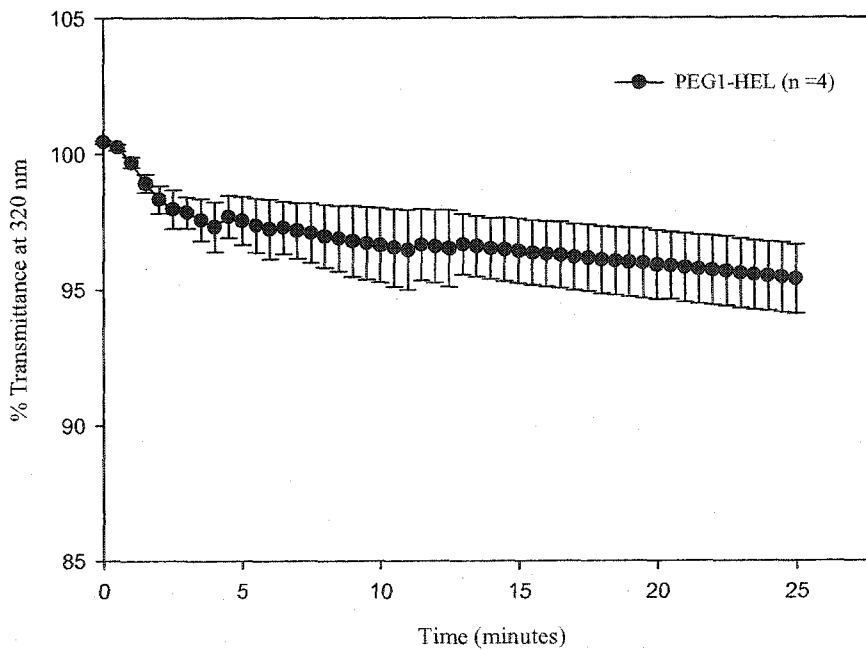


Figure 48. A plot depicting the aggregation of PEG2-HEL monitored turbidimetrically at 320 nm. Experiments ($n = 3$) conducted with 1 mg/mL PEG2-HEL in a 25 mM sodium phosphate, 125 mM NaCl, pH 7.5 buffer at 75 °C.

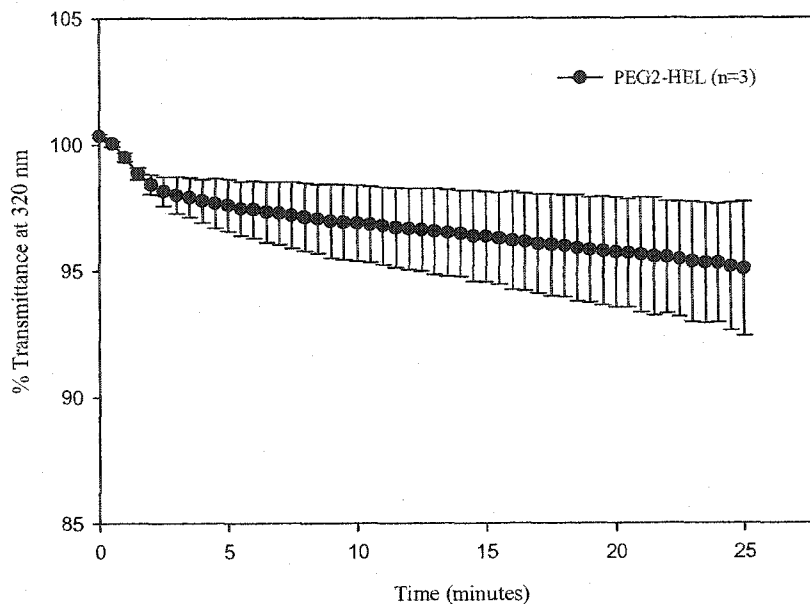
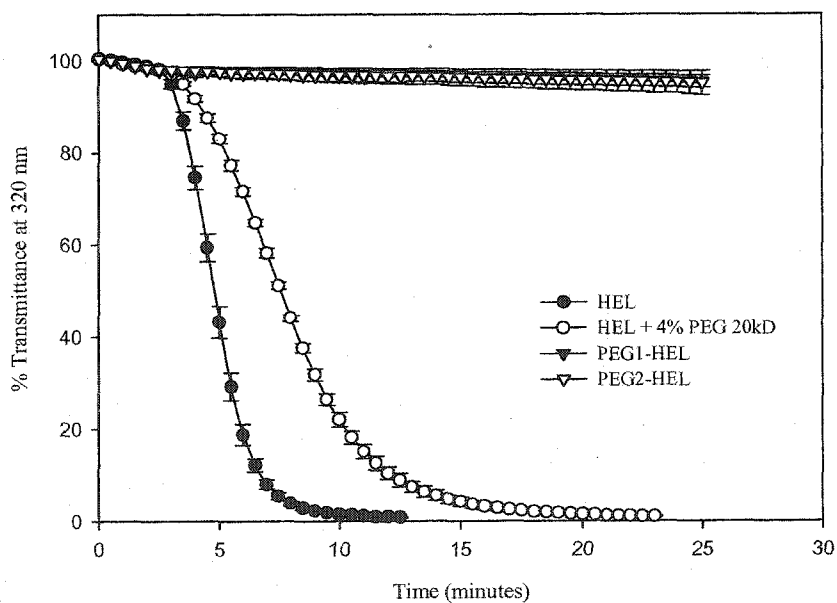


Figure 49. A plot depicting the effect of PEGylation on the heat induced aggregation of HEL. Experiments conducted with 1 mg/mL HEL, 1 mg/mL HEL + 4 % PEG 20 kD, 1 mg/mL PEG1-HEL, and 1 mg/mL PEG2-HEL respectively in a 25 mM sodium phosphate, 125 mM NaCl, pH 7.5 buffer. The aggregation reaction was monitored turbidimetrically at 320 nm at 75 °C.



These results are consistent with the hypothesis proposed in this dissertation. The covalently tethered PEG chains being readily available in the immediate microenvironment of the protein, interact with the hydrophobic patches exposed in the unfolded HEL and inhibit further interactions that lead to aggregation. Evidence for the presence of such the protein-PEG interactions has previously been reported by other researchers for HEL [84] and for carbonic anhydrase [83]. An equally important factor to be considered is the steric hindrance by the large PEG chains in inhibiting the aggregation reaction. It is quite likely that the covalently attached polymer sterically blocks interactions involving the unfolded HEL (D) molecules.

Although minimal, there still was some aggregation observed in both PEG1-HEL and PEG2-HEL in the turbidimetric assay. To better understand the nature of these aggregates and to ensure that there was no degradation in the PEGylated HEL molecules during the assay, both PEG1-HEL and PEG2-HEL were subjected to SDS-PAGE analysis post turbidimetric assay. Experiments were conducted under both reducing and non-reducing conditions to test for any covalent aggregates. Digital images of the SDS-PAGE gels are presented in Figure 50 and Figure 51, respectively. The protein bands were visualized using the Coomassie Blue Stain and the BaI₂ stain was employed to visualize the PEG bands. As seen from the figures, there is no degradation or dePEGylation observed in either of the two PEGylated molecules. However, the non-reducing gels revealed the presence of disulfide linked, covalent aggregates, as these are not present in the samples that were run under reducing conditions. Under reducing conditions only a single band corresponding the denatured, PEG1-HEL or PEG2-HEL monomers was observed in all lanes.

Figure 50. Non-reducing SDS-PAGE analysis of PEG1-HEL and PEG2-HEL post turbidimetric aggregation assay (incubation at 75 °C for 25 minutes). Panel (a): Gel stained with the Coomassie Blue Stain. The PEG1-HEL, and PEG2-HEL controls (prior to heat treatment) are in lanes 1 and 5 respectively, while the heat treated PEG1-HEL & PEG2-HEL samples (n =3) are in lanes 2-4, and 6-8 respectively. Panel (b): Gel stained with a barium iodide stain, specific for PEG. The PEG1-HEL, and PEG2-HEL controls (prior to heat treatment) are in lanes 4 and 8 respectively, while the heat treated PEG1-HEL & PEG2-HEL samples (n = 3) are in lanes 1-3, and 5-7 respectively.

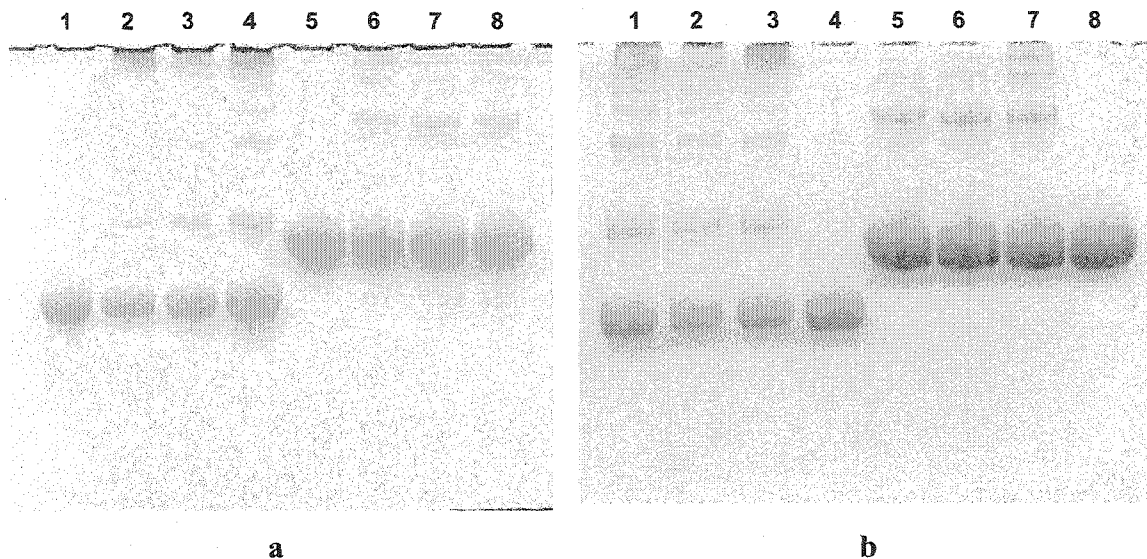
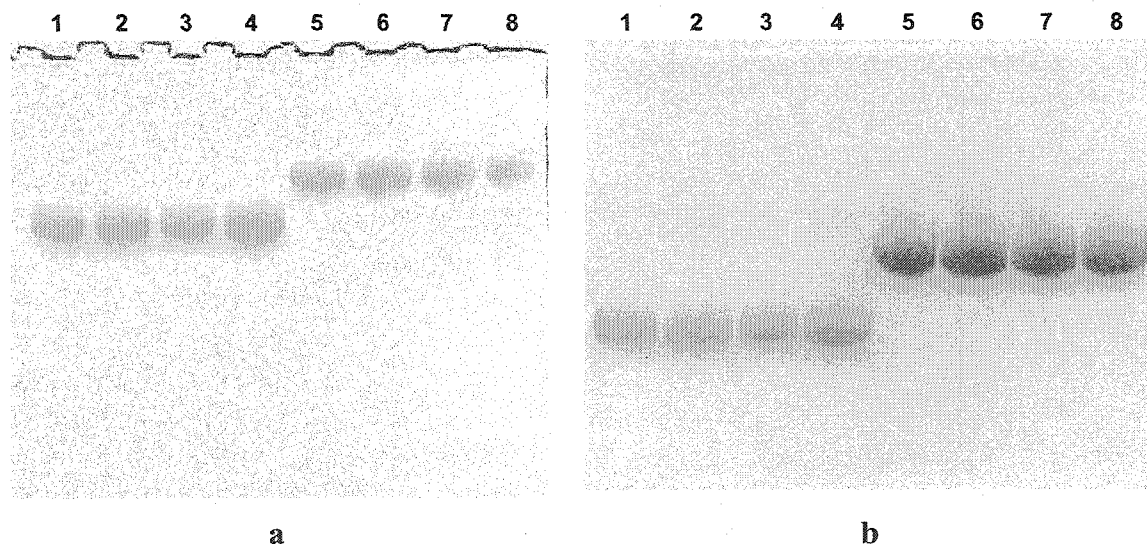


Figure 51. Reducing SDS-PAGE analysis of PEG1-HEL and PEG2-HEL post turbidimetric aggregation assay. Panel (a): 12% gel stained with the Coomassie Blue Stain. The PEG1-HEL, and PEG2-HEL controls (prior to heat treatment) are in lanes 1 and 5 respectively, while the heat treated PEG1-HEL & PEG2-HEL samples (n =3) are in lanes 2-4, and 6-8 respectively. Panel (b): 4-15% gel stained with a barium iodide stain, specific for PEG. The PEG1-HEL, and PEG2-HEL controls (prior to heat treatment) are in lanes 4 and 8 respectively, while the heat treated PEG1-HEL & PEG2-HEL samples (n =3) are in lanes 1-3, and 5-7 respectively.



It should be noted that the turbidimetric assay was conducted under non-reducing conditions (pH 7.5) and at an elevated temperature of 75 °C. Inter-molecular disulfide bond formation between unfolded molecules would be expected to occur under these conditions.

3.5.4 Aggregation Studies Using SE-HPLC

The turbidimetric assay demonstrated that PEGylation drastically reduced the aggregation in HEL. However, it did not provide any information about aggregates at a molecular level. Insoluble aggregates were mainly detected in the turbidity measurements. Further, the results from SDS-PAGE analysis were limited to covalent aggregates; no information about the presence of non-covalent aggregates could be obtained using this technique. Also, the turbidimetric technique may not have been sensitive enough to discern the differences, if any, between the aggregation rates of PEG1-HEL and PEG2-HEL. For these reasons, size-exclusion HPLC was employed to study heat induced aggregation of HEL and the PEGylated HEL molecules.

Aggregation experiments for SE-HPLC analysis were conducted using the experimental conditions as employed in the turbidity measurements. Briefly, the HEL, PEG1-HEL, or PEG2-HEL samples were incubated at 75 °C for 25-30 minutes and then immediately cooled to room temperature. After this, SE-HPLC analysis was conducted on these samples and the monomer remaining of each species (HEL, PEG1-HEL, or PEG2-HEL) was determined. The SE-HPLC results are presented graphically in Figure 52. Only 34 % of HEL as a monomer remained after the heat treatment, while substantially larger amounts of the PEG1-HEL and PEG2-HEL monomers, 68 and 79 percent respectively, were observed to be present. Importantly, these data demonstrate

that the aggregation of HEL is reduced in half by the covalent attachment of a single 20 kD PEG chain. The addition of a second PEG chain leads to a further decrease in aggregation rate, although the magnitude of this effect is smaller.

The effect PEGylation has in enhancing the thermal stability of HEL can be seen visually in Figure 53. The HEL solution turns milky after incubation at 75 °C for 25 minutes, while the PEG1-HEL and PEG2-HEL samples remain clear.

Figure 52. Comparison of the rates of heat induced aggregation in HEL, PEG1-HEL and PEG2-HEL. Experiments were conducted with 0.9 mg/mL HEL, PEG1-HEL and PEG2-HEL respectively in a 25 mM sodium phosphate, 125 mM NaCl, pH 7.5 buffer. The aggregation reaction was conducted 75 °C for 25-30 minutes (s indicated below). Samples were analyzed using SE-HPLC in terms of % monomer remaining post reaction.

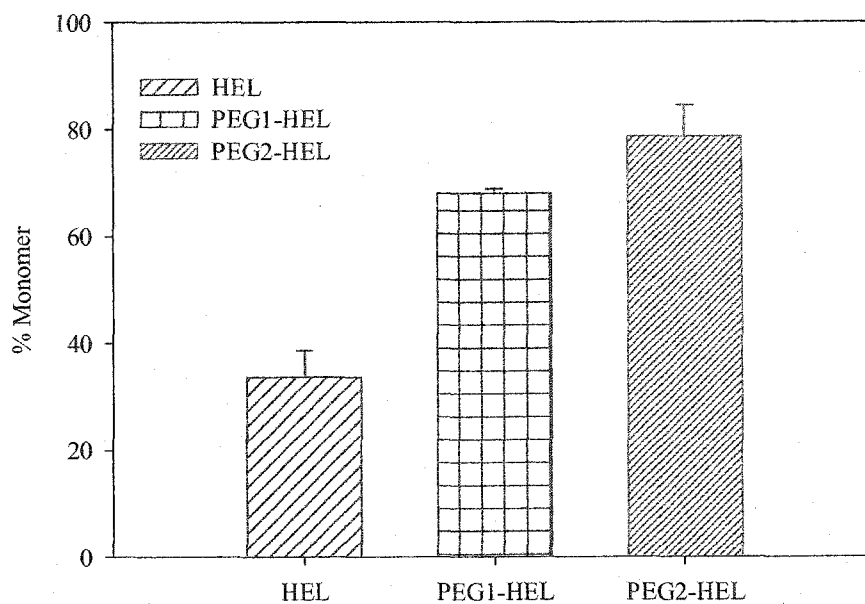
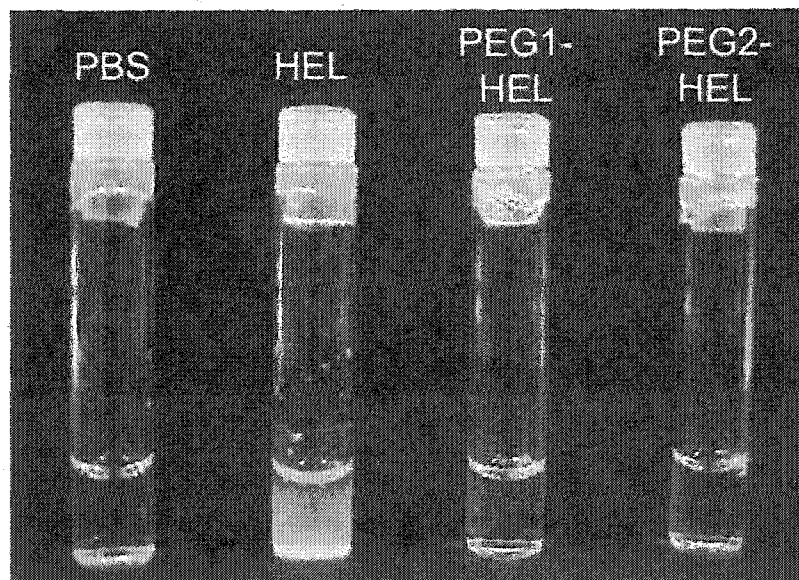


Figure 53. Visualization of the heat induced aggregation of HEL, PEG1-HEL and PEG2-HEL. Vials containing PBS (25 mM sodium phosphate, 125 mM NaCl, pH 7.5), and 0.9 mg/mL HEL, PEG1-HEL & PEG2-HEL in PBS were incubated at 75 °C for 25 minutes, and then digitally photographed.



Chapter 4

SUMMARY AND CONCLUSIONS

4.1 Characterization of PEG-HEL Molecules

4.1.1 Purity Analysis

Hen Egg Lysozyme was modified with linear, 20-kD, methoxy-PEG propionaldehyde chains using the reductive amination reaction of aldehydes and primary amines. Three PEGylated HEL molecules - PEG1-HEL, PEG2-HEL, and PEG3-HEL were purified, each containing one, two or three PEG chains respectively.

The SDS-PAGE and MALDI-TOF analyses indicated that PEG1-HEL and PEG2-HEL were homogeneous with respect to the degree of PEGylation. Trace amounts of PEG2-HEL were observed to be present in the purified PEG3-HEL. Importantly, no unreacted HEL was present in any of the purified PEG-HEL molecules.

Minimal amounts of non-covalent aggregates were observed to be present in PEG1-HEL (2.0 %) and PEG2-HEL (2.3 %). The polydispersity in the PEG, PEG1-HEL and PEG2-HEL monomers was quantified using static light scattering. All three molecules were observed to be fairly monodisperse with polydispersity indices of 1.03, 1.03, and 1.04 respectively.

Taking advantage of the differential pK_as of the α -amine (pK_a = 5.2 – 7.8) and the ϵ -amines (pK_a = 11.1) of lysines [64-66], the PEGylation reaction pH was optimized (pH 4.5) to selectively modify the N-terminal amine of HEL. Hence it is very likely that the PEG is attached at the amino terminus in the case of PEG1-HEL. This reaction has previously been shown to yield fairly homogenous (> 95 %), N-terminally modified products for several other proteins [67]. The positional homogeneity offered by the reductive amination reaction in the case of monoPEGylated species could not be utilized to synthesize homogeneous, higher order PEGylated species. Differentiation on the basis of pK_a was not possible between the ϵ -amines. Consequently, positional isomers may be present in PEG2-HEL and PEG3-HEL.

4.1.2 Molecular Weights

Although SDS-PAGE was an effective tool for the qualitative characterization of the homogeneity of the PEGylated HEL molecules, gross overestimates of the apparent molecular weights for the three PEG-HEL molecules were obtained using this technique. PEG-proteins exhibit an anomalous electrophoretic behavior on a sieving matrix. This is because of their large hydrodynamic radii, branching in the polypeptide chain introduced by PEG, and an uneven distribution of SDS molecules around the PEG-polypeptide. Hence, the molecular weights of the PEGylated HEL molecules were determined using the absolute techniques of MALDI-TOF, sedimentation velocity (SV), and static light scattering (SLS).

MALDI measurements yielded molecular weights of 36280, 58200, and 79,800 kD for PEG1-HEL, PEG2-HEL and PEG3-HEL respectively. These values are in excellent agreement with their expected, nominal values of 34305, 54,305, and

74305 kD. The MALDI data suggest that the actual molecular weight of the PEG employed for HEL modification is $\sim 21,900$ (by subtracting the HEL MW and dividing by the degree of PEGylation). This is consistent with the molecular weight value of 21470 for PEG determined using SLS measurements. One drawback of the MALDI measurements is that the MW values represent only the respective, peak intensity values and do not account for the polydispersity of the samples. Solution molecular weights (M_w) of the PEGylated HEL molecules were possible using SLS and SV measurements

The weight average molecular weights of PEG1-HEL (34,430) and PEG2-HEL (53,870) determined using SE-HPLC coupled static light scattering were in excellent agreement with their respective nominal values (within 5 %), MALDI-TOF (within 5-8 %), and SV measurements (within 5 %). Size exclusion HPLC coupled static light scattering is a very powerful technique for the analysis of PEGylated proteins. With one experiment, information about aggregation, polydispersity, and the solution molecular weight of a molecule can be obtained via this technique.

On the other hand, information regarding both size and shape of a molecule can be obtained simultaneously from SV studies as obtained for HEL (14540, 19 Å), PEG1-HEL (32840, 49 Å), and PEG2-HEL (52940, 68 Å) in the present case. One drawback of sedimentation velocity is that highly pure samples are required for obtaining good estimates of molecular weights and Stokes radii. Further, significant hydrodynamic non-ideality effects were observed for both PEG1-HEL and PEG2-HEL. These effects were accounted for by conducting experiments at different concentrations to obtain s and D values extrapolated to infinite dilution (s° and D°). In the case of PEG1-HEL and

PEG2-HEL (which were ~ 98 % pure), very good estimates of molecular weights and Stokes radii were obtained using their respective s° and D° values.

4.1.3 Effect on HEL Structure

The Far UV CD experiments conducted with HEL, PEG1-HEL and PEG2-HEL indicated that PEGylation had no effect on the secondary structure of HEL. The far UV CD spectra of the three molecules were almost coincident (Figure 17). In the fluorescence experiments, significant signal quenching was observed for both PEG1-HEL and PEG2-HEL, however, their λ_{\max} remained unchanged at 342 nm. The reason for the observed quenching remains unclear. Additional studies are required to understand this phenomenon. The fluorescence and near UV CD studies suggest that the PEGylated HEL molecules are folded, and that there are no major conformational changes in HEL as a result of PEGylation.

4.2 Hydrodynamic Behavior of PEG-HEL molecules

4.2.1 Sedimentation Properties & Hydrodynamic Radii

The sedimentation properties of HEL were altered upon PEGylation. Consistent with observations for other PEG-proteins in a previous study by the author [40], the sedimentation coefficient of HEL (1.8 s) decreased upon PEGylation. Despite significant differences in the molecular weights of PEG1-HEL, PEG2-HEL, and PEG3-HEL, their sedimentation coefficients were nearly identical, between 1.0 and 1.1 s (at a protein concentration of 0.4 – 0.5 mg/mL for all three molecules). This indicated that the PEGylated molecules experience an increase in frictional drag. For the higher order

PEGylated species, the increase in frictional drag was almost exactly compensated by the increase in their molecular weights. Consequently, the sedimentation coefficient remained invariant with increasing degree of PEGylation. Further, almost coincidental the $g(s^*)$ patterns were observed for all three PEG-HEL molecules. This indicates that the heterogeneity with respect to the degree of PEGylation for a given PEG-protein mixture will be resolved poorly via sedimentation velocity experiments.

The sedimentation experiments also revealed the presence of hydrodynamic non-ideality for PEG1-HEL and PEG2-HEL. These effects were manifested in terms of a concentration dependence of s and D . The hydrodynamic non-ideality increased with increasing degree of PEGylation and its effect was more severe on the diffusion coefficient (Figure 23) than on the sedimentation coefficient (Figure 22). Importantly, the Stokes radii of PEG1-HEL and PEG2-HEL estimated from D° values were in excellent agreement with those determined using dynamic light scattering (within 5- 8 %).

The R_h of HEL increased from 20 Å to ~ 50 Å for PEG1-HEL. PEG2-HEL and PEG3-HEL had even larger radii of ~ 68 Å and 74 Å. These results demonstrate that PEGylation causes a dramatic increase in the hydrodynamic volume of a protein. They also suggest that for a small protein, modification with a single large PEG chain may be sufficient to increase its size past the threshold (> 36 Å) for renal clearance.

4.2.2 Solution Conformation

The dynamic light scattering studies with various PEG molecules (MW: 5000 – 40,000) suggest that the polymer exhibits a near random-coil conformation in solution. A value of $n = 2.07$ was obtained for PEG by applying the power law equation (Equation 21: $MW = k \times R_h^n$). For perfect random-coil behavior, the value of n is 2.

Interestingly, the 20-kD and 40-kD bi-PEGs also were observed to exhibit random coil behavior. In fact, the Stokes radii of the linear 20 kD PEG and that of the 20-kD bi-PEG were found to be identical (43 Å). Branching at a single point appears to have no effect on the overall conformation of the polymer.

The R_h of PEG1-HEL (49 Å) and PEG2-HEL (68 Å) were measured to be only ~ 10 % larger than the 20-kD (43 Å) and 40-kD (60 Å) PEG chains. These data suggest that the covalently tethered PEG(s) predominantly govern the solution conformation of the PEG-HEL molecules. Further evidence for this is provided by the value of the exponent $n = 1.8$ (Equation 21) for the PEG-HEL molecules. The PEG-protein can be imagined to be a random coil (like PEG), with the polymer chains hanging freely in solution with one end fixed at the protein surface.

4.3 Effect of PEGylation on the Thermal Stability of HEL

4.3.1 Equilibrium Unfolding Studies

HEL was observed to exhibit a two state ($N \leftrightarrow D$) unfolding process under the chosen conditions (40 mM glycine-HCl, pH 3.0). The thermodynamic parameters determined from the difference spectrum method and DSC were in excellent agreement (within 5 -10 %). This agreement was indicative of the validity of the two-state model. The $\Delta H_{cal}/\Delta H_v$ ratio for HEL unfolding was between 0.96-1.02, which further supported the two-state transition model. However, the $\Delta H_{cal}/\Delta H_v$ ratio decreased to 0.8 for PEG2-HEL, suggestive of intermolecular cooperativity resulting from the PEG. The covalently attached PEG may chaperone and facilitate the unfolding process via interactions with the exposed, hydrophobic interior.

Similar to the effects of free PEG 400, and PEG 20,000 on the unfolding of HEL, a decrease in the melting temperature (T_m) of HEL was observed with increasing degree of PEGylation. A T_m drop of up to 2.5 °C (DSC) and 4.0 °C (Difference Spectrum method) was observed for the PEG-HEL molecules. By comparing the T_m drop of the PEGylated HEL molecules with that observed in the presence of free PEG 20,000, the local concentration of PEG around the a PEGylated HEL molecule can be viewed to be as high as 15-25 %. These results support the hypothesis that the covalently attached PEG chains are available in the immediate microenvironment of the protein to interact with, and stabilize its denatured form. A decrease in the melting temperature of unfolding can be explained by the stabilization of the denatured protein by PEG.

4.3.2 Kinetic Aggregation Studies

The Aggregation reaction of HEL was monitored at an elevated temperature of 75 °C. This was done to ensure the presence of a substantial amount of the protein in denatured form. Under these conditions, HEL exhibited a nucleation-propagation type of aggregation process that is indicative of amyloid fibril formation. The aggregation of HEL was observed to be slower in the presence of 4 % PEG 20,000. However, a dramatic decrease in the aggregation rate was observed in the case of the PEG-HEL molecules.

The aggregation of HEL, PEG1-HEL and PEG2-HEL was also monitored using Size exclusion HPLC. These results indicated that the extent of aggregation decreased with increasing degree of PEGylation. Only 34 % of the HEL monomer remained after incubation at 75°C for 30 minutes, while 68 % and 79 % of the PEG1-HEL and PEG2-HEL monomers were present. These data suggest that the thermal stability of PEGylated HEL is kinetically controlled.

4.3.3 Reaction Model for the Aggregation of PEGylated Proteins

The thermal stability of PEGylated HEL was evaluated by employing the Eyring-Lumry model ($N \xrightleftharpoons{T_m} D \xrightarrow{k_a} A$)⁸ for protein aggregation. A decrease in the T_m for HEL unfolding was observed with increasing degree of PEGylation. This was indicative of an increasing thermodynamic instability with increasing degree of PEGylation. In contrast, the kinetic studies demonstrated that aggregation of HEL decreases with increasing degree of PEGylation. Thus, both the thermodynamic unfolding studies and the kinetic aggregation studies are in support of the aggregation model proposed in Reaction Scheme-II.



The model states that even if a PEGylated protein is thermodynamically unstable, it can still resist aggregation. The melting temperature may not be a true indicator of the stability of PEGylated proteins as their aggregation appears to be kinetically controlled. This has practical significance for the design of PEGylated proteins. Caution should be exercised when interpreting the thermodynamic, melting temperature data for PEGylated proteins. A decrease in the T_m of a PEGylated protein may not be relevant to its stability with respect to aggregation. Instead, it may be more appropriate to evaluate the thermal stability of PEGylated proteins on the basis of kinetic assays.

⁸ N – native state, D – denatured state, A – aggregate

REFERENCES

1. Working, P.K., Newman, M. S., Johnson, J., Cornacoff, J. B., "Safety of Poly(ethylene glycol) and Poly(ethylene glycol) Derivatives" in Poly(ethylene glycol) Chemistry and Applications, Harris, J. M. & Zalipsky, S. Ed., American Chemical Society Press, Washington D. C. (1997) pp 45-57
2. Johnston E, Crawford J, Blackwell S, Bjurstrom T, Lockbaum P, Roskos L, Yang BB, Gardner S, Miller-Messana MA, Shoemaker D, Garst J, Schwab G., "Randomized, dose-escalation study of SD/01 compared with daily filgrastim in patients receiving chemotherapy", *J Clin Oncol.* (2000) (13): 2522-8.
3. Katre, N.V. "Immunogenicity of Recombinant IL-2 modified by Covalent Attachment of Polyethylene Glycol." *J. Immunology*, 1990, vol. 144. pp. 209-213
4. Goodson, R. J. & Katre, N.V. "Site -Directed PEGylation of Recombinant Interlukin-2 at its Glycosylation Site", *Bio/Technology* (1990) 8: 343 - 346.
5. Mabrouk, P. A., The use of Polyethylene glycol-Enzymes in Nonaqueous Enzymology. In: *Poly(ethylene glycol) Chemistry and Applications*. Harris, J. M., & Zalipsky S. Eds. American Chemical Society, Washington D. C., pp. 118-133.
6. Molineux, G. "Pegfilgrastim: using Pegylation technology to improve neutropenia support in cancer patients." *Anti-Cancer Drugs* 2003, vol. 14, pp. 259-264
7. *Thomson Physician's Desk Reference (2002-2003)* Electronic Edition.
8. Luxon, B., Grace, M., Brassard, D., & Bordens, R. "Pegylated Interferons for the treatment of Chronic Hepatitis C Infection." *Clinical Therapeutics* 2002, Vol. 24, No. 9, pp. 1363-1379
9. Holle, L., M., "Pegaspargase: an alternative?" *Ann Pharmacother* (1997) May; 31(5) 616-24.
10. Francis, G.E, Delgado, C & Fisher, D, "PEG-Modified Proteins" in Stability of Protein Pharmaceuticals, Part B: In Vivo Pathways of degradation and strategies for protein stabilization, edited by Ahern, T. J. & Manning, M. C. Plenum Press, New York (1992) pp. 236-263.
11. Suzuki, T., Kanbara, N., Tomono, T., Hayashi, N., & Shinohara, I. "Physico-chemical and biological properties of poly(ethylene glycol)-coupled Immunoglobulin G", *Biochim. Biophys. Acta* 788: 248-255

12. Sorensson, J., Ohlson, M. & Haraldsson, B. "A quantitative analysis of the glomerular charge barrier in the rat", *Am J Physiol Renal Physiol* (2001), 280: F646 - F656.
13. Lumry R, Eyring H.. "Conformational changes of proteins". *J Phys Chem* (1954) 58: 110-120
14. Roberts, C.J., Darrington, R.T., Whitley, M.B. "Irreversible Aggregation of Recombinant Bovine Granulocyte-Colony Stimulating Factor (bG-CSF) and Implications for Predicting Protein Shelf Life." *J. Pharm. Sci.*, May 2003, Vol. 92, No. 5, pp. 1095-1111.
15. Dill, K.A., Alonso, D.O.V. & Hutchinson, K. "Thermal Stabilities of Globular Proteins." *Biochemistry* 1989, 28, pp. 5439-5449
16. Remmele, R.L., Nightlinger, N.S., Srinivasan, S. & Gombotz, W.R. "Interleukin – 1 Receptor (IL-1R) Liquid Formulation Development Using Differential Scanning Calorimetry." *Pharm. Res.* 1998, Vol. 15, No.2, pp. 200-208
17. Remmele, RL., Gombotz, WR., "Differential Scanning Calorimetry: A practical tool for elucidating stability of liquid biopharmaceuticals "BioPharm. (2000) June: 36-45.
18. Arakawa, T. & Timasheff, S. N., "Stabilization of Protein Structure by Sugars", *Biochemistry* (1982) 21: 6536 -6544.
19. Arakawa, T. & Timasheff, S. N. "The Stabilization of Proteins by Osmolytes", *Biophys. J* (1985) 47: 411-414.
20. Eberlein GA, Stratton PR, Wang YJ. "Stability of rhbFGF as determined by UV spectroscopic measurements of turbidity", *PDA J Pharm Sci Technol.* (1994) 48(5): 224 - 230.
21. Bam NB, Cleland JL, Yang J, Manning MC, Carpenter JF, Kelley RF, Randolph TW., "Tween protects recombinant human growth hormone against agitation-induced damage via hydrophobic interactions" *J Pharm Sci.* (1998) Dec; 87(12): 1554-9.
22. Hinds, K. D., Kim, S. W., "Effects of PEG conjugation on insulin properties." *Adv Drug Deliv Rev.* 2002 Jun 17; 54(4): 505-30.
23. Francis, G.E., Delgado, C. & Fisher, D. "PEG- Modified Proteins" in *Stability of protein Pharmaceuticals, Part B: In Vivo Pathways of Degradation and Strategies for Protein Stabilization*, edited by Tim J. Ahern and Mark C. Manning. Plenum Press, New York, 1992.

24. Callahan WJ, Narhi LO, Kosky AA, Treuheit MJ. "Sodium chloride enhances the storage and conformational stability of BDNF and PEG-BDNF", *Pharm Res.* (2001) 3: 261-266.
25. Kinstler, O. B., Brems, D.N., Lauren, S.L., Paige, A.G., Hamburger, J.B. & Treuheit, M.J., "Characterization and Stability of N-terminally PEGylated rhG-CSF", *Pharmaceutical Research* (1996) 13: 7, 996 - 1002.
26. Nodake, Y. & Yamasaki, N. "Some Properties of a Macromolecular Conjugate of Lysozyme Prepared by Modification with a Monomethoxypolyethylene Glycol Derivative." *Biosci, Biotechnol, Biochem* (2000) 64 (4) pp. 767 -774.
27. So, T., Ueda, T., Abe, Y., Nakamata, T., Imoto, T., "Situation of monomethoxypolyethylene glycol covalently attached to lysozyme" *J/Biochem* (Tokyo) (1996) 119(6) pp. 1086-93.
28. Lee, LL-Y. & Lee, JC. , Thermal Stability of Proteins in the Presence of Poly(ethylene glycols), *Biochemistry* (1987) 26: 7813 - 7819.
29. Arakawa, T., & Timasheff, S. N. "Mechanism of Poly (ethylene glycol) Interaction with Proteins." *Biochemistry* (1985) vol. 24, pp. 6756 -6762
30. Tencer, J., Frick, I-M., Oquist, B. W., Alm, P. & Rippe, B. "Size-selectivity of the glomerular barrier to high molecular weight proteins: Upper size limitations of stunt pathways". *Kidney Int.* (1998) 53: 709 - 715.
31. Lindstrom, K. E., Blom, A., Johnsson, E., Haraldsson, B. & Fries, E. "High glomerular permeability of bikunin despite similarity in charge and hydrodynamic size to serum albumin". *Kidney Int.* (1997) 51: 1053 - 1058
32. Ohlson M, Sorensson J, Haraldsson B. "Glomerular size and charge selectivity in the rat as revealed by FITC-ficoll and albumin", *Am J Physiol Renal Physiol.* (2000) 279(1): F84-91.
33. Bowen, S., Tare, N., Inoue, T., Yamasaki, M., Okabe, M., Horii, I. & Eliason, J.F. "Relationship between molecular mass and duration of activity of polyethylene glycol conjugated granulocyte colony- stimulating factor mutein". *Exp. Hemat.* (1999) 27: 425 - 432.
34. Lee LS, Conover C, Shi C, Whitlow M, Filpula D. "Prolonged circulating lives of single-chain Fv proteins conjugated with polyethylene glycol: a comparison of conjugation chemistries and compounds", *Bioconjug Chem.* (1999) 10(6): 973-981.
35. Koumenis, I.L., Shahrokh, Z., Leong, S., Hsei, Deforge, L. and Zapata, G. "Modulating pharmacokinetics of an anti-interleukin-8 F(ab')₂ by amine-specific PEGylation with preserved bioactivity", *Int. J. Pharmaceutics* (2000) 198: 83 -95.

36. Knauf, M. J., Bell, D.P., Hertzner, P., Luo, Z-P, Young, J.D. and Katre, N.V. "Relationship of Effective Molecular Size to Systemic Clearance in Rats of Recombinant Interleukin-2 Chemically Modified with water soluble polymers", *J. Biol. Chem.* (1988) 263:29 pp 15064 -15070.
37. Nucci ML, Olejarczyk J, Abuchowski A. "Immunogenicity of polyethylene glycol-modified superoxide dismutase and catalase", *J. Free Radic. Biol. Med.* (1986) 2(56): 321-325.
38. Oliver, J.D.III & Deen, W. M. "Random-Coil Model for Glomerular Sieving of Dextran." *Bulletin of Mathematical Biology*, 1994, vol. 56, No. 3, pp. 369-389.
39. Kozlowski A, Charles S. A., Harris, J. M., "Development of pegylated interferons for the treatment of chronic hepatitis C." *BioDrugs* (2001) 15(7): 419-29.
40. Gokarn, Y. R., "Biophysical Characterization of PEGylated Proteins", *Master's Thesis*, University of New Hampshire (1998)
41. Chipman, D.M., Pollock, J.J., & Sharon, N. "Lysozyme -catalyzed Hydrolysis and transglycosylation Reactions of Bacterial Cell Wall Oligasaccharides." *J. Biol. Chem.* (1968) vol. 243 No.3. Feb. pp. 2698-2707
42. Canfield, R.E. "The Amino Acid Sequence of Egg White Lysozyme." *J. Biol. Chem.* (1963) vol. 238 No. 8. Aug. pp. 2698-2707.
43. Vocadlo, D.J., Davies, G.J., Laine, R., & Withers, S.G. "Catalysis by hen egg-white Lysozyme proceeds via a covalent intermediate." *Nature* (2001) Aug. vol. 412 pp. 835-838
44. Laurents, D.V. & Baldwin, R.L. "Characterization of Unfolding Pathway of Hen Egg White Lysozyme." *Biochemistry* (1997) vol. 36, pp. 1496-1504
45. Redfield, C., & Dobson, C.M. "Sequential H NMR Assignments and Secondary Structure of Hen Egg White Lysozyme in Solution." *Biochemistry* (1988) vol. 27, pp. 122-136
46. Estimated from the primary sequence using the program SEDNTERP
47. Allison, S. A., & Tran, V. T., "Modeling the electrophoresis of rigid polyions: Application to Lyosyme" *Biophysical J.* (1995) vol. 68: 2261-2270.
48. Bell, L. N., Hageman, M. J., Muraoka, L. M. "Thermally induced denaturation of lyophilized bovine somatotropin and lysozyme as impacted by moisture and excipients." *J Pharm Sci.* 1995 Jun; 84(6): 707-12.
49. Diwan, M. & Park, T.G. "Pegylation enhances protein stability during encapsulation in PLGA microspheres." *J. Controlled Release*, 2001, 73, pp. 233-244

50. So, T., Ito, H. -O, Hirata, M., Ueda, T. & Imoto, T. "Extended blood half-life of Monomethoxypolyethylene Glycol-conjugated hen Lysozyme is a key parameter controlling immunological tolerogenicity." *CMLS, Cell. Mol. Life Sci.* 55 (1999) pp. 1187-1194
51. So, T., Ito, H. -O, Tsujihata, Y., Hirata, M., Ueda, T. & Imoto, T. "The Molecular Weight Ratio of Monomethoxypolyethylene glycol (mPeg) to Protein determines the Immunotolerogenicity of mPEG proteins." *Protein Engineering* (1999) Vol. 12, No. 8, pp. 701-705.
52. Laemmli, UK. "Cleavage of structural proteins during the assembly of the head of bacteriophage T4", *Nature* (1970) 227(259): 680-685.
53. Kurfurst, M. M., Detection and MW Determination of PEG-modified Hirudin by Staining after SDS-PAGE Anal. *Bio Cehm* (1992) 200: 244- 248
54. Wen, J., Arakawa, T. and Philo, J.S. "Size Exclusion Chromatography with On-Line Light Scattering, Absorbance, and Refractive Index Detectors for Studying Proteins and Their Interactions", *Anal. Biochem.* (1996) 240: 155 -166.
55. The dn/dc value of 0.167 for proteins at laser wavelength was communicated by Precision Detectors, Inc.
56. Personal communication with Dr. Edward Remsen - Monsanto, 8th August 2000.
57. Kunitani, M., Dollinger, G., Johnson, D. & Kresin, L., "On-line characterization of polyethylene glycol-modified proteins". *J. Chromatography* (1991) 588:125-137.
58. Edsall, J. T. Apparent molar volume, heat capacity, compressibility and surface tension of dipolar ions in solutions in *Proteins, Amino acids and Peptides as Ions and Dipolar Ions*, Cohn, E. J. & Edsall, J. T., Ed. (1943) Pheinfeld, New York, pp. 155-176
59. Stafford W. F., Methods for Obtaining Sedimentation Coefficient Distributions. In: analytical ultracentrifugation in Biochemistry and Polymer Science. Harding S. & Rowe, A. Eds. The Royal Society of Chemistry, Cambridge, pp. 359-393.
60. Philo JS. "An improved function for fitting sedimentation velocity data for low-molecular-weight solutes", *Biophys J.* (1997) 72(1): 435-44.
61. Jackson WM, Brandts JF. "Thermodynamics of protein denaturation. A calorimetric study of the reversible denaturation of chymotrypsinogen and conclusions regarding the accuracy of the two-state approximation", *Biochemistry* (1970) 9(11): 2294 - 2301.

62. Remmele, R.L., Bhat, S.D., Phan D.H. & Gombotz, W.R. "Minimization of Recombinant Human Flt3 Ligand Aggregation at the T_m Plateau: A Matter of Thermal Reversibility." *Biochemistry* (1999) vol. 38, pp. 5241-5247
63. Lehearne, S., Chowdhry, B., "Thermodynamic background to Differential Scanning Calorimetry" in *Biocalorimetry: Applications of Calorimetry in the Biological Sciences*, Edited by J. E. Ladbury & Chowdhry, B. Z. (1998) John Wiley and Sons Ltd.
64. Antosiewicz, J., Briggs, J., Elcock, A., Gilson, M., and McCammon, A. "Computing Ionization States of Proteins with a Detailed Charge Model." *Journal of Computational Chemistry* **17**, 1633-1644 (1996).
65. Bashford, D and Karplus, M. "pK_as of ionizable groups in proteins: atomic detail from a continuum electrostatic model." *Biochemistry* **29**, 10219-10225 (1990).
66. Kuramitsu, S. & Hamaguchi, K. "Analysis of the Acid-Base Titration Curve of Hen Lysozyme." *J. Biochem.* **87**, 1215-1229 (1980).
67. Kinstler, O., Molineux, G., Treuheit, M., Ladd, D., & Gegg, C., "Mono-N-terminal poly(ethylene glycol)-protein conjugates" *Advanced Drug Delivery Reviews* **54** (2002) 477-485
68. Lepori, L. & Mollica, V., *J. Polymer. Sci. Polym. Phys. Ed.*, Vol 16 (1978) 1123-1134.
69. Barnes, K.P., Warren, J.R. & Gordon, J.A. "Effect of Urea on the Circular Dichroism of Lysozyme." *J. Biol. Chem.* (1972) vol. 247 No.6. Mar. pp. 1708-1712
70. Nishimote, E., Yamashita, S., Yamasaki, N., & Imoto, T. "Resolution and Characterization of Tryptophyl Fluorescence of Hen-Egg white Lysozyme by quenching and Time-Resolved Spectroscopy." *Biosci, Biotechnol, Biochem* (1999) **63** (2) pp. 329 -336
71. *Jasco Application Note*. "Automated Thermal Denaturation of Hen-egg Lysozyme with Concurrent CD and Fluorescence Detection."
72. Furness E. L., Ross A., Davis T. P., King G. C. "A hydrophobic interaction site for lysozyme binding to polyethylene glycol and model contact lens polymers." *Biomaterials*. (1998) **15**: 1361-1369.
73. Kerwin, B.A., Chang, B.S., Gegg, C.V., Gonnelli, M., Li, T. & Strambini, G.B. "Interactions between PEG and type I soluble tumor necrosis factor receptor: Modulation by pH and by PEGylation at the N terminus." *Protein Science* (2002) **11**. pp. 1825-1833.

74. Harris, J. M., Chess, R. B. "Effect of PEGylation on Pharmaceuticals" *Nature Review: Drug Discovery* (2003) Vol 2: 214-219
75. Yamaski, N., Matsuo, A., & Isobe, H. "Novel Polyethylene Glycol Derivatives for Modification of Proteins" *Agric. Biol. Chem.* 52: 2125-2127 (1988)
76. Dishon, M., Weiss, G. H., & Yphanistis, D. A. Numerical Solutions to the Lamm Equation III Velocity Centrifugation Biopolymers (1967) 5: 697 – 713.
77. DSC Data Analysis in Origin: Tutorial Guide Version 5.0, Oct. 1998 – MicroCal™, Inc.
78. Liu, Y., & Sturtevant, J.M. "The Observed Change in heat Capacity accompanying the thermal Unfolding of Proteins depends on the Composition of the Solution and on the Method Employed to change the Temperature of Unfolding." *Biochemistry* 1996, 35, pp. 3059-3062.
79. Branchu, S., Forbes, R. T., York, P. & Nyquist, H., "The effect of Cyclodextrins on Monomeric Protein Unfolding" in *Biocalorimetry: Applications of Calorimetry in the Biological Sciences*, Edited by J. E. Ladbury & Chowdhry, B. Z. (1998) John Wiley and Sons Ltd.
80. Gomez, J., Hilser, V. J., Xie, D., & Friere, E. (1995) *Proteins: Struct. Func. Genet.* 22:404-412.
81. Yonezawa Y, Tanaka S, Kubota T, Wakabayashi K, Yutani K, Fujiwara S. "An Insight into the pathway of the amyloid fibril formation of hen egg white lysozyme obtained from a small-angle X-ray and neutron scattering study" *J Mol Biol.* (2002) Oct 18; 323(2):237-51.
82. Uversky, V.N., Cooper, Bower, K.S., Li, Jie & Fink, A.L. "Accelerated α -synuclein fibrillation in crowded milieu." *FEBS Letters* 515 (2001) pp. 99-103.
83. Cleland, J.L. & Randolph, T.W. "Mechanism of Polyethylene Glycol Interaction with the Molten Globule Folding Intermediate of Bovine Carbonic Anhydrase B", *J. Biol. Chem.* (1992) Vol. 267, No. 5, Feb 15. pp. 3147-3153.
84. Lee J. C., and Lee, L. L. Y. "Preferential Solvent Interactions between Proteins and Polyethylene Glycols" *J. Biol. Chem.* (1981) Vol. 256. No. 2, pp. 625-631.